



RTI Report No. TRR-30

ARO# 6030:1

AD686538

Final Technical Report
RTI Program RU-224

A SURVEY OF AVAILABLE INFORMATION RELATIVE TO
ACHIEVING ULTIMATE ANTENNA BANDWIDTHS

by

G. V. Borgiotti

Contract DA 31-124-ARO-D 396

Submitted to

U. S. Army Research Office - Durham
Box CM, Duke Station
Durham, North Carolina

Code 1

CLEARINGHOUSE FOR FEDERAL SCIENTIFIC AND TECHNICAL INFORMATION			
Hardcopy	Microfiche		
\$ 4.00	\$ 0.75	127 pp	SL
ARCHIVE COPY			

July 31, 1966



RESEARCH TRIANGLE INSTITUTE • DURHAM, NORTH CAROLINA

RTI Project No. RU-224

A SURVEY OF AVAILABLE INFORMATION RELATIVE TO
ACHIEVING ULTIMATE ANTENNA BANDWIDTHS

by

G. V. Borgiotti
Radiation Systems Laboratory
Research Triangle Institute

Final Technical Report
Contract DA 31-124-ARO-D 396
July 31, 1966

Submitted to: U. S. Army Research Office - Durham, N. C.

Requests for additional copies by Agencies of the Department of Defense, their contractors, and other Government agencies should be directed to:

Defense Documentation Center
Cameron Station
Alexandria, Virginia 22314

Department of Defense contractors must be established for DDC services or have their "need-to-know" certified by the cognizant military agency of their project or contract. All other persons and organizations should apply to the:

U. S. Department of Commerce
Clearinghouse for Federal Scientific
and Technical Information
Washington 25, D. C.

FOREWORD

The study described in this report was performed during FY 1966 under the sponsorship of the U. S. Army Research Office - Durham, N. C., contract DA 31-124-ARO-D-396. Technical coordinators for the Government have been Messrs A. P. Sheppard and J. R. Suttle, ARO-D.

ABSTRACT

This report is concerned with a survey of the presently available literature concerning broadband antennas, in order to determine the capabilities and the limitations of the various techniques which have been investigated.

The report is divided into three main parts, concerned with the following subjects:

- I. Frequency Independent Antennas
- II. Logarithmic Periodic Antennas
- III. Electrically Small Antennas

In the first part the present state of the theory of frequency independent antennas is discussed. The experimental work on these structures is then briefly reviewed. In Section II, a parallel treatment is made for log periodic antennas. Section III is mainly concerned with the theoretical question of the bandwidth limitation of an antenna "small" in terms of wavelength.

TABLE OF CONTENTS

	<u>Page</u>
INTRODUCTION	1
SECTION I. FREQUENCY INDEPENDENT ANTENNAS	3
1.1 INTRODUCTION	3
1.2 GEOMETRY OF FREQUENCY INDEPENDENT ANTENNAS	5
1.3 THEORETICAL WORK ON FREQUENCY INDEPENDENT ANTENNAS	5
1.3.1 General Considerations	5
1.3.2 An Exact Solution for the Planar Log Spiral with an Infinite Number of Arms	7
1.3.3 Other Miscellaneous Contributions to the Problem of Planar Spiral Antennas	16
1.3.4 Pseudo Frequency-Independent Antennas	16
1.3.5 A General Approach to the Analysis of Frequency Independent and Log Periodic Structures	18
1.3.5.1 "Slowly-Varying" Periodic Structures	18
1.3.5.2 Elementary Discussion of the Types of Waves Supported by Open Uniform Structures	18
1.3.5.3 Waves in Periodic Structures and Application to F.I. and L.P. Structures	24
1.3.5.4 Use of Dispersion Diagram for Log-Spiral Antennas	29
1.4 EXPERIMENTAL WORK ON LOG-SPIRAL ANTENNAS	32
1.4.1 Two-Arm Spirals	32
1.4.2 Miscellaneous Modifications of the Basic Geometry	37
1.5 DESIGN OF FREQUENCY-INDEPENDENT ANTENNAS	41
SECTION II. LOGARITHMICALLY PERIODIC ANTENNAS	45
2.1 GENERAL CONCEPT OF LOG-PERIODIC ANTENNAS	45
2.2 STATE OF THE THEORY OF LOG-PERIODIC ANTENNAS	48
2.2.1 Mathematical Models	48
2.2.2 The Sinusoidally Anisotropic Surface	49
2.2.3 The Periodic Array of Dipoles	52
2.2.4 Log-Periodic Loaded Lines	55
2.3 NUMERICAL ANALYSIS OF THE LOG-PERIODIC DIPOLE ARRAY	63
2.3.1 Numerical Approach	63
2.3.2 Formulation of the Problem	64
2.3.3 The Interior Problem	67
2.3.4 Radiation Pattern	70
2.3.5 Numerical Computations	70
2.3.6 Design Data	78

Table of Contents (Continued)

	<u>Page</u>
2.4 MISCELLANEOUS LOG-PERIODIC ANTENNAS	80
2.5 DESIGN OF LOG PERIODIC ANTENNAS	91
SECTION III. BROADBANDING CONVENTIONAL ANTENNAS	95
3.1 THE "SMALL ANTENNA" PROBLEM	95
3.2 THE Q OF A RADIATING ELECTROMAGNETIC SYSTEM	96
3.3 EXPRESSION OF THE FIELD OF AN OMNIAZIMUTHAL ANTENNA	97
3.4 EQUIVALENT CIRCUITS OF THE VARIOUS MODES	98
3.5 THE MINIMUM Q OF A SMALL LOSSLESS ANTENNA	102
3.6 QUALITATIVE DISCUSSION	104
3.7 NETWORK THEORETICAL APPROACH	106
SECTION IV. CONCLUSIONS AND RECOMMENDATIONS	111
4.1 CONCLUSIONS	111
4.2 RECOMMENDATIONS FOR FURTHER STUDIES	113
SECTION V. REFERENCES	115

LIST OF ILLUSTRATIONS

<u>Figure No.</u>		<u>Page</u>
1	Geometry of equiangular spiral.	6
2	Self-complementary multiarm log spiral structure.	8
3	Radiation pattern of the log spiral antenna with an infinite number of arms for different values of n .	12
4	Radiation pattern of the log spiral antenna with an infinite number of arms for different values of $ a $.	13
5	Radial current behavior in the log spiral antenna with an infinite number of arms.	14
6	Radial phase variation in the log spiral antenna with an infinite number of arms.	15
7	Radiation pattern of a multiarm spiral antenna (with a ground plane), excited by a monopole.	17
8	Dispersion (β, k) diagram for a uniform structure.	21
9	Geometry of a leaky wave structure.	23
10	Dispersion diagram for complex waves.	23
11	Modified dispersion diagram.	26
12	Dispersion (or Brillouin) diagram for a periodic structure.	26
13	Different character of the space harmonics.	28
14	Brillouin diagram for monofilar helix.	31
15	Brillouin diagram for bifilar helix.	31
16	Spiral antenna feeding zone with "infinite balun."	33
17	Radiation patterns of a typical planar spiral antenna (r = axial ratio of the polarization ellipse on the peak of the radiation pattern).	34
18	A mechanically simple form of conical log-spiral antenna.	36
19	Radiation patterns of the conical spiral of Fig. 18.	36
20	"Square spiral" antenna.	38
21	"Square" spiral and log spiral radiation patterns.	38
22	Feeding system of the four arm spiral.	39
23	Radiation patterns of the four arm spiral.	39
24	Frequency independent array of log-spiral antennas (A, B, C phase centers).	40
25	Saw tooth log periodic array.	46
26	Sinusoidal zigzag antenna.	47
27	Plot of θ vs $\ln r$ for one of the component structure of Fig. 25.	47
28	Sinusoidally anisotropic surface.	50
29	Unreversed element uniform dipole array.	53
30	Reversed elements uniform dipole array.	53

List of Illustrations (Continued)

<u>Figure No.</u>		<u>Page</u>
31	Transmission line model for the uniform array of dipoles.	54
32	Uncoupled load transmission line model for the uniform dipole array.	54
33	Brillouin diagram for reversed uniform dipole array.	56
34	Brillouin diagram for unreversed uniform dipole array.	56
35	Transmission-line voltage amplitude and phase curves for LP dipole array (theoretical) and comparison with experiment (Carrel [1]).	57
36	Voltage amplitude and phase vs electrical distance with matched termination $R_o = 0.5$ and $Q = 2$.	60
37	Voltage amplitude and phase vs electrical distance open circuit termination $R_o = 0.5$ and $Q = 2$.	60
38	Comparison of voltage amplitude and phase on LP and CS transmission lines with $\tau = 0.9$, $D = 0.5$, $R_o = 0.5$, $Q = 2$, and $z_o = 1$.	62
39	Log-periodic array of reversed dipoles.	65
40	A schematic of the log-periodic dipole antenna, including symbols used in its description.	66
41	Schematic circuits for the LPD interior problem.	68
42	Coordinate system used in the computation of the far field radiation patterns.	71
43	Relative magnitude and phase of feeder voltage vs R/λ at f_3 , $\tau = 0.888$, $\sigma = 0.089$, $\alpha = 17.5^\circ$, $N = 8$, $Z_o = 100$, $h/a = 125$, short circuit termination 0.128λ behind element number one.	72
44	Bandwidth of action region B_{ar} vs α for several values of τ , for $Z_o = 100\Omega$, $h/a = 125$.	74
45	Relative magnitude and phase of element base current vs R/λ at f_3 , $\tau = 0.888$, $\sigma = 0.089$, $\alpha = 17.5^\circ$, $N = 8$, $Z_o = 100\Omega$, $h/a = 125$, short circuit termination 0.128λ behind element number one.	75
46	Computed and measured patterns, $\tau = 0.888$, $\sigma = 0.089$, $\alpha = 17.5^\circ$, $Z_o = 100\Omega$, $h/a = 125$, $Z_T = \text{short at } 0.1\lambda_{\max}$ behind element number one.	76
47	Computed contours of constant directivity vs τ , σ , and α ; $Z_o = 100$, $Z_T = \text{short at } h_1/2$, $h/a = 177$.	77
48	Location of the phase center in wavelengths from the apex.	79
49	Log periodic, folded monopole array.	83
50	Log-periodic folded slot array.	84
51	Some radiation patterns of the slot array of Fig. 50.	86
52	A circularly polarized log periodic dipole array.	87

List of Illustrations (Continued)

<u>Figure No.</u>		<u>Page</u>
53	Log periodic zigzag antenna on a ground plane.	88
54	Log periodic helical zigzag antenna on a ground plane.	90
55	Pattern characteristics of wire trapezoidal tooth element for: ——— approximate minimum value of τ . - - - A larger value of τ .	92
56	Relation between element beamwidth and n .	92
57	Effect of angle ψ on pattern characteristics for antenna with $\alpha = 60^\circ$ and $\tau = 0.6$.	93
58	Equivalent circuit of a vertically polarized omni-directional antenna.	99
59	Equivalent circuit of TM_n spherical wave.	101
60	Equivalent circuit of electric dipole.	101
61	Q_n of the equivalent circuit.	103
62	Bandwidth of an ideal dipole with ideal matching network.	107

INTRODUCTION

The long term objective of the research documented in this report is to find promising techniques that will lead to the realization of ultimate operating bandwidths for any given class of antennas. As a first step toward the accomplishment of this objective, a literature review has been conducted to determine promising theoretical approaches to broadband antenna design.

The immense quantity of both experimental and theoretical information available on antennas in the frequency range of interest (100 Kc to 100 Gc) obviously prevents consideration in depth of all antenna classes, hence this survey primarily considers wideband structures that are characterized by self-congruent (log spiral) and log periodic geometry. In addition, several approaches to the general problem of broadbanding conventional "small" antennas are reviewed, with emphasis placed on those papers that contain general results independent of specific antenna configurations.

The reader will find that the theory of frequency-independent antenna structures is not well developed at the present time. The only approach having thus far been developed is the analysis of the periodic component of the structures, and the array of dipoles is apparently the only practical structure which has been solved. In the dipole array case, approximations are made which degrade solution accuracy at dipole spacings less than a wavelength.

For antennas small with respect to the operating wavelength, the theory in its present form allows prediction of an upper bound on the bandwidth obtainable from a certain structure, but is not able to predict the actual behavior of a practical antenna given its configuration.

In the following, Section I reviews the present state of the theory of antennas derived from log spiral geometry, Section II considers the class of log periodic antennas, and in Section III, the problem of the minimum Q or maximum bandwidth of small lossless antennas is discussed.

Several promising approaches that may provide a better insight into the behavior of frequency independent antennas are outlined in Section IV, along with recommendations for future studies.

I. FREQUENCY INDEPENDENT ANTENNAS

1.1 INTRODUCTION

Carrel, in a very important paper, (reference [1]^{*}) which we will examine in detail in Section II, gave this crystal clear definition of frequency independent antennas:

"By frequency independence, as applied to an antenna, it is meant that the observable characteristics of the antenna such as the field pattern and input impedance vary negligibly over a band of frequencies within the design limits of the antenna, and that this band may be made arbitrarily wide merely by properly extending the geometry of the antenna structure. The ultimate band limits of a given design are determined by non-electrical restrictions. Size governs the low frequency limit, and precision of construction the high frequency limit."

It is well known that as a rather immediate consequence of Maxwell equations, all the electromagnetic properties of a lossless passive structure are determined by its shape and size evaluated in terms of wavelengths. This seems at first glance to deny the possibility of existence of an antenna satisfying the above quoted definition. However, this turns out not to be correct: the basic idea underlying the invention of frequency independent antennas (FIA) is just the recognition that there exist structures for which the geometrical properties are independent of linear dimension and can be specified by angles alone [2]. When scaled by an arbitrary factor they are transformed into others congruent to the original one. However, this is not the only requirement a structure must satisfy in order to be a frequency independent antenna. In addition, it is necessary that the current have a particular behavior along the structure.

To clarify this point let us consider the infinite biconical antenna. It is obviously a self congruent geometry in the sense specified above. However, it is not a FIA. If we cut the conducting cones at any distance from the apex, the resulting finite structure behaves differently at different wavelengths. We cannot increase the band by simply "extending the geometry of the antenna structure." The reason is that the total current is constant along the structure, and therefore there is the above mentioned end effect, which causes a difference of behavior at different frequencies; in fact the surface density of current in the biconical case is decreasing as $\frac{1}{r}$, where r is the distance from the feeding point (apex of the cones). In order not to have end effects, the current at the end of the structure must be negligible. This implies that the density of current must decay faster than $\frac{1}{r}$ (going away from the

* Numbers in square brackets refer to references listed in the Bibliography.

feeding point). In such a case, the structure can be truncated at a certain distance from the feeding point, (proportional to the largest wavelength of operation). The rate of decay of the current depends, of course, upon the particular structure under analysis. From these considerations it is apparent that the behavior of a frequency-independent antenna is quite different from that of the biconical case. Roughly speaking, in the latter the energy is guided from the feeding point along the "biconical guide," and the radiation occurs because of an end discontinuity which transforms the guided modes in radiating ones. In the frequency-independent antennas the energy reaches a region (whose location depends upon frequency) of very strong attenuation, beyond which the current is practically zero. In this region (the "active zone") the guided energy must be transformed in radiation. No role is played in this mechanism by the edge of the structure except at the lowest frequency when the active region reaches it.

In summarizing we can say that a structure, in order to work as a FIA, must satisfy the following requirements (one of geometrical and two of electrical nature):

- (a) self congruency (a scaling must transform the structure in itself);
- (b) the current density must decay along the structure faster than $1/r$, where r is the distance from the feeding point; and
- (c) in the active zone there must be an efficient transformation of guided modes into radiating modes.

These various points (a), (b), and (c), will be examined in more detail in the next sections.

We want at this point to stress the fact that it is very difficult to predict whether the electromagnetic behavior of a certain structure which satisfies (a), will obey (b) and (c). This makes the design of novel types of frequency-independent antennas very difficult. Quoting Mittra and Jones [3] about this point:

"The conditions prescribed¹ . . . are undoubtedly necessary, but far from being sufficient. Most of the authors in the field report only the successful antennas and tacitly forego the discussion on those which, although built on the same principle as the others, fail to work as broadband antennas. For every successful antenna built, there are perhaps several which were failures. Even today, after many years of experience, it is not possible to predict, a-priori, whether or not a given log-periodic antenna (LPA) will have broadband performance in the design range."

The design of frequency-independent antennas is largely based on experimental and cut-and-try procedures. However, as we will see later, substantial steps

¹i.e., The geometrical condition we have denoted by (a).

have been made in recent years toward an understanding of these interesting and peculiar structures.

1.2 GEOMETRY OF FREQUENCY INDEPENDENT ANTENNAS

An antenna satisfies the angle condition [(a) in Section 1.1] when expansion by an arbitrary ratio τ about the feed point O , generates a structure that either coincides with the original one, or differs only by a rotation about some axis D passing through the point O .

The most general structure having this property must satisfy the following conditions [2,4]:

- (a) the axis of rotation D must be independent of τ , and
- (b) the angle of rotation φ about D must be proportional to the logarithm of the expansion factor τ :

$$\tau = \frac{r_2}{r_1} = e^{a\varphi} \quad (1.1)$$

where r_2 and r_1 are the radius vectors defining two correspondent points before and after the expansion.

As a consequence of (a) and (b) the surfaces bounding the antenna structure must have polar equations of the form:

$$F(\theta, re^{-a\varphi}) = 0$$

For $\theta = \theta_0 = \text{const}$, the points of the structure are described by the equations:

$$r = r_0 e^{a\varphi} = e^{a(\varphi + \varphi_0)} \quad (1.2)$$

which are equiangular spirals (Fig. 1). They make a constant angle ψ with the radius vector. The φ_0 is the angle such that $r(0) = r_0 = e^{a\varphi_0}$. When φ_0 is varied the entire curve is rotated about D .

In spite of the fact that the spiral is surrounding the origin, infinitely many times the arc length s from the origin O is finite and proportional to distance r :

$$s = \frac{r}{\cos\psi}$$

The parameter a of the spiral has a simple geometrical significance. It is simple to show that a is related to ψ and θ_0 by the relationship:

$$a = \frac{\sin\theta_0}{\tan\psi} \quad (1.3)$$

1.3 THEORETICAL WORK ON FREQUENCY INDEPENDENT ANTENNAS

1.3.1 General Considerations

The geometrical shape of an equiangular spiral conical antenna is not a simple one. The surface of the conductors are not coincident with any coordinate system for

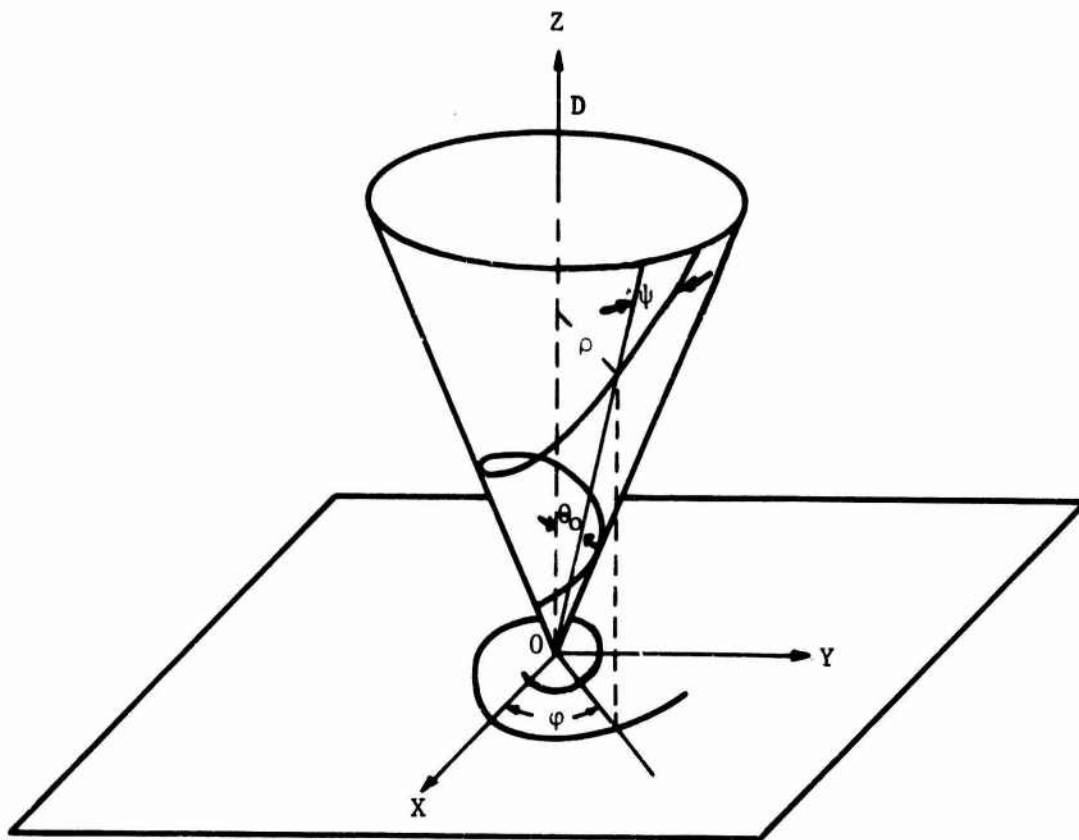


Fig. 1. Geometry of equiangular spiral.

which the wave equation is separable. Therefore the analysis of this structure is a formidable task and an exact solution for the general conical case has not yet been found. On the other hand, the planar spiral has been analyzed by resorting to a very simplified mathematical model, an idealization of the structures practically used. Although this solution does not explain all the experimental results, it performs one of the two major steps toward an understanding of the way in which frequency-independent antennas operate.

The other basic theoretical advancement has been the introduction and systematic use of the fruitful and powerful idea of considering these antennas (and the log periodic as well) as slowly tapered versions of (uniformly) periodic structures. If the properties of the latter are known, it is thus possible to deduce in an approximate way the properties of the antennas by considering its "local" behavior (as will be discussed at length in Section 1.4).

In the next sub-section, we will examine in some detail the solution for the planar spiral antenna found by Rumsey, Cheo, and Welch. Then we will consider in 1.3.3 other theoretical contributions (exact and approximate solutions). Then 1.3.5.1 and 1.3.5.2 will be devoted to an elementary discussion of the various possible waves which can be supported by uniform and periodic structures. The discussion of this question will give the background necessary in order to use the approach mentioned above of considering a conical spiral as locally periodic (Sub-section 1.3.5.4). This study will also be useful for a qualitative analysis of log-periodic antennas (Section II).

1.3.2 An Exact Solution for the Planar Log Spiral with an Infinite Number of Arms

The solution of the electromagnetic problem posed by a FIA is a formidable task, which so far has proved to be intractable. Therefore, it has been necessary to consider some simpler problem (which could be considered an idealization of the real one) amenable to theoretical solution. The mathematical model, posed by Rumsey, et al., consists of an infinite number of perfectly conducting wires of spiral shape infinitely close together [5]. It is apparent that this structure is the limiting case of a multi-arm antenna, of the self-complementary type (i.e., such that the angular widths of the metallic elements and of the space between two elements are equal, Fig. 2), when the number of arms is increased with limit. The antenna takes the form of an anisotropic sheet perfectly conducting in the direction of spiral lines and perfectly transparent in the perpendicular direction. This implies that on the plane of the antenna the component of the electric field along the wires is zero

$$\underline{E}_t \cdot \underline{t} = 0 \quad (1.4)$$

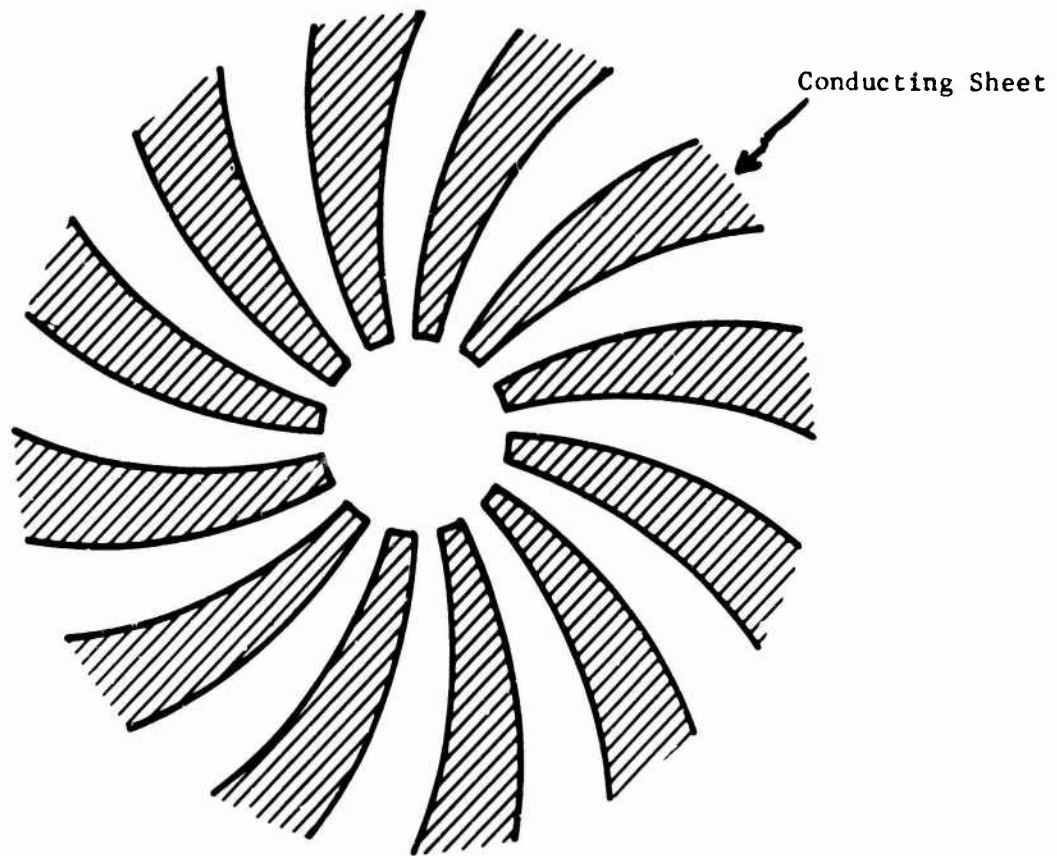


Fig. 2. Self-complementary multiarm log spiral structure.

where \underline{E}_t is the tangential component of the electric field (component on the plane $z = 0$) and \underline{t} is a unit vector in the direction of the wires. It is of interest to note that the tangential magnetic field must satisfy the same boundary condition

$$\underline{H}_t \cdot \underline{t} = 0 \quad (1.5)$$

This is because the current must necessarily flow along the direction defined by \underline{t} (i.e., along the wires). The identity of condition (1.4) and (1.5) suggests trying a solution in which \underline{E} and \underline{H} have the same behavior (i.e., they are proportional). It is however clear that the proportionality constant cannot be the same in the half spaces, $z > 0$ and $z < 0$ of Fig. 1, because \underline{H}_t is discontinuous at $z = 0$ (since there is a current flow on the arms of the spiral) while \underline{E}_t is continuous. It is possible to show that solutions with \underline{E} proportional to \underline{H} can exist only if the proportionality constant is either $+j\eta$ or $-j\eta$ with η the characteristic impedance of the medium [6]; therefore one of the following sets of solutions must be satisfied:

$$\left. \begin{aligned} \underline{E}_1 &= +j\eta \underline{H}_1 & \text{for } z > 0 \\ \underline{E}_2 &= -j\eta \underline{H}_2 & \text{for } z < 0 \end{aligned} \right\} \quad (1.6)$$

or

$$\left. \begin{aligned} \underline{E}_2 &= -j\eta \underline{H}_2 & \text{for } z > 0 \\ \underline{E}_1 &= +j\eta \underline{H}_1 & \text{for } z < 0 \end{aligned} \right\} \quad (1.7)$$

Let us consider for example solution (1.6). The field \underline{E}_1 (or \underline{E}_2) can be derived from a potential U_1 (or U_2), satisfying the wave equation as it follows [5]:

$$\underline{E}_1 = -\beta \nabla x(zU_1) + \nabla x \nabla x(zU_1) \quad (1.8)$$

$$\underline{E}_2 = \beta \nabla x(zU_2) + \nabla x \nabla x(zU_2) \quad (1.9)$$

where β is the propagation constant of free space and z is a unit vector in the z direction. When (1.8) and (1.9) are satisfied the field is completely specified by (1.6). To the functions U_1 and U_2 , which satisfy the wave equation and the radiation condition and have an angular variation of the type $e^{jn\phi}$, the following integral representation can be given:

$$\text{for } z > 0 \quad U_1 = e^{jn\phi} \int_0^{\infty} g(\lambda) J_n(\lambda \rho) e^{-jz \sqrt{\beta^2 - \lambda^2}} \lambda d\lambda \quad (1.10)$$

$$\text{for } z < 0 \quad U_2 = e^{jn\phi} \int_0^{\infty} g(\lambda) J_n(\lambda \rho) e^{jz \sqrt{\beta^2 - \lambda^2}} \lambda d\lambda \quad (1.11)$$

with $g(\lambda)$ to be determined. $J_n(\lambda \rho)$ is the Bessel function of the first kind and order n . The introduction of the boundary condition (1.3) and the use of (1.6) gives [5 and 7]:

$$-a E_{1\rho} = E_{1\varphi}$$

which, by utilizing (1.8), (1.9), (1.10) and (1.11), yields in turn the integro-differential equation:

$$\int_0^{\infty} g(\lambda) \left\{ \left(-jna\beta + n\sqrt{\beta^2 - \lambda^2} \right) \frac{\lambda J_n(\lambda \rho)}{\rho} + \left(-ja\sqrt{\beta^2 - \lambda^2} + \beta \right) \lambda^2 J_n'(\lambda \rho) \right\} d\lambda = 0 \quad (1.12)$$

It is possible to transform (1.12) into a differential equation for $g(\lambda)$, which can be solved. In this way the expression for the potential U_1 of the field in the half space $z > 0$ is obtained:

$$U_1 = A e^{jn\varphi} \int_0^{\infty} \left[\frac{1 - \sqrt{1-y^2}}{1 + \sqrt{1-y^2}} \right]^{n/2} \frac{\left[1 - aj\sqrt{1-y^2} \right]^{-1+j(n/a)}}{y} e^{-j\sqrt{1-y^2}\beta z} J_n(\beta \rho y) dy \quad (1.13)$$

where A is a constant. For $z < 0$ a similar expression for the potential U_2 can be obtained from (1.13), (1.10) and (1.11). It is possible to prove that the signs in (1.6) and (1.7) could not be chosen in a different way, because that would have led to divergent expressions for U_1 and U_2 unless the sign of n were changed too. In fact, with the radiation conditions fixed, the choice of the plus or minus sign in (1.6) and (1.7) determines the polarization of the far field [6]. On the other hand, the sign of n specifies the sense of the polarization of the source. Therefore, the physical significance of such a constraint is that the far field must have the same polarization as the source.

In their paper, Rumsey, et al., considered in detail the various features of their solution. A check of its behavior at the feeding point showed that when the distance ρ from the origin tends to zero the magnitude of the current flowing in an angular sector of the antenna from the source tends to a constant as it must be. Since the field is circularly polarized at infinity, the radiation pattern can be characterized by a single scalar. The expression of the far zone electric field, obtained by using stationary phase method is the following:

$$E(\theta, \varphi) = A(\theta) e^{-j\psi(\theta)} e^{jn(\varphi + \frac{\pi}{2})} \frac{e^{-j\beta r}}{r}$$

where the amplitude pattern is

$$A(\theta) = \frac{\cos\left(\text{tg} \frac{\theta}{2}\right)^n e\left(-\frac{n}{a}\right) \text{tg}^{-1}(-a\cos\theta)}{\sin\theta \sqrt{1+a^2\cos^2\theta}} \quad (1.14)$$

and the phase pattern:

$$\psi(\theta) = -\frac{n}{2a} \ln |1+a^2\cos^2\theta| + \text{tg}^{-1}(-a\cos\theta) \quad (1.15)$$

The pattern $A(\theta)$ is plotted in Figs. 3 and 4 for various values of n and a and it is amazing that they agree reasonably well with the experimental results found by Dyson for the two arm spirals (see Subsection 1.4.1).

In order to determine the current on the structure it is necessary to introduce (1.13) in (1.8). For this computation it is not possible for arbitrary ρ to utilize the asymptotic expressions which hold in the neighborhood of the origin or in the far zone. Therefore the authors found it necessary to resort to a series expansion of the integrand of (1.13) and a numerical integration.

It is worth spending some time in discussing these numerical results, also because they are illuminating for the comprehension of the general features of frequency-independent antennas.

In Fig. 5 and Fig. 6, the amplitude and phase of the current flowing in a sector of the antenna (normalized at the input value I_0) are plotted vs $\beta\rho = \frac{2\pi}{\lambda} \rho$ (for $n=1$). This means that the abscissa axis corresponds to the length of the circumference at the radius ρ (measured in wavelengths). The amplitude distribution clearly shows the characteristic current attenuation of frequency-independent antennas (see Section 1.1). The parameter a is related, as already pointed out, to the curvature of the wires constituting the antenna. For $a = \infty$ (the wires are straight) and no attenuation of current is found; this case corresponds to the infinite biconical structure degenerate into a plane. Current attenuation increases with a ; for example, $a = 0.1$ causes a current reduction to about 10% at $\beta\rho = 2$, i.e., $\rho \approx \frac{\lambda}{3}$. The behavior of the phase is rather peculiar, exhibiting a sign change of the phase velocity (which is proportional to the reciprocal of the slope of the curve in Fig. 6) at a certain distance from the feeding point. For large $\beta\rho$ phase velocity tends to the velocity of light (this occurs where the current is already extremely attenuated). The wave is a slow one (phase velocity less than velocity of light) in the neighborhood of the origin and then becomes a fast wave with increasing ρ . It is clear that the zone of the antenna for $1 < \beta\rho < 2$ plays a fundamental role in the radiation mechanism. In this "active zone" the radial variation of the phase is slow (see Fig. 6) and adjacent wires are approximately in phase. In points closer to the origin, the radiation from the currents is small because of the rapid variation of the phase (much in the same way as the input resistance of two dipoles close to each other when they are fed in opposition of phase is much lower than when they are in phase). Roughly speaking, we can say that the flux of power from the feeding point is guided along the surface until it reaches the active zone where it is transformed into radiation. This interpretation is in agreement with the ideas generally accepted concerning the radiation mechanism of conical-spiral and log periodic antennas.

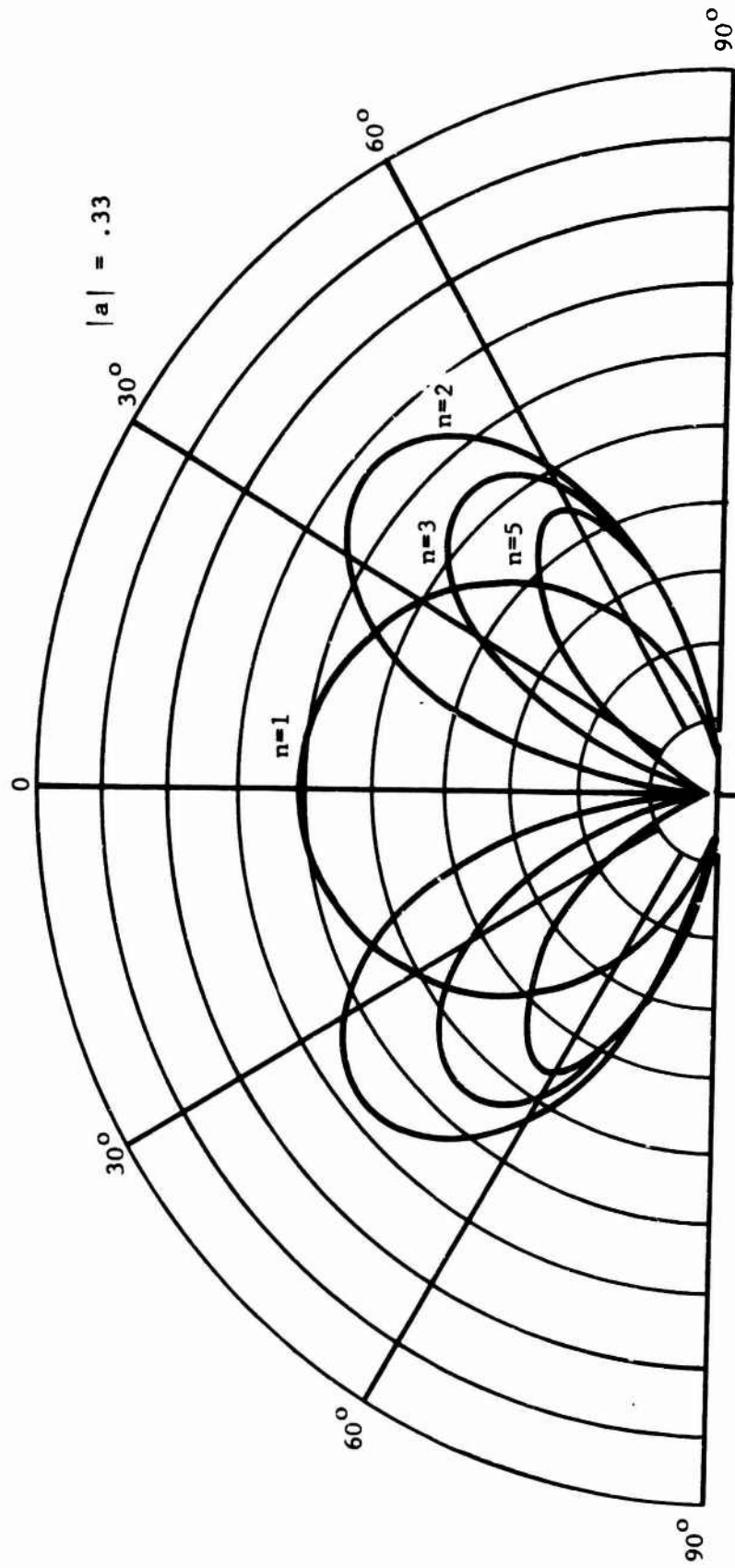


Fig. 3. Radiation pattern of the log spiral antenna with an infinite number of arms.

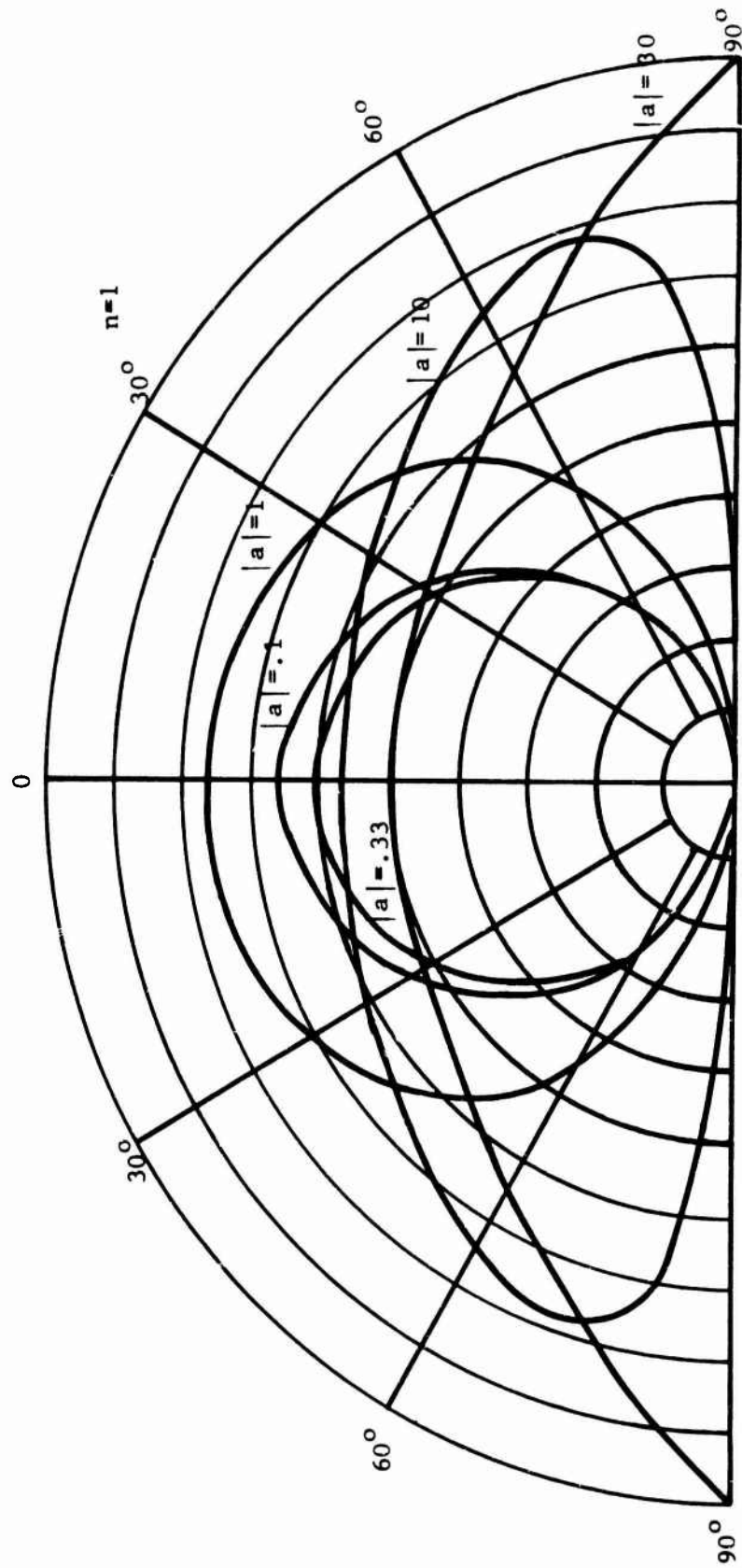


Fig. 4. Radiation pattern of the log spiral antenna with an infinite number of arms.

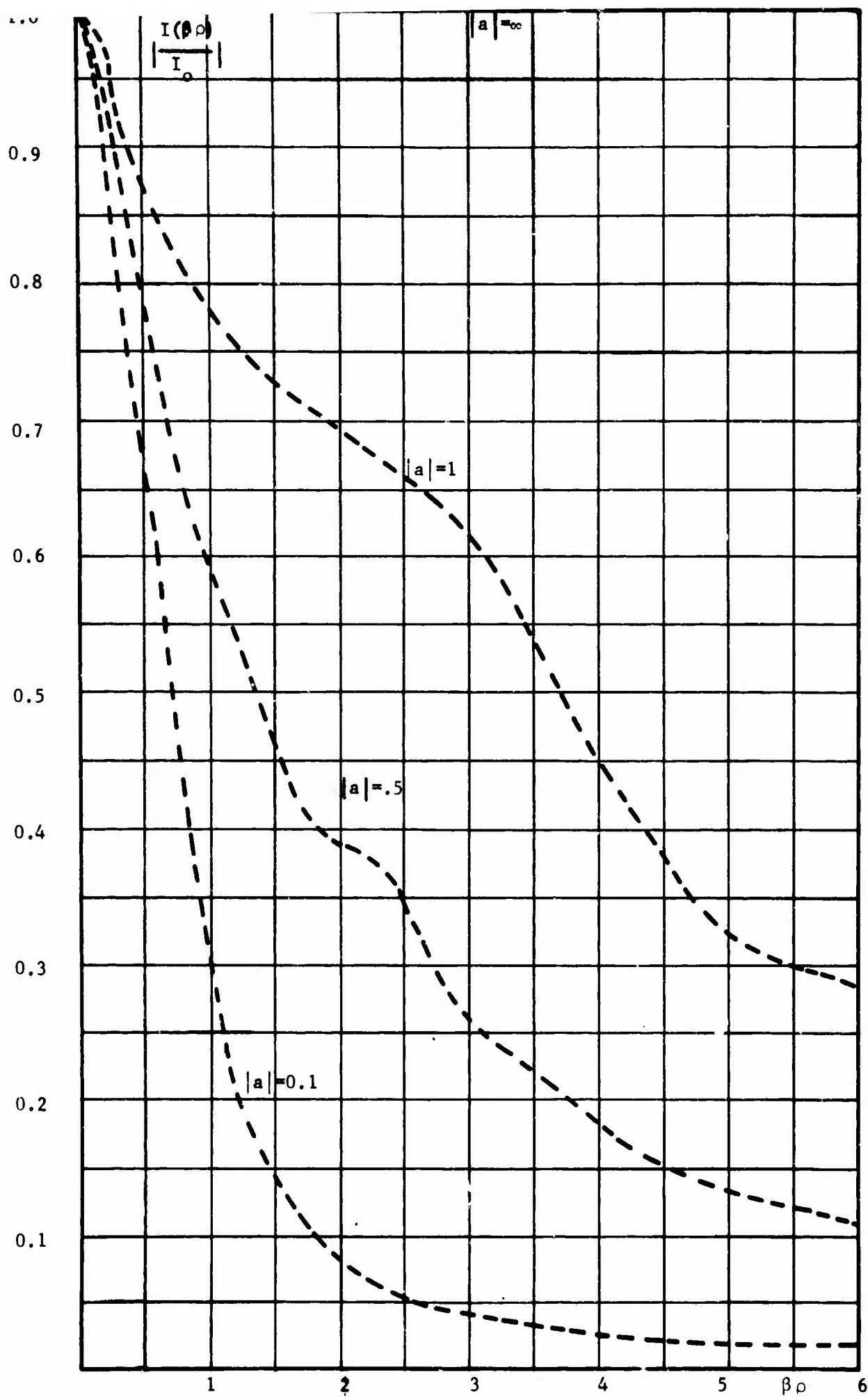


Fig. 5. Radial current behavior in the log spiral antenna with an infinite number of arms.

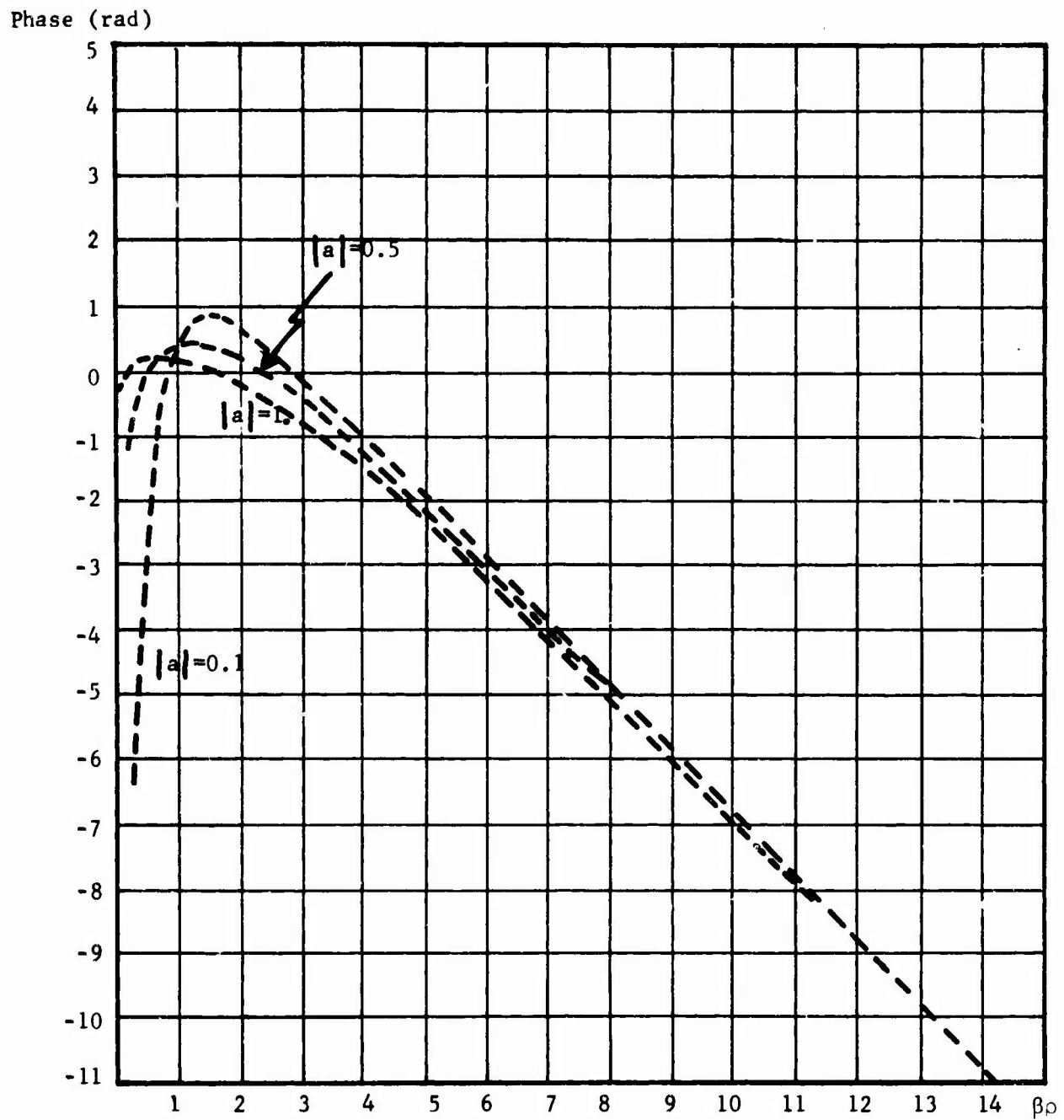


Fig. 6. Radial phase variation in the log spiral antenna with an infinite number of arms.

1.3.3 Other Miscellaneous Contributions to the Problem of Planar Spiral Antennas

After the basic work of Rumsey et al., other people have tried to make use of the same or similar mathematical model to treat theoretical problems concerning planar spiral antennas. Particularly remarkable the paper of Bernard and Ishimaru [8] in which the solution for the planar log spiral excited by a dipole orthogonal to the plane of the antenna is found by using an integral representation for the Hertz Potential (of the type considered in the previous section). An interesting feature of the solution is that the field is linearly polarized, (showing that the solution is a combination of the two types of circularly-polarized modes with $n=0$, considered in the previous section). Furthermore the radiation obtained is at a very small angle with respect to the surface. In this paper the effect of the presence of a ground plane is considered and for generality, the case of a dielectric filling the space between the antenna and the ground plane is analyzed. The radiation is bounded to half space, a property desired in most practical applications. The frequency independence of the form of the radiation beam has been numerically checked, and experimental tests have confirmed the theoretical predictions. A typical radiation pattern of an experimental model is reported in Fig. 7. It refers to the vertical beam of a multi-arm antenna similar to that pictured in Fig. 2. The structure is made by using copper clad dielectric sheets with spiral slots photo-etched out of the copper surface. The feed (not shown in Fig. 2) is a monopole protruding out of the small hole in the center of the back plane. The band is limited by the presence of the ground plane. However bands of 2:1 with very satisfactory radiation patterns have been obtained.

From the point of view of possible applications, the work of Bernard and Ishimaru is particularly interesting because it indicates the possibility of obtaining omnizimuthal coverage with linear polarization on a very large band.

On a different line of thought some approximate analyses of log-spiral antennas have been performed by assuming certain current distributions and then computing the radiation patterns (e.g. Copeland [9]). This approximate type of analysis can be very useful, since the numerical results are often remarkably close to the experimental ones; however, it does not lead to an understanding of the operation of these structures (e.g., since the current is assumed a-priori no insight is obtained about the mechanism by which the current is attenuated along the structure.)

1.3.4 Pseudo Frequency-Independent Antennas

Before passing on to the discussion of uniform and periodic structures, it is worth while to mention briefly some studies performed (analytically and experimentally) on structures which are not frequency independent (in the sense defined in Section 1.2), but which operate over bandwidths never reached before.

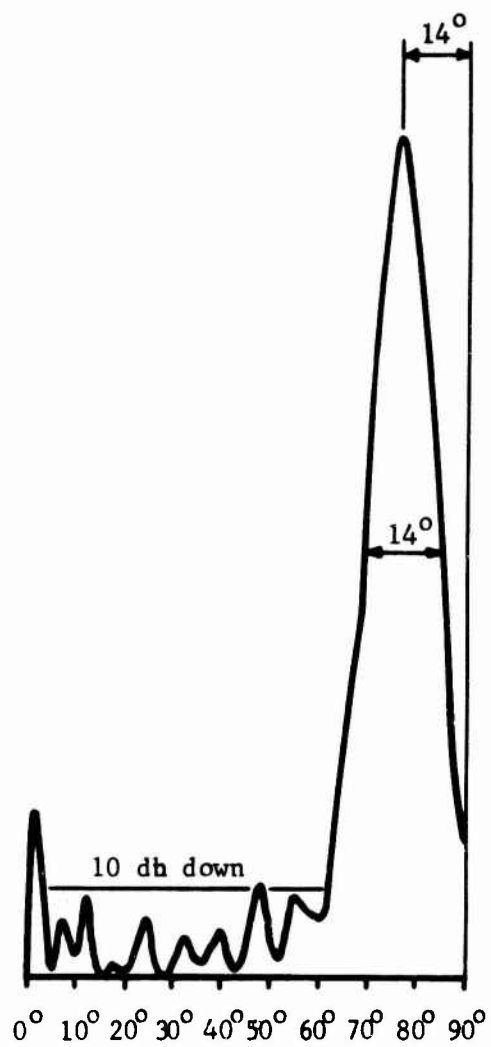


Fig. 7. Radiation pattern of a multiarm spiral antenna (with a ground plane), excited by a monopole.

Turner was perhaps the first to propose a spiral antenna in 1955 [10]: two flat, rather narrow, constant-width metallic arms, wound in the form of an Archimedean Spiral (which clearly is not a self-scaling structure). Fed at the center in a balanced manner, it radiates a broad circularly-polarized lobe on each side of the plane of the antenna. Subsequent investigations and development of this antenna produced forms that have stable pattern and impedance characteristics over a bandwidth up to 10 to 1 [11-15].

Curtis [17] treated analytically the radiation of the archimedean spiral. He approximated the geometry of the structure with a series of semicircles of different radii. He assumed a certain distribution of current on the arms and then calculated the radiation field. In spite of the fact that this approach is not theoretically correct, the radiation patterns calculated are surprisingly close to the experimental data.

1.3.5 A General Approach to the Analysis of Frequency Independent and Log Periodic Structures

1.3.5.1 "Slowly-Varying" Periodic Structures

A great deal of work has been made in the last thirty years in the theoretical analysis and experimental study of electromagnetic waves on uniform and periodic structures. The propagation of guided waves on open structure (surface waves) has been thoroughly investigated in the last decade and in the last few years the more difficult and elegant theory of "complex" or "leaky" waves has been amply developed [18 - 20]. It is therefore understandable why various authors have recently attempted to adapt these theories, already at a high degree of development, to the analysis of spiral and log-periodic structures. The essential idea underlying this approach consists in assuming that if the structure changes its geometrical property gradually (e.g., for a conical spiral if the angle θ is not too large), then the electromagnetic behavior is locally very similar to that occurring in a uniform or periodic structure with its section equal to that in the point under analysis. It is essentially the same idea which is at the basis of the WKB method i.e., roughly speaking, to consider the medium "locally homogeneous" (with the obvious mathematical simplifications in the wave equation).

In the two following subsections the types of waves which can be supported by a uniform and a periodic structure will be analyzed briefly, following essentially the simple exposition of [18].

1.3.5.2 Elementary Discussion of the Types of Waves Supported by Open Uniform Structures

A long radiating structure can be considered a guiding configuration [19]. Although the antenna is open to free space, the surface and leaky waves are supported in a manner similar to that whereby modes propagate in a closed (shielded) waveguide.

The knowledge of the field configuration in the neighborhood of a radiating structure allows prediction of the far field (via the Huygen's principle). On the other hand, the capability of selectively exciting the various types of waves on the structure allows control of the radiation pattern in synthesis problems.

Let us consider a smooth structure, which for simplicity will be assumed bi-dimensional, bounded by the plane $x = 0$. If z is the direction of the propagation, the waves in the upper medium (free space region) $z > 0$ have a spatial and temporal dependence of the type

$$e^{j(\omega t - k_t x - wz)} \quad (1.16)$$

where w and k_t are, respectively the wave numbers in the longitudinal (z) and transverse (x) directions, and are related to free-space wave number k via the dispersion relation

$$w^2 + k_t^2 = k^2 \quad (1.17)$$

w and k_t are generally complex:

$$w = \beta - j\alpha \quad (1.18)$$

$$k_t = b - ja \quad (1.19)$$

While the expression (1.16) for the elementary component wave and (1.17) are general relationships, the actual values of k_t and w depend of course upon the nature of the medium below the interface. To determine these values, the boundary value problem must be solved, and this is an extremely difficult task. However, in order to discuss the behavior of these various types of waves this analysis is not necessary; in what follows we will consider surface and complex waves in free space without relating the discussion to a specific structure.

The simplest types of waves on an open structure are the surface waves, propagating in the direction of the interface without loss. This implies that k_t is purely imaginary and w purely real, i.e.

$$k_t = -j|k_t| \quad (1.20)$$

From (1.17):

$$w^2 > k^2 \quad (1.21)$$

Therefore the surface waves are slow waves. The power is flowing in the z direction and the power flow occurs at the group velocity v_g which, for physical reasons, is always less than the velocity c of light:

$$\left| \frac{v_g}{c} \right| = \left| \frac{dk}{dw} \right| \quad (1.22)$$

An example of a possible dispersion curve is given in Fig. 8. For the wave represented by this curve the group velocity and the phase velocity,

$$V_f = \frac{\omega}{\beta} = c \frac{k}{\beta} \quad (1.23)$$

have the same sign in some frequency regions; opposite signs in others. The former case corresponds to forward waves and the latter to backward waves. The forward waves are the most usual, occurring in dielectric slabs, Gouban lines etc.; the backward ones are less widely known and occur in dispersive and/or anisotropic media. In this kind of wave the phase delay occurs in the direction opposite to that of the flow of power. This behavior can seem at first glance somehow unfamiliar, but it does not contradict any physical principle.

Complex waves are characterized by complex values of w even if the media are lossless. An example of a structure capable of supporting such waves is the slotted rectangular metallic waveguide. From (1.17) it clearly appears that if w is complex, then k_t must be complex too. Splitting (1.17) in its real and imaginary parts, the two following relationships are obtained.

$$\begin{aligned} \beta^2 + b^2 - \alpha^2 - a^2 &= k^2 \\ \alpha\beta + ba &= 0 \end{aligned} \quad (1.24)$$

In order to gain a better picture of the physical characteristics of these waves, polar coordinates are introduced:

$$\begin{aligned} x &= r \cos\theta & b &= B \cos\theta_0 \\ z &= r \sin\theta & \beta &= B \sin\theta_0 \end{aligned} \quad (1.25)$$

Equation (1.25) defines θ_0 and B implicitly. Notice that θ_0 is positive in all directions for which z is positive, i.e., the angle between the direction θ_0 and the direction of the flow of the feeding power is smaller than $\frac{\pi}{2}$. We can write

$$e^{-j(wz+k_t x)} = e^{-j(\beta z+bx)} e^{-j(\alpha z+ax)} = e^{-jk(\theta)r-D(\theta)r} \quad (1.26)$$

where $k(\theta)$ and $D(\theta)$ are the wave numbers and the decay terms in the radial direction defined by θ . By using (1.26) and the basic relationship (1.24) we obtain

$$\begin{aligned} k(\theta) &= B \cos(\theta-\theta_0) \\ D(\theta) &= \alpha \frac{\sin(\theta-\theta_0)}{\cos\theta_0} \end{aligned} \quad (1.27)$$

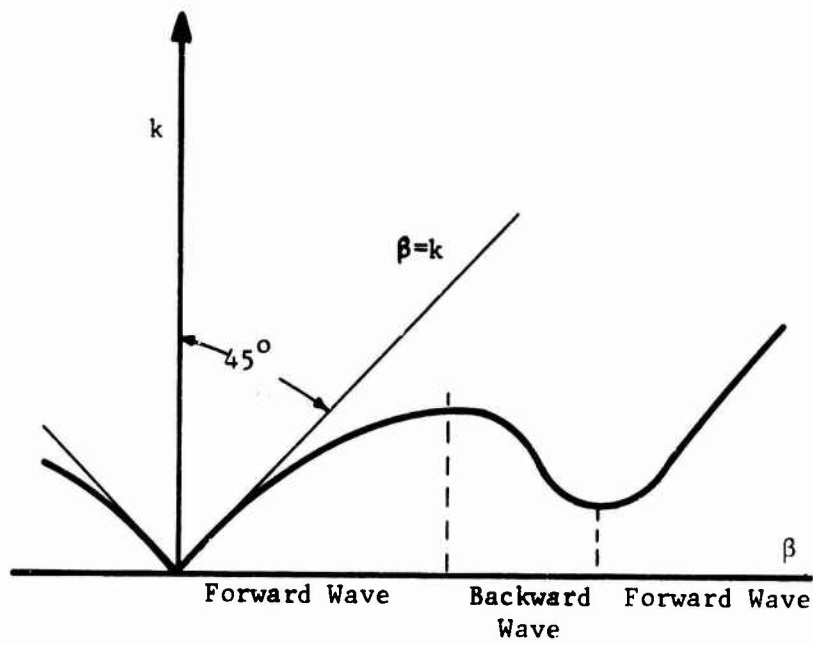


Fig. 8. Dispersion (β, k) diagram for a uniform structure.

It is seen in this way that, given complex w and k_t , a direction θ_0 is found on which the gradient of the phase is maximum and the attenuation zero. We can assume b positive. B is always positive (the orientation of the propagation vector is defined by θ_0 , and B is its length.) Furthermore, the amplitude of the wave propagating along the interface $x=0$ decreases progressively with z , because there is a leakage of energy from the guiding structure to free space. This means that α cannot be negative and $D(\theta)$ will change sign when θ crosses the value θ_0 . It is then apparent that where $D(\theta)$ is less than zero, the "leaky" wave cannot exist in the entire half space of radiation, because it could not satisfy the radiation condition; in other words, it must be restricted to the angular region of space where $D(\theta) > 0$. This region can be promptly found from inspection of (1.27). Let us consider separately the two cases $\theta_0 > 0$ and $\theta_0 < 0$.

Case (a): $\theta_0 > 0$ (Fig. 9)

For this case

$$\begin{aligned} D(\theta) &> 0 && \text{for } \theta > \theta_0 \\ D(\theta) &= 0 && \text{for } \theta = \theta_0 \\ D(\theta) &< 0 && \text{for } \theta < \theta_0 \end{aligned}$$

Therefore, the region of existence of the wave is given by

$$\frac{\pi}{2} > \theta > \theta_0 \quad (1.28)$$

It could be simple to check from (1.26) that the wave is attenuated in the z direction but increases in the x direction. This type of wave (not satisfying the radiation condition) is a "non-spectral" wave.

Case (b): $\theta_0 < 0$

In this case similar considerations show that the wave exists in the region $\theta_0 < \theta < \frac{\pi}{2}$ and it is attenuated in both x and z directions. This wave is therefore of "spectral" type.

From (1.25) it is apparent that for waves of type (a) and (b), β is respectively positive and negative. Consequently, (since we have assumed that along the interface the source feeds power in the z direction) the (a) type of wave is forward, and the (b) type is backward.

If we plot k vs β in a dispersion diagram (Fig. 10) it is possible to get information about leaky waves in a way analogous to that of surface waves. A bounded wave is one with $\beta \gg k$. In fact from (1.27) and (1.25), it can be established that in this case $b \simeq B > k$. The wave travels essentially at the interface ($\theta \simeq \frac{\pi}{2}$). In the Brillouin diagram this corresponds to a point of the type B or A of Fig. 10 (forward

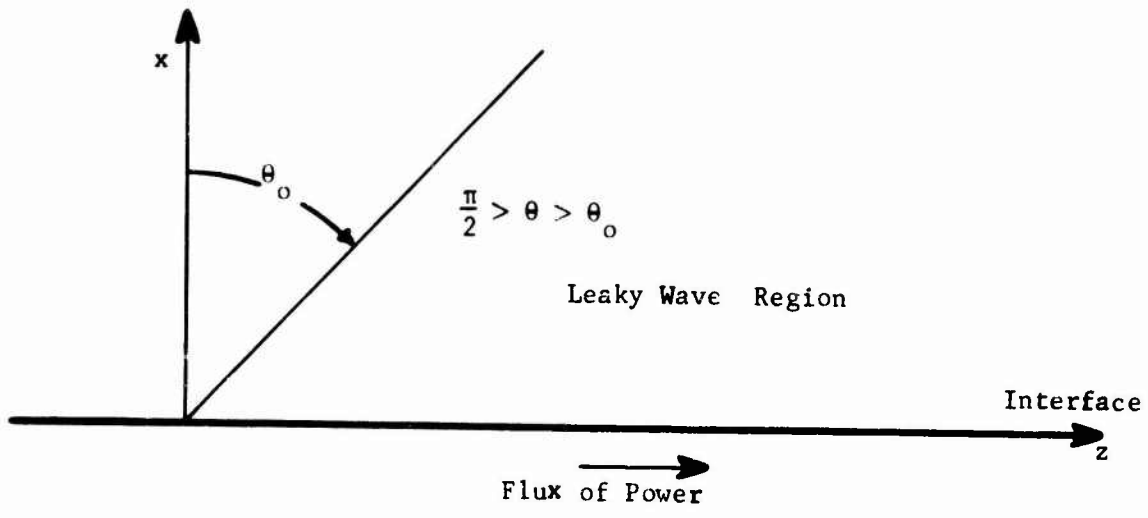


Fig. 9. Geometry of a leaky wave structure.

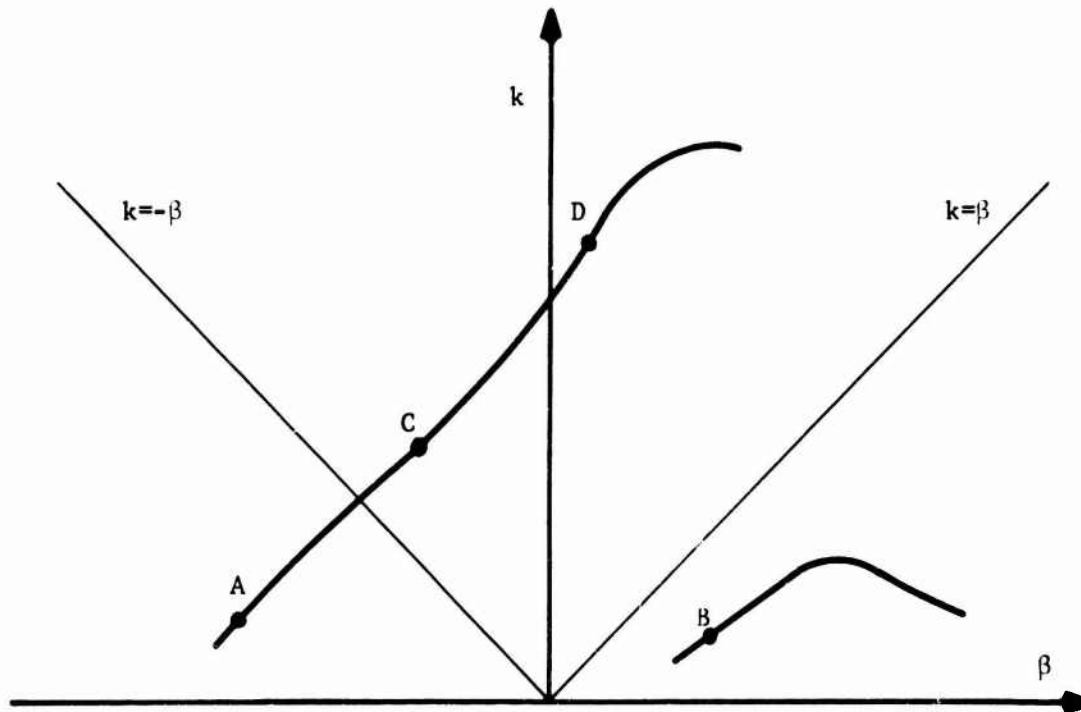


Fig. 10. Dispersion diagram for complex waves.

and backward slow waves). In the case that $\beta < k$ (points C and D) it can be shown similarly that the wave is essentially radiating. From the antenna design viewpoint this is very interesting since one can predict the radiating behavior of a given structure if the plot of k vs β on the Brillouin diagram is given. For example, if the representative point moves from a point of the type A, to points of the type C and D, it is possible to predict that the structure will begin to radiate effectively as a backfire antenna when the point crosses the line at -45° , then the squint angle of the beam will move toward broadside, and finally it reaches a zone where the antenna will radiate end-fire. Notice the importance of the straight lines $k = \beta$ and $k = -\beta$ which divide the zones of "fast" and "slow" waves.

For what follows, it is convenient to put in abscissae and ordinates of the dispersion diagram βa , and ka , where "a" is a characteristic dimension of the structure (Fig. 11). For example, if we are considering the propagation along a dielectric rod, "a" can be its radius. This modification of the dispersion diagram, mathematically trivial, is however conceptually very important and is the key for a qualitative understanding of tapered (conical) structures. If, as already mentioned, we assume that the structure is "slowly" changing its cross section we can assume that in every point ("approximately") its behavior is similar to that of a uniform structure with the same characteristic length "a". Therefore, we can apply the Brillouin diagram to tapered structures by considering k constant (i.e., for a certain frequency) and "a" as a variable. Suppose the dispersion pattern for the smooth structure is that one of Fig. 10. From it we can deduce that, for a fixed frequency (i.e., fixed k), the tapered version will be able to support a forward wave in the zone characterized by:

$$0 < ka < ka_1$$

or simply

$$0 < a < a_1$$

In the zone,

$$a_1 < a < a_2 \quad , \quad (1.29)$$

it will be able to support two forward waves and a backward wave. For

$$a_2 < a \quad ,$$

the only possible wave is a forward wave. Notice that for any wave propagating in the z direction there is a possible wave in the $-z$ direction.

1.3.5.3 Waves in Periodic Structures and Application to F.I. and L.P. Structures

The electromagnetic behavior of a periodic structure will now be considered. The basic tool for this study is given by Floquet theorem [23,24]. Essentially this

theorem states that in a structure which is periodic in the z direction with period d , if $\varphi(z)$ denotes any field component, then

$$\varphi(z) = e^{-jw_0 z} P(z) \quad (1.30)$$

where $P(z)$ is a periodic function of z with period d and w_0 is a constant wave number. Because of its periodicity, one may expand $P(z)$ in a Fourier Series

$$P(z) = \sum_{n=-\infty}^{\infty} P_n e^{-j \frac{2\pi n}{d} z} \quad (1.31)$$

If we put:

$$w_n = w_0 + \frac{2\pi}{d} n \quad (1.32)$$

we can write for the various terms of (1.31), making explicit the dependence upon x and t :

$$\varphi_n = P_n e^{j(\omega t - k_{tn} x - w_n z)} \quad (1.33).$$

with P_n a constant. Since the various space harmonics (1.33) must satisfy the wave equation, (1.17) and (1.24) must hold, and for each of the harmonics the treatment of the previous section can be applied. The real part of (1.32) (multiplied by d for convenience) will be written:

$$\beta_n d = \beta_0 d + 2\pi n, \quad (1.34)$$

Plotting $k d$ versus d we obtain a periodic diagram of the type of Fig. 12. It is clear from the expression of the propagation constant β_n that all the space harmonics have different phase velocities:

$$v_{fn} = \frac{\omega}{\beta_n} = \frac{\omega}{\beta_0 + \frac{2\pi n}{d}} \quad (1.35)$$

and the higher harmonic are slow waves. On the other hand, the group velocity is equal for all the harmonics:

$$v_g = \frac{\partial \omega}{\partial \beta} = \frac{1}{\frac{\partial \beta}{\partial \omega}} = \frac{1}{\frac{\partial \beta_0}{\partial \omega}}. \quad (1.36)$$

This can be expected since the space harmonics form a single physical unit which accounts for the wave in question and the group velocity is the speed of the energy carried by the wave.

An interesting point is that if w_0 is a complex, all the w_n are also complex with the same attenuation constant α (as it can be immediately seen from eq 1.32). However,

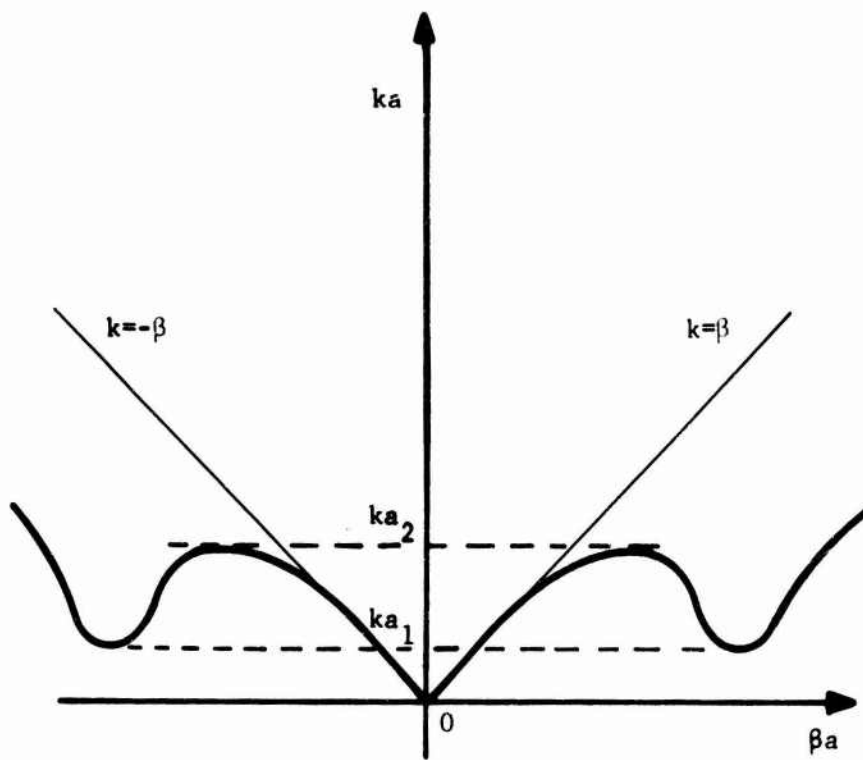


Fig. 11. Modified dispersion diagram.

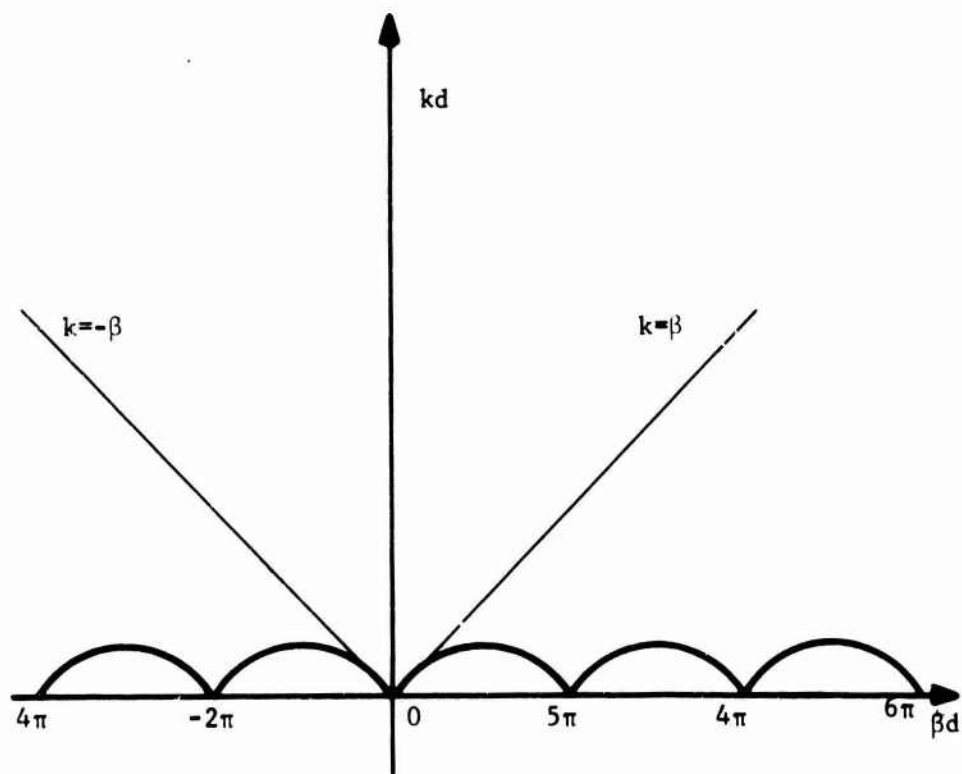


Fig. 12. Dispersion (or Brillouin) diagram for a periodic structure.

the physical interpretation of this attenuation term is different for the various harmonics, since some of them are essentially bounded waves and other essentially radiating according to the discussion in the previous section. For example, suppose that for a certain frequency the harmonic $n = -1$ is represented by the point A_{-1} in the $\beta d, kd$ plane (Fig. 13). This represents a leaky wave which, since A_{-1} is located in the zone above the $\pm 45^\circ$ lines, is essentially radiating. The points A_{-2}, A_0, A_1 , etc. which (according to eq 1.32) represent space harmonics, correspond instead to waves essentially bounded (they are below the $\pm 45^\circ$ lines). They are strongly attenuated in the transverse direction (as it could be seen from eq 1.24), and for very large n in the transverse attenuation constant tends to β_n .

A basic point which helps explain the manner of log-spiral and log-periodic antennas, is that under certain hypothesis (approximately verified in some practical cases) we can deduce from the Brillouin Diagram that the first radiating wave is a backward wave. This is a well known experimental feature which is typical for this kind of structure (which radiate toward the feeding point). Suppose that β_0 is proportional to the frequency; and larger than the free space wave number:

$$\beta_0/k = \text{constant} > 1 \quad . \quad (1.37)$$

Equation (1.37) applies if the antenna behaves exactly as a delay structure. This hypothesis is approximately verified for helical structures. Let us consider what happens when the frequency is increased. β_0 and all the space harmonics of order $n > 0$ are non radiating (see eq 1.34) since their wave numbers are larger than k , i.e. they are forward slow waves. On the other hand, the wave number of the backward wave of order $n=-1$,

$$\beta_{-1} = \beta_0 - \frac{2\pi}{d} \quad , \quad (1.38)$$

increases with k , (and β_0), and reaches a value equal to $-k$ for

$$\beta_0 - \frac{2\pi}{d} = -k \quad (1.39)$$

A further increase of the frequency makes the $n=-1$ wave change character from backward slow wave to backward fast wave, i.e. a radiating wave since $\beta_{-1} > -k$, and the point A_{-1} representing the wave crosses the -45° line in the Brillouin Diagram. A further increase of the frequency eventually makes other harmonics radiate, also. If a slowly-tapered periodic structure is not considered, following a line of reasoning similar to that developed in the end of Section 1.4.2, we recognize that the above discussion can be applied to this case, as well. Considering the diagram of Fig. 12, it is clear that we can move to the various parts of the diagram either by

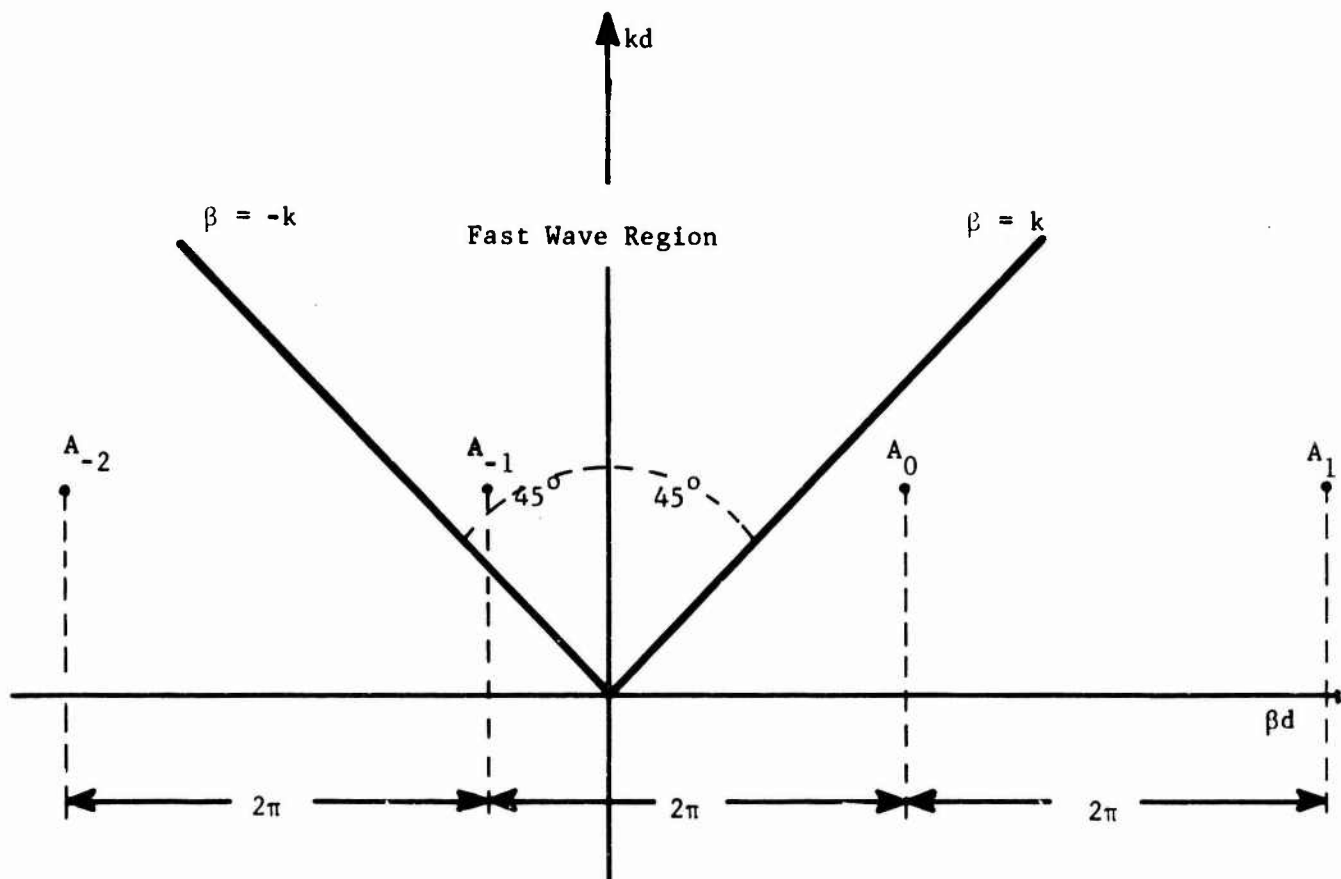


Fig. 13. Different character of the space harmonics.

changing k with d constant (periodic structures) or by keeping k constant and changing d (the spatial period being proportional to the transverse dimension. A change of d means simply that we consider different points of the antenna. For example, if the structure under analysis is a conical spiral (the tapered version of the helix) the above discussion shows that going away from the apex of the cone (the feeding point) a slow forward wave zone is found, followed by a zone where a backward radiating wave is present, which is responsible essentially for all the radiative phenomena on the structure [25,26].

In conclusion, when the k - β plot is known, an invaluable tool for the investigation of long radiating tapered structures is available. It allows prediction of the types of waves which will be present. However, all pertinent information cannot be obtained by simple inspection of this diagram. For example, no information is available about the relative strength of space harmonics. For example, in the log-spiral case discussed above, the existence of a fast backward wave in a certain zone of the structure can be predicted, but it is not clear whether this wave efficiently converts the guided energy into radiating wave, or whether the radiation is due to more than one space harmonic. These questions can be answered only by a complete solution of the electromagnetic problem.

We terminate this section by recalling that the above approximate qualitative discussion has been made in terms of radiative behavior. It is possible also to build transmission line models of the antenna which allow prediction of the input behavior of the structure (i.e., impedance, standing-wave ratio on the feeding line). The proposed model will be discussed in the next chapter in connection with log-periodic structures.

1.3.5.4 Use of Dispersion Diagram for Log-Spiral Antennas

The periodic counterpart of the log spiral is the helix, and the analysis of this structure is by no means simple. However, extensive study has been performed because of its importance to traveling-wave tubes. A solution of the problem was given by Sussner [27]. The most important result of his analysis as far as the applications of log-spiral antennas are concerned, is that the propagation constant along the helix, in extended regions of the Brillouin Diagram, turns out to have an approximate expression which is surprisingly simple and conforms closely with intuitive reasoning. In fact, referring to Fig. 1, for the harmonic of zero order, the following relationship holds approximately:

$$k = \beta_0 \cos\psi \cos\theta_0, \quad (1.40)$$

and it is very simple to see that this can be interpreted as a wave progressing at the speed of light along the helix. Since (1.40) is in the form (1.37) all the

deductions made in 1.4.3 can be applied; in particular the antenna will radiate a backward endfire beam. Let us investigate this question in detail. Let $\rho = r \sin\theta_0$ (Fig. 1) be the radius of the circle, cross section of the cone of the antenna (i.e. $2\pi\rho$ is the length of the circumference on the plane at a distance $r \cos\theta_0$ from the feeding point). In the helix theory it is customary to modify the usual Brillouin Diagram by plotting $\frac{k\rho}{\tan\psi}$ vs $\frac{\beta\rho}{\tan\psi}$. In a similar way for the spiral we will plot $\frac{k\rho}{\tan\psi} \cos\theta_0$ vs $\frac{\beta\rho \cos\theta_0}{\tan\psi}$. With this normalization the period of the Brillouin diagram is equal to unity. For the monofilar helix it takes the form in Fig. 14. We see that the relation between β and ρ follows the law indicated by (1.40) up to the neighborhood of the point A where the law of dependence changes rapidly (and the latter fact could be explained by resorting to the theory of coupled modes [28]). As a first approximation, we can assume that the dependence of k on β in the radiating region can be approximated by segments of straight lines. For a bifilar helix, (with the two wires excited in opposition of phase) which corresponds to the widely used two-arm antenna, the approximate Brillouin Diagram takes the form of Fig. 15. This is due to the fact that all the harmonics of even order are zero [29]. In order to explain the radiation mechanism, we only need to consider the $n=1$ and $n=-1$ harmonics.

A peculiarity of the Brillouin Diagram for the two-arm spiral, Fig. 14, is that the curve for the lowest order forward harmonic starts at the point $k=0$; $\frac{\beta\rho \cos\theta_0}{\tan\psi} = 1$. In other words, the $n=0$ harmonic has zero amplitude. This may seem strange at first glance, but it is quite logical since, even for frequencies tending to zero, the difference of phase between the two arms is still 180° . From the study of the Brillouin Diagram the following quantities can be obtained:

- (a) The approximate position of the beginning of the active zone
- (b) The phase shift between two successive turns.

If on Fig. 15 we move on the line from A_1 to A_2 , this corresponds on the antenna to moving away from the feeding points. The ordinate of the point A_2 (which can be found with simple geometrical consideration (by approximating A_1 and A_2 with a straight line) gives the value of ρ which in our approximation corresponds to the beginning of the active zone. We see, from the Brillouin Diagram, that when the point representing the first forward harmonic has reached A_2 , the point corresponding to the first backward harmonic reaches A_3 and afterwards the $n=-1$ harmonic begins to radiate. This mechanism has already been discussed in Section 3.3.3 and will not be repeated here. The ordinate of A_2 corresponds to

$$\frac{2\pi\rho}{\lambda_0} = \frac{\sin\psi \cos\theta_0}{1 + \cos\psi \cos\theta_0} \quad (1.41)$$

where λ_0 is the free space wavelength. For values of pitch angle in the usual range ($70^\circ - 80^\circ$) this means that the active zone begins at a distance from the feeding point

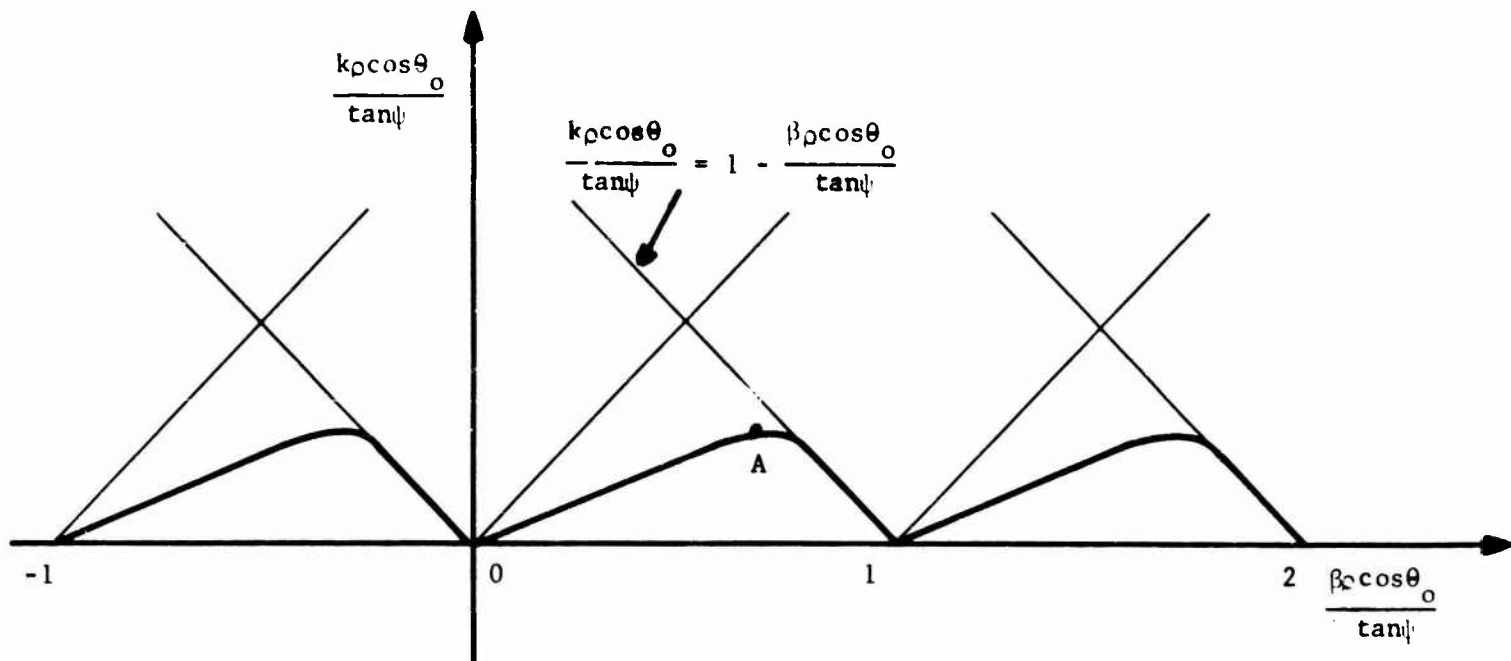


Fig. 14. Brillouin diagram for monofilar helix.

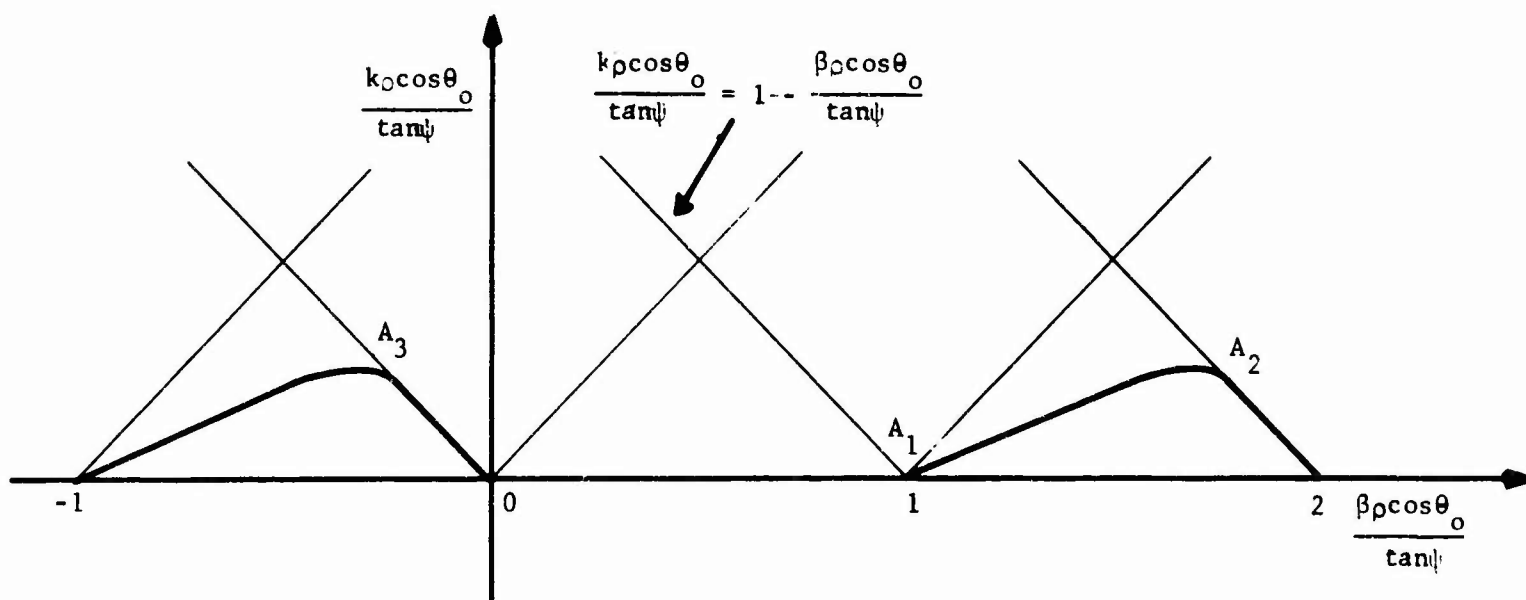


Fig. 15. Brillouin diagram for bifilar helix.

where the circumference section of the conical surface with a plane orthogonal to the axis is less but not greatly different from the free space wavelength. The propagation constant of the first forward harmonic along the axis of the cone is given by

$$\beta_1 = \frac{2\pi}{\lambda_0} + \frac{4\pi}{\lambda_0 \cos\psi \cos\theta_0} \quad (1.42)$$

The pitch distance of two terms (of the same arm) at the beginning of the active region is:

$$p = \lambda_0 \frac{\cos\psi \cos\theta_0}{1 + \cos\psi \cos\theta_0} \quad (1.43)$$

An inspection of Brillouin Diagram gives the phase constant of the (radiating) backward leaky harmonic in the active zone

$$\beta_{-1} = -\frac{2\pi}{\lambda_0} \quad (1.45)$$

(1.45) clearly shows that the radiation is backward endfire.

1.4 EXPERIMENTAL WORK ON LOG-SPIRAL ANTENNAS

1.4.1 Two-Arm Spirals

As we mentioned in Section I, Rumsey was the first to advance (in 1955) the theory that an antenna constructed in the form of an equiangular spiral would be frequency independent with regard to pattern and impedance, and proposed that the characteristics of finite size antennas be investigated. The first practical implementation of this structure was made at the University of Illinois in 1955 [30]. Two forms of the antenna were used, the plane conductor antenna, i.e., metallic arms suspended in free space, and the slot antenna, which consists of spiral slots cut in large conducting screen. These antennas, of course, had a bidirectional pattern. The technique of feeding the antenna with what can be called an "infinite balun" was used (probably for the first time); this method consists of soldering the coaxial feed cable to the ground plane (Fig. 16). One of the two arms is connected to the generator (in transmission) or to the receiving load (in reception.) The inner conductor of the coaxial of the feed arm is connected to the outer conductor of the coaxial of the other arm. A perfect balance is in this way obtained (at least for the frequencies high enough to cause the gap to be a significant part of a wavelength. Fig. 17 illustrates radiation patterns (from [30]) in two planes orthogonal to the antenna plane (See Fig. 1 for geometrical representation). The antenna has a remarkably constant behavior with frequency in a band of 20:1. Notice the excellent circular polarization on the peak of the radiation beam. Because of the bi-directionality of the radiation, these structures are not very practical and these early experiments have mainly an historical interest. At

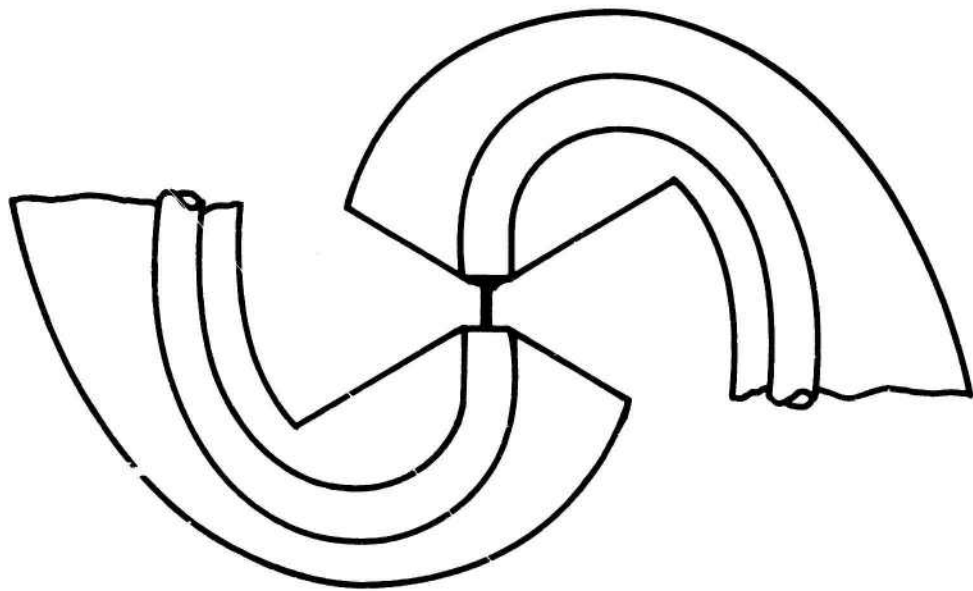


Fig. 16. Spiral antenna feeding zone with "infinite balun."

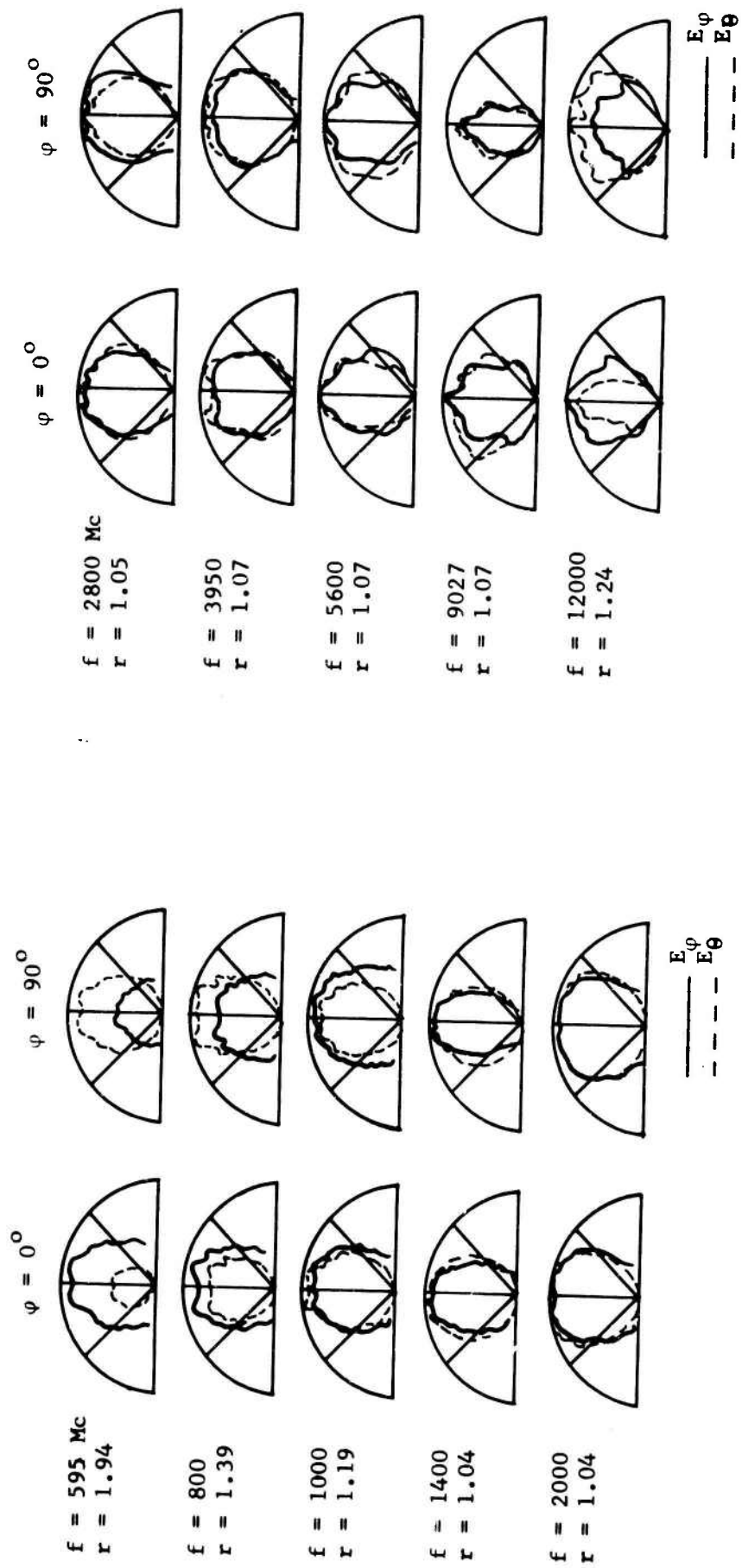


Fig. 17. Radiation patterns of a typical planar spiral antenna (r = axial ratio of the polarization ellipse on the peak of the radiation pattern).

that moment, however, they were very significant, because they showed that a practical (i.e., truncated) structure behaved correctly, provided the diameter of the antenna was larger than about one-half wavelength.

The spiral conical antenna, which gives a unidirectional radiation, began to be experimentally studied in 1958 [32]. For included cone angle less than about 45° , the radiation is confined to one broad circularly-polarized lobe with maximum radiation toward the apex of the cone. As in the planar case, the antenna is a balanced structure with the feed voltage applied between the two arms at the apex of the cone. Dyson tested many different structures. The most interesting for its simplicity and ease of construction is perhaps that one of Fig. 18; the cables of the infinite balun constitute the radiating structure, with the feed cable forming one of the arms. At the apex the center conductor is carried over and bonded to the outer braid of a dummy cable which forms the opposite arm of the antenna. The cables are mechanically supported by polystyrene ribs. Rigorously speaking, the antenna is not frequency independent. However, the experimental data show that the behavior is rather insensitive to the width of the arms. Fig. 19. illustrates the radiation patterns and SWR of this structure. In [31] it was reported that decreasing the ψ angle (Fig. 1) from 76° to 45° caused the beamwidth to change from around 70° to approximately 180° .

The effect of the angle θ_0 on the beamwidth is rather minor, while a small θ_0 ($10^\circ - 20^\circ$) improves the front-to-back ratio. Dyson obtained a front-to-back ratio of about 15 db for $\theta_0 = 10^\circ$. The input impedance does not show a definite trend as a function of ψ . It increases as the arm width decreases, passing from values around 80 ohms (for very large arms) to about 300 ohms (for very small arms). For self-complementary structures (i.e., equal arm width and spacing) the measured values are close to 190 ohms (a value which can be shown to be characteristic of all self-complementary structures).

It is worth briefly mentioning that measurements of the near field of the spirals were made to determine whether the approximate theory sketched in Section 1.3.5 reflected the physical situation, [33]. A small magnetic loop was used to measure the relative amplitude and phase of the current flowing along the conductor of the antenna. The results indicated:

- (a) a rapid decay in the amplitude over the first portion of the structure, and
- (b) the average phase velocity along the arms in the initial region was always equal to or slightly greater than the speed of light. The second result confirms the result of the approximate analysis of Section 1.4.

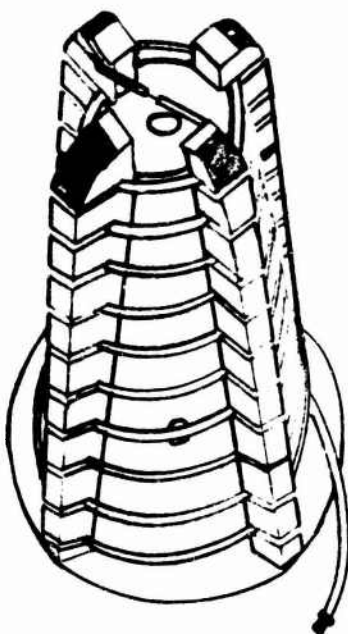


Fig. 18. A mechanically simple form of conical log-spiral antenna.

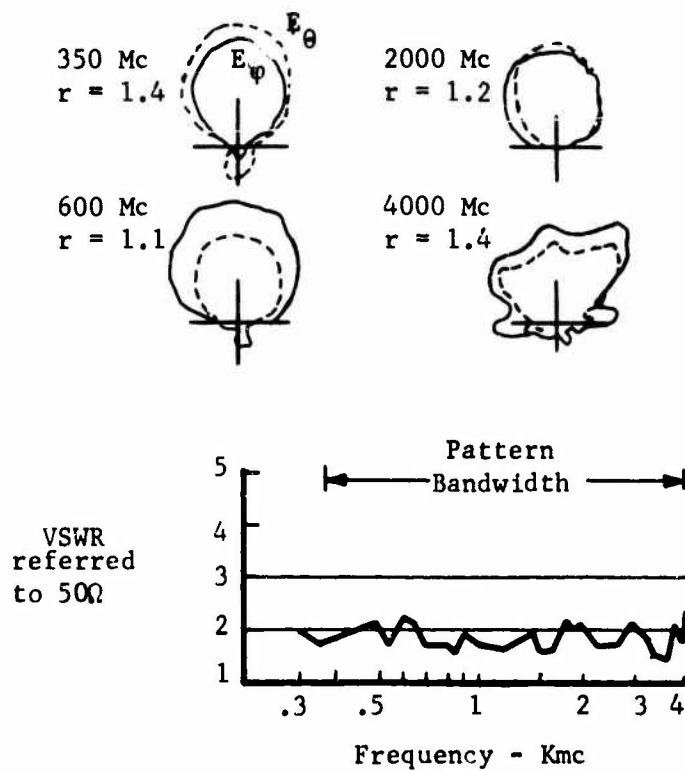


Fig. 19. Radiation patterns of the conical spiral of Fig. 18.

It is possible to modify the log-conical geometry, making it simpler to fabricate. Tang has proposed a "poligonal" form of log spiral [34]. This type of antenna is non-frequency independent but is rather log-periodic. However, the geometrical and electrical characteristics are very close to that of a true log-spiral (Fig. 20 and 21). For the same pitch angle, the square antenna presents characteristics practically identical (with respect to radiation pattern and impedance) to the conical one.

1.4.2 Miscellaneous Modifications of the Basic Geometry

The basic two-arm conical structure is satisfactory for many applications, when a moderate gain is required with an end-fire type radiation, and when the size of the antenna is not a problem. To cope with special requirements, a number of modifications of the basic structure has been proposed; some of these will be briefly considered.

It is desirable in some cases to have a "conical" or beacon type beam. The log-spiral antennas properly modified, are ideally suitable for this kind of application. A "conical" beam can be obtained by constructing an antenna with more than two spirals and symmetrically connecting these arms to provide a suppression of the radiated fields on the axis of the antenna [35]. The arrangement used in a four arm spiral antenna is shown in Fig. 22. Typical patterns which have been obtained are shown in Fig. 23. The angle α of Dyson corresponds to ψ , in the notation we used throughout this report. Increasing the pitch angle causes the angle of rotationally-symmetrical radiation with respect to the horizon to increase also. For $\psi = 45^\circ$, we have a coverage of "azimuthal" type. The SWR is reported to be less than 2:1 over a band of about 10:1 (the pattern bandwidth).

Another type of (planar) log-spiral antenna with very similar type of coverage (and having the advantage of the possibility of being flush-mounted) has been proposed by Mei and has already been described in Section 1.3.3.

Arrays of spiral antennas have been studied in an effort to devise a radiating structure having bandwidth capability similar to that of a conical antenna, but greater directivity and gain. It is possible to do this to a limited extent with log-spiral antennas. The limitation arises because the frequency-independent characteristics can be preserved only by making the vertices of the cones coincident, Fig. 24. In this way, the phase center of the component's antennas lie on a circle. Therefore, a large phase error is introduced. Naturally, this effect is present only for arrangements of more than two elements. It is possible to arrange the elements in a parallel fashion; but, of course, in this case the antenna has a beamwidth (and a gain) which varies with the frequency. In order to predict the input SWR of these structures over the band it is necessary to know the mutual impedances of two spirals for different spacings. An exhaustive experimental analysis has been performed by Dyson who has given the mutual coupling between conical log spirals for many different geometries [36]. The main results of this work are the following:

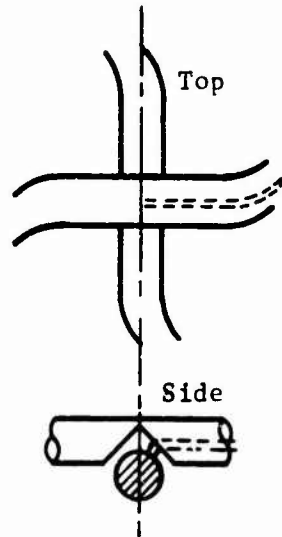


Fig. 22. Feeding system of the four arm spiral.

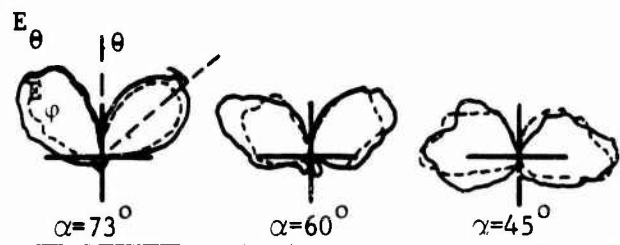


Fig. 23. Radiation patterns of the four arm spiral.

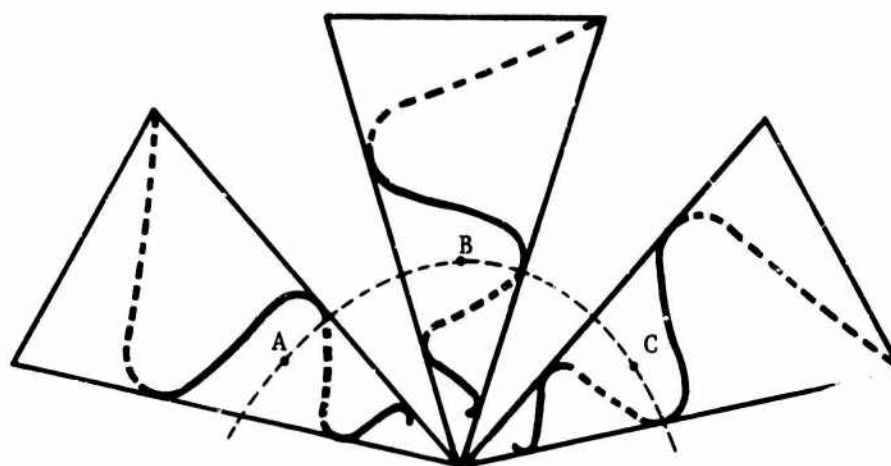


Fig. 24. Frequency independent array of log-spiral antennas (A, B, C phase centers).

- (a) the coupling among the elements in a parallel (therefore, frequency independent) array is low, of the order of -30 db or greater for element-to-element spacing of $\frac{\lambda}{2}$ or more; this coupling varies with rotation, being a minimum for a 90° rotation between elements;
- (b) coupling is on the order of -20 db in the conical array; minimum coupling for 15° cones occurs at an array angle of approximately 35° to 50° depending upon the spiral angle ψ ;
- (c) changes in the basic element pattern caused by the presence of other elements are minor for an element-to-element spacing of at least one-half wavelength and consists mainly of a broadening of the element pattern beamwidth in the plane of the array; and
- (d) a good approximation to the array pattern of small arrays can be obtained by using the pattern of the isolated element.

Before concluding this survey of the various miscellaneous structures derived from spiral antennas, we will briefly mention some attempts to reduce the size of conical spirals. Some experimenters loaded log spiral conical antennas with ferrite in various ways [37]. One of the techniques used consisted in loading the two arms of the spiral with ferrite layers. Also loading with a complete cone of ferrite coaxial with the antenna has been tried, with the antenna located in free space and in a cavity open in a ground plane. It is reported that a reduction of about one-half the size of the equivalent air antenna can be expected. However, the loading produced a drop of the efficiency to 13% for the antenna in the cavity and 23% for free space antenna and the temperature dependence of ferrite was found very critical.

Slightly more successful attempts at reducing the size of the antennas have been obtained with log-periodic structures (see Section II).

1.5 DESIGN OF FREQUENCY-INDEPENDENT ANTENNAS

The analysis of log-spiral structures is very difficult. However, the design of an equiangular antenna is usually a relatively simple matter. This is because the radiation pattern and impedance are not critically dependent upon the geometrical parameters of the structure. In other words, although in designing an antenna of this type, it is difficult to predict exactly the electrical parameters, the approximate characteristics can be predicted reliably. Thus there is generally no serious problem in designing a log spiral, at least if the antenna specifications are not unusually stringent. Difficulty may arise if, for some special purposes, the beamwidth or the impedance must be accurately specified over a wide frequency band. As an example, this case occurs in some electromagnetic surveillance systems, when it is intended to find the direction of a source by beam-comparison techniques. The development of antennas having controlled beam shapes over a large band can require a

considerable amount of development work (experimental).

We will now sketch briefly the design procedure for a log-spiral antenna. Suppose that the given specifications are:

- (a) a frequency band of operation between f_1 and f_2 ;
- (b) a nominal impedance with permissible deviations over the band;
- (c) a nominal beamwidth, with permissible deviations over the band.

Frequency Band

We assume that in order to have a balanced input the technique of the infinite balun considered in Section 1.5.1 is adopted. The specification of minimum frequency, f_1 , establishes the maximum radius r_1 of the feeding region. As a reasonable value $r_1 = \frac{\lambda}{8}$, can be chosen where λ_1 is the free space wavelength. Notice that this specification can result in practical difficulties from the point of view of mechanical tolerances and of the possibility of arcing, if the frequency is very high (e.g., in the microwave spectrum). In some cases particular types of miniaturized coaxial cable must be used, since the arm width at radius r_1 must be at least equal to the coaxial cable diameter d . For ease of construction, it is generally convenient to use the coaxial itself as the arm of the spiral (according to the technique considered in Section 1.4.1). The overall size of the antenna will be determined by the upper frequency of operation f_2 . The diameter of the cone base will be chosen from $\frac{1}{2}$ to 1 times the wavelength λ , to prevent spoilage of the beamwidth and of the circular polarization experienced at the lowest frequency of the band. The lower value of cone base may be used at higher values of ψ ($70^\circ - 80^\circ$). With this choice, the ratio between r_1 and r_2 (vector radii corresponding to spiral points closest and farthest from the apex of the cone, respectively) is actually larger than f_2/f_1 , because of the finite size of the active zone. With this choice of parameters, the maximum axial ratio of the polarization ellipse on the peak of the beam can be expected to be about 2:1.

Impedance

The impedance of the antenna can be controlled to a limited extent by varying the width of the arms. As mentioned in Section 1.5.1, it is possible to obtain a variation in the range from 80 to 300 ohms. When the coaxial cable is used as the arm of the spiral, an average impedance of about 200 ohms can be expected. For proper choice of a line of suitable characteristic impedance, the standing-wave ratio can always be less than 2:1. The impedance is rather insensitive to variations in ψ and ϵ_0 .

Beamwidth

The geometric element which provides the main control over the beamwidth is the pitch angle ψ . Higher values of ψ (spiral closely wound) correspond to narrower

half-power beamwidths. Proper design can result in beamwidths of about 70° and 180° for values of ψ equal to 75° and 45° , respectively, as mentioned in 1.5.1. In the last case, an almost hemispherical coverage is obtained. The angle θ_0 controls the front-to-back ratio; for small θ_0 ($10^\circ - 15^\circ$), a front-to-back ratio of 15 db can easily be obtained.

It is to be emphasized again that the development of an antenna of this type is essentially experimental. Naturally, the theory is important to give the basic criterion of design through the understanding of the radiation mechanism of the structure. However, at the present state-of-the art, the theory supplies only guidelines of a qualitative nature.

BLANK PAGE

II. LOGARITHMICALLY PERIODIC ANTENNAS

2.1 GENERAL CONCEPT OF LOG-PERIODIC ANTENNAS

Logarithmically periodic antennas are the class of extremely wideband antennas receiving wide use. Modifying the basic idea of Rumsey of specifying antenna geometry solely by angles, DuHamel and Isbell introduced a new principle in broadband antenna design, yet closely related to the frequency-independent antenna concept. They considered a class of structures scaling to themselves log periodically, rather than in a continuous manner [38]. In Fig. 25, a typical log periodic antenna is shown. Two metal sheet structures are fed against each other by a generator placed between their vertices. The four sets of teeth are defined by similar curves expressed in polar coordinates as

$$\theta = f(\log r) \quad (2.1)$$

where f is a periodic function of its argument. From (2.1) it can be seen that the structure expands with r , but is always angularly limited between the maximum and the minimum value of θ . The simplest of this type of geometry is defined by the equation (Fig. 27):

$$\theta = \sin(\log r), \quad (2.2)$$

corresponding to an expanded sinusoid structure, which has been used as a practical antenna. The periodic functions defining the structure will be in general more complicated. For example in Fig. 26 the curves defining the upper half structure of Fig. 25 are plotted vs $\log r$. If

$$\tau = \frac{R_n + 1}{R_n} \quad (2.3)$$

(independent of n) is the distance from the vertex to the outer edge of the tooth, it is seen that period of the curve is equal to $\log(1/\tau)$. From (2.3) it is apparent that all similar sets of dimensions form a geometric sequence with the same geometrical ratio τ . The geometry is clearly not "defined by angles" as discussed in 1.2, and the antenna, therefore, is not frequency independent. However, a scaling of a factor τ , with n any integer, transforms the structure into itself. Therefore, all the electrical characteristics of the antenna will remain unchanged when the frequency is scaled by the factor τ_n . In the case

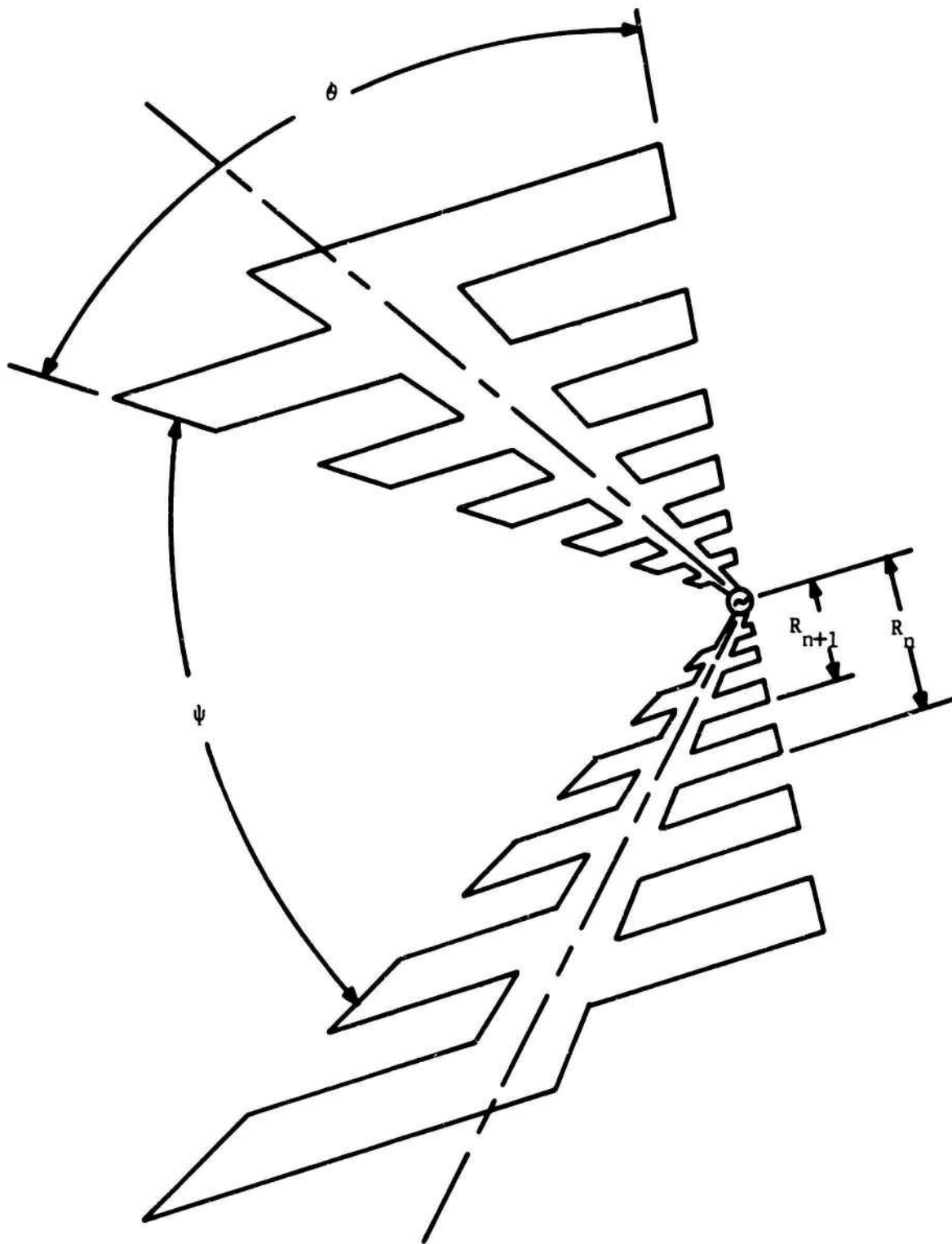


Fig. 25. Saw tooth log periodic array.

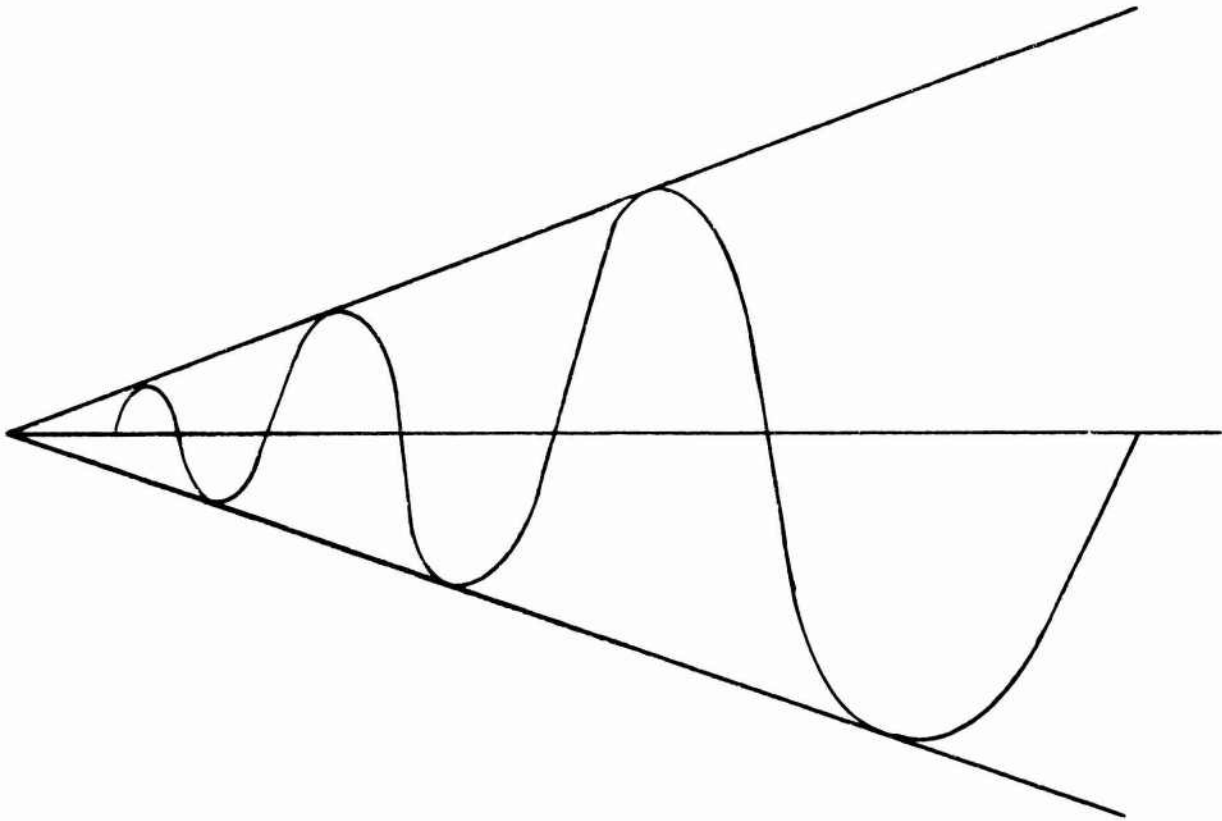


Fig. 26. Sinusoidal zigzag antenna.

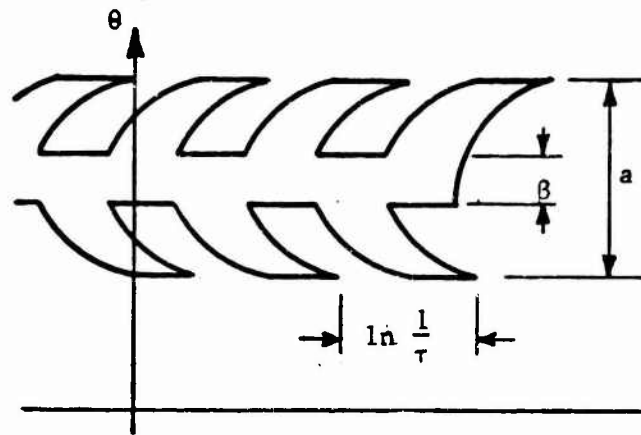


Fig. 27. Plot of θ vs $\ln r$ for one of the component structures of Fig. 25.

of structures of the type of Fig. 25, because of their special left-right symmetry the period of the impedance curve is $\frac{1}{2} \log 1/\tau$ rather than $\log 1/\tau$. The radiation pattern has instead a periodicity of $\log 1/\tau$. If we assume that the variation of impedance and radiation pattern is not too large over one period of the frequency, the structure may be considered frequency independent for all practical purposes.

Much of the discussion of the previous chapter concerning frequency-independent antennas can be applied to log-periodic structures (Section 1.4.2 and 1.4.3). In particular, it can be seen that the log-periodic geometrical condition is necessary; however, it is not sufficient, and does not guarantee that the current on the structure dies off rapidly after a certain zone (the active zone) where an efficient conversion to radiating modes must take place. This attenuation is necessary to avoid on frequency-dependent end effects (as discussed in Section 1.2).

In summary, a log-periodic antenna is an antenna which is not rigorously frequency independent, since if it is expanded by a scale factor K the resulting structure is in general not self congruent to the original one. However, for an infinite discrete set of values of K :

$$K_i = \tau^i$$

the structure is scaled in itself. The electrical behavior of the structure is therefore the same for frequencies having the ratio τ^i . It is therefore clear that if τ is close to unity, the behavior with frequency is not far from that of a truly frequency-independent structure.

2.2 STATE OF THE THEORY OF LOG-PERIODIC ANTENNAS

2.2.1 Mathematical Models

The theory of log-periodic antennas is still relatively undeveloped. Not a single structure has been solved exactly and the only general approach for an analytical study is the one outlined in Section 1.3.5. The structure is considered as "slowly" expanding. Its periodic counterpart is analyzed (in an exact or an approximate manner) and it is in this way possible to determine its local properties. In particular, from the knowledge of the dispersion diagram the location of the active zone can be determined. However, it is not a simple matter to determine the Brillouin diagram for practical structures. Section 1.3.5.3 contains a discussion of the types of waves an open periodic structure can support. Clearly, such a treatment can be applied to the present case.

The analytical works on log-periodic antennas can be loosely grouped in four broad different classes:

- (a) Exact analysis of very simplified mathematical structures. Although the results cannot be applied directly to practical problems, they can give a qualitative insight on the nature of the phenomena.
- (b) Approximate analysis of a periodic array of dipoles (as a periodic counterpart of the log-periodic array of the same type of elements).
- (c) Approximate analysis of the "interior" problem (mathematically modeling the antenna as a loaded line). This approach is useful for predicting the impedance properties and the location of the active zone, (but not the radiation properties).
- (d) Numerical analysis of the interior and exterior problems of the exact structure idealized as a bipolar transmission line loaded with dipoles of different lengths.

Carrel, in a beautiful and exhaustive paper followed the approach (d). His numerical analysis of the electromagnetic problem is not based on the concept of the periodic counterpart and the work (which will be discussed in Section 2.3) is therefore somewhat atypical.

The above approaches will be respectively considered in Sections 2.2.2, 2.2.3, and 2.2.4.

2.2.2 The Sinusoidally Anisotropic Surface

In Subsection 1.3.2, we saw that a special type of anisotropic plane surface was adopted as a mathematically tractable model for the planar spiral antenna. Following a similar idea, a reasonably simple model for a log-periodic antenna was devised by Rumsey, which, although extremely idealized, still explains some of the features experimentally observed [39].

If we consider the periodic counterpart of the simple structure depicted in Fig. 27, we obtain a sinusoidal wire. A mathematically simpler structure, less difficult to analyze, is obtained by considering a surface made of an infinite number of sinusoidal wires infinitely close together, in such a way as to form an anisotropic surface with sinusoidally variable properties. An approximate physical realization can be obtained by using coplanar sinusoidal metal strips as in Fig. 28.

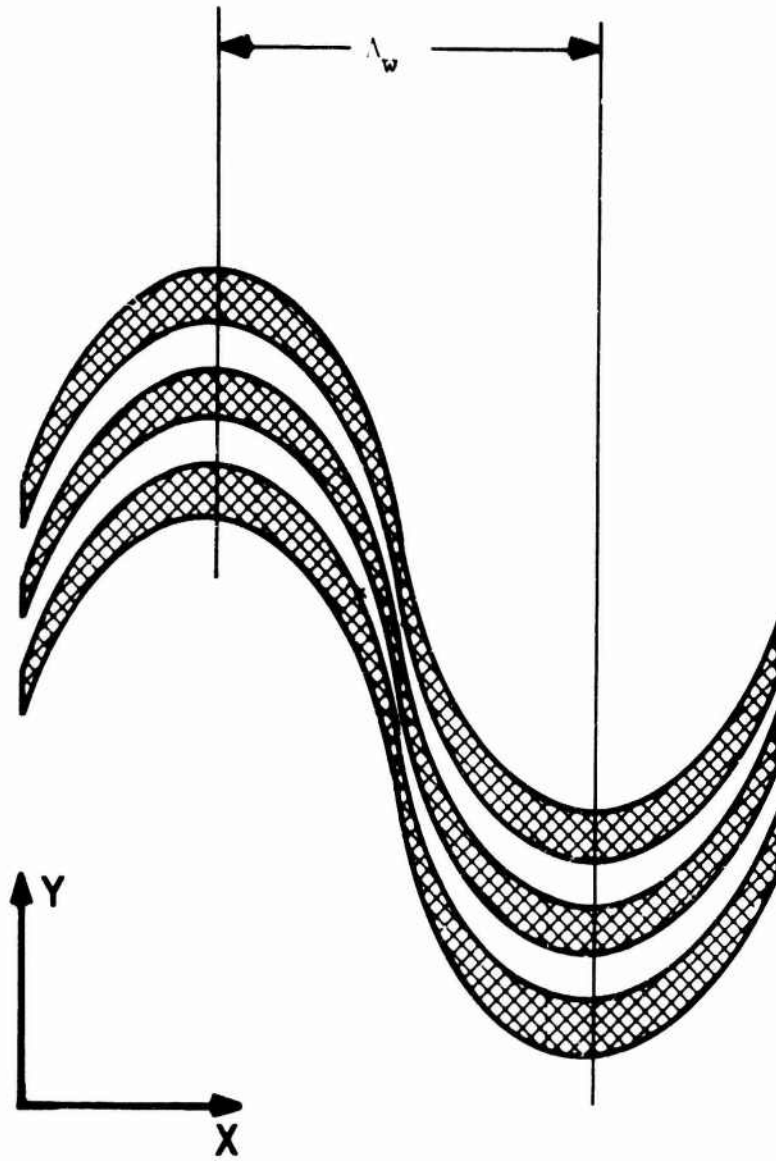


Fig. 28. Sinusoidally anisotropic surface.

Many of the considerations developed in Subsection 1.3.2 are applicable to this structure. For example if \underline{t} is a unit vector in the direction of the wires, it follows immediately that the same boundary conditions apply to \underline{E} and \underline{H} (with the same meaning of the symbols of Subsection 1.3.2)

$$\underline{E}_t \cdot \underline{t} = 0 \quad (1.4)$$

$$\underline{H}_t \cdot \underline{t} = 0 \quad (1.5)$$

It is possible to find a solution of the type (1.6) or (1.4), which in accordance with the discussion of Section 1.4.3 must be in the form of a Floquet series. Only an outline of this type of approach will be included here. By introducing the Floquet's series for the electric (or the magnetic) field and imposing the boundary condition, a recurrence formula is obtained relating the $n-1$, n , and $n+1$, amplitudes of the space harmonics. This recurrence formula can be thought of as an homogeneous system of infinite equations in an infinite number of unknowns. The coefficients of the system depend upon the propagation constant. In order for the system to have solutions it is necessary to equate the (infinite) determinant to zero; thus, an equation for the propagation constant is obtained. It is possible to show that the convergence is very rapid, or in other words, the infinite determinant can be replaced by another one having a finite number of rows [39]. We then obtain an equation which in the surface wave zone can be numerically solved in a reasonably easy way. In the leaky-wave region, the numerical solution is more difficult. However, drastic simplifications are obtained in both the cases of slightly-curved or extremely-curved wires. In this latter case, when the free-space wavelength is much smaller than the wavelength Λ_w of the wires (see Fig. 28), an extremely high attenuation occurs (of the order of hundreds of db per Λ_w). This attenuation occurs both in the slow-wave and fast-wave frequency regions. Therefore, from this treatment it does not seem easy to determine whether the attenuation will be caused by slow-wave stop-band reflection, or by leaky-wave radiation.

We will not discuss longer this mathematically interesting approach. We will only mention that a subject of current research at the University of California is the analysis of propagation on two parallel anisotropic sinusoidal sheets of the type considered in this subsection. This structure is a highly idealized model of the antenna of Fig. 25, in the same way the single anisotropic plane is a model of the single-sheet structure.

2.2.3 The Periodic Array of Dipoles

It is very difficult to obtain the Brillouin diagram for periodic structures. In the case of the helix (Section 1.4.4) the analysis was drastically simplified by the possibility of assuming that the propagation along the structure occurred with a phase velocity proportional to that of the light, (see equation 1.37). Unfortunately, the only periodic structure for which this "constant slowness" property is approximately valid is the zigzag. The periodic structures corresponding to the antenna depicted in Fig. 25 pose analytical problems which are unsolvable at the present state-of-the-art.

A "non-constant slowness" structure which can be analyzed "almost" exactly is the dipole loaded transmission line [40]. Mittra and Jones considered uniform dipole arrays with non-reversed and reversed elements as shown in Figs. 29 and 30. The latter case is the periodic counterpart of an antenna which was invented by D. E. Isbell in 1958 [41] (Fig. 39). The technique they used for finding the k - β diagram is the following. It is clear that the structures of Fig. 29 and 30 are equivalent to transmission lines periodically loaded with a network described by an admittance matrix having a periodic property (Fig. 31). This matrix has an infinite number of terms (since we are dealing with an infinite periodic structure). It is apparent that the impedance Z' seen at a pair of terminals (for example $A A'$ of Fig. 31) is equal to the impedance seen at any other pair of terminals. Therefore, for a certain frequency and from the point of view of the phenomena on the transmission line, the circuit of Fig. 31 is equivalent to the one of Fig. 32 (i.e., to a line periodically loaded with mutually uncoupled bipolar networks). It is possible to compute these ϵ loads by simple circuit analysis. In order to do this, however, the mutual impedance among the dipoles must be calculated and this can be done by the well known induced e.m.f. method (see for example Ref. [43]). It is convenient to assume that any dipole is coupled to only a finite number of other dipoles. Let us limit ourselves, as a first approximation, to consideration of only the nearby elements. This means that in Fig. 31 the port n is coupled only with the port $n-1$ and $n+1$. Moreover, it is clear from the periodic character of the structure that the self and mutual impedances Z_{nn} , $Z_{n, n+1}$, $Z_{n, n-1}$ are independent of the subscript n . From this it can be deduced that in order to find the propagation constant of the loaded line, we have only to solve a transcendental equation, obtained by equating a third order determinant to zero. Of course, it is possible to improve the approximation by using a larger number of mutual impedances, in which case many values for the propagation constants are

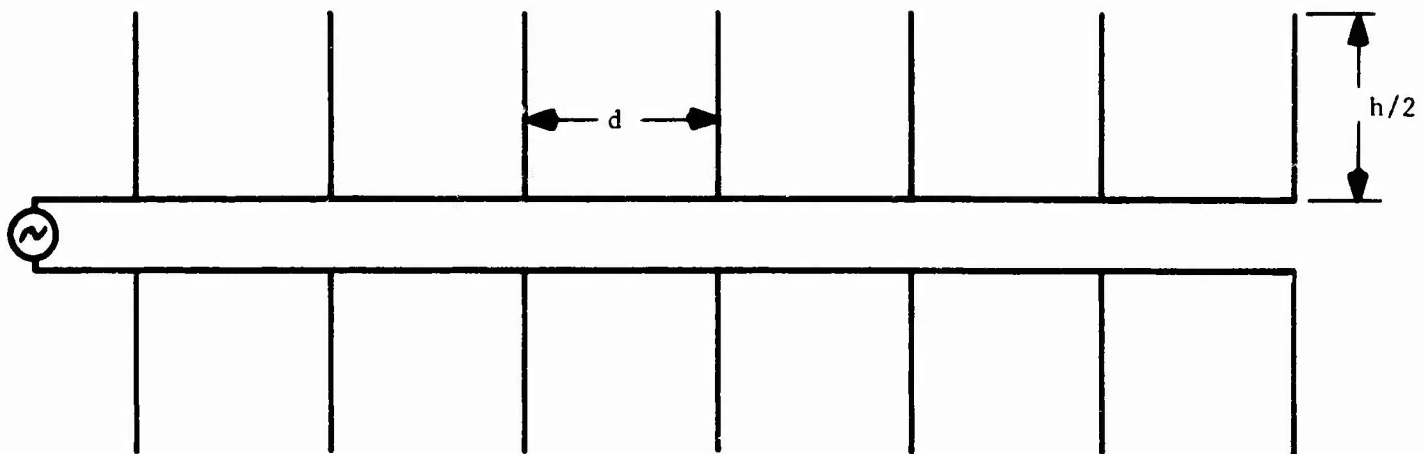


Fig. 29. Unreversed element uniform dipole array.

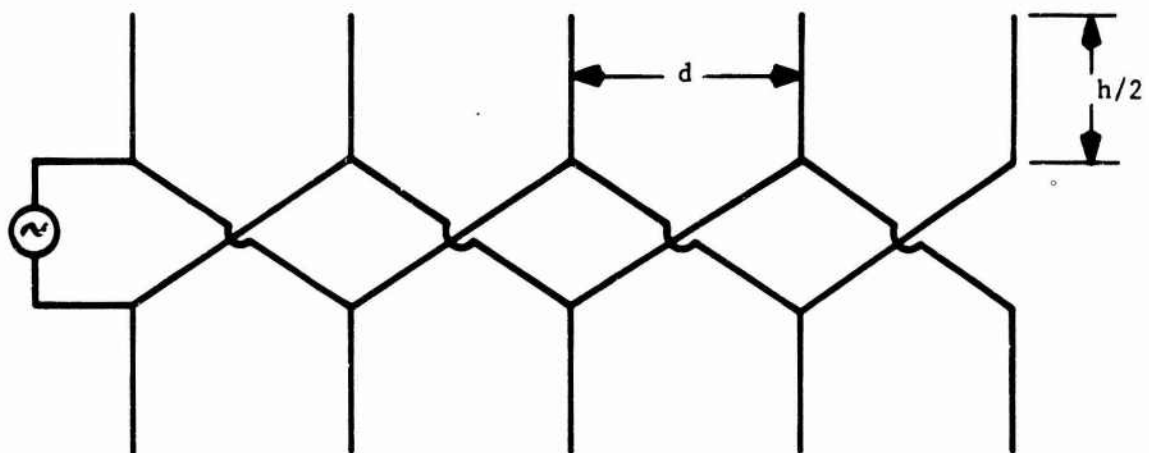


Fig. 30. Reversed elements uniform dipole array.

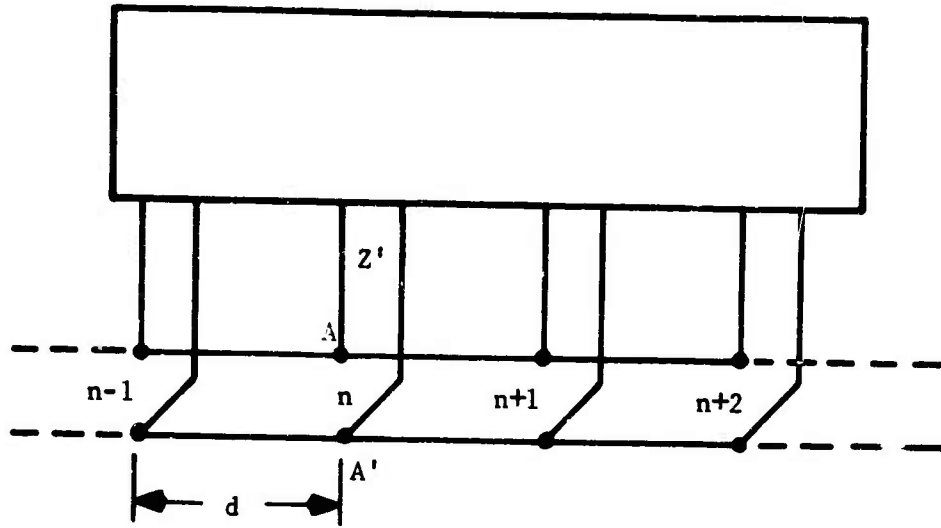


Fig. 31. Transmission line model for the uniform array of dipoles.

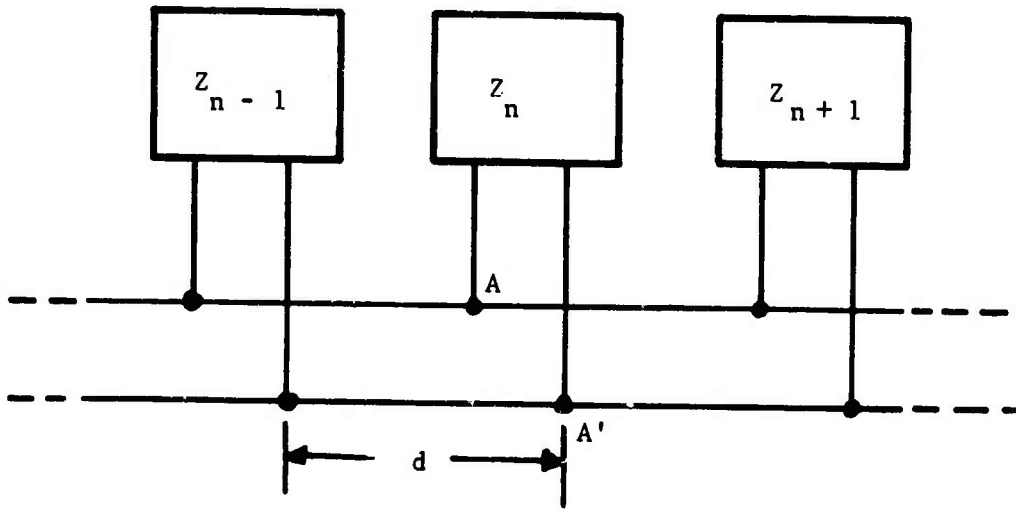


Fig. 32. Uncoupled load transmission line model for the uniform dipole array.

obtained ; these correspond to different modes on the structure, which can have different relative strengths. The problem cannot be solved without source considerations. However, the first approximation gives a sufficiently accurate picture of the physical phenomena. In Fig. 33 and 34 the Brillouin diagram experimentally measured by Mayes and Ingerson [42] is compared with computed data. The agreement is indeed excellent. It is even more impressive the comparison with the experimental data found on a log-periodic array by Carrel [1]. To obtain the curves of Fig. 35, Mittra and Jones calculated the phase shift and attenuation for the local kd, where d changes now from cell to cell, and used these values considering k constant and d variable, as we have already discussed. These theoretical curves were calculated by using a distance d between the elements equal to 0.112 times the length of the dipole (to correspond to Carrel's choice of the parameters). It is worth pointing out that once the behavior of the voltage along the line is obtained the input current of an element is also found (since the input impedance of the equivalent network of Fig. 32 is known). From an assumed sinusoidal current on the dipoles (i.e., having the same form utilized for the calculation of mutual impedance), the radiation pattern can be evaluated. Therefore, it seems possible to use this model for optimizing some parameters of a log-periodic array (e.g., the distance among the elements).

In conclusion it seems that the mathematical model here considered can be very useful for design purposes. However, from a theoretical point of view, it does not clarify some problems concerning log-periodic arrays. For example, the possibility of existence of, α the role played by higher modes in log-periodic array is a question which cannot be answered by using this type of analysis.

2.2.4 Log-Periodic Loaded Lines

In Section 1.3.5, the radiation mechanism of the log-periodic and frequency-independent antennas was discussed in a qualitative way. Very concisely, the approximate physical picture of the phenomena was the following: the structure acts in its first part as a surface waveguide whose characteristics are slowly varying. In the active zone, the modes become radiating, or in other words, a conversion of the guided into radiated energy takes place. If the structure is an efficient antenna the conversion is almost total, with small reflection toward the input. It is clear from this that, if it is possible to schematize the antenna as a (variable impedance) transmission line with distributed or lumped loading (progressively changing), the antenna "internal" behavior can be investigated without solving the electromagnetic problem. Thus, in a rather

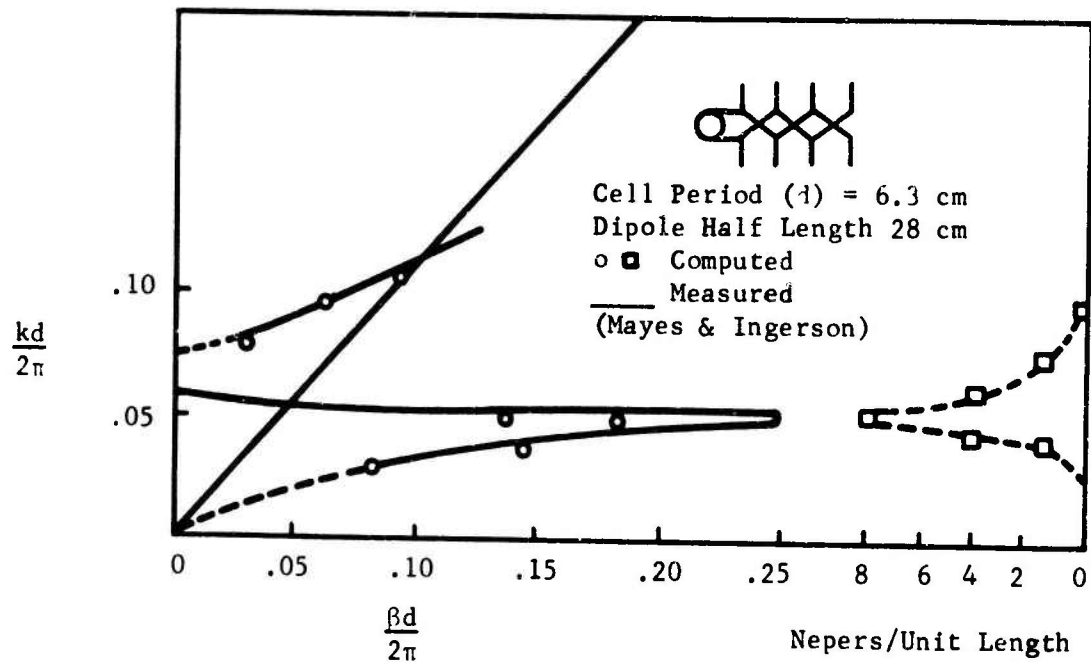


Fig. 33. Brillouin diagram for reversed uniform dipole array.

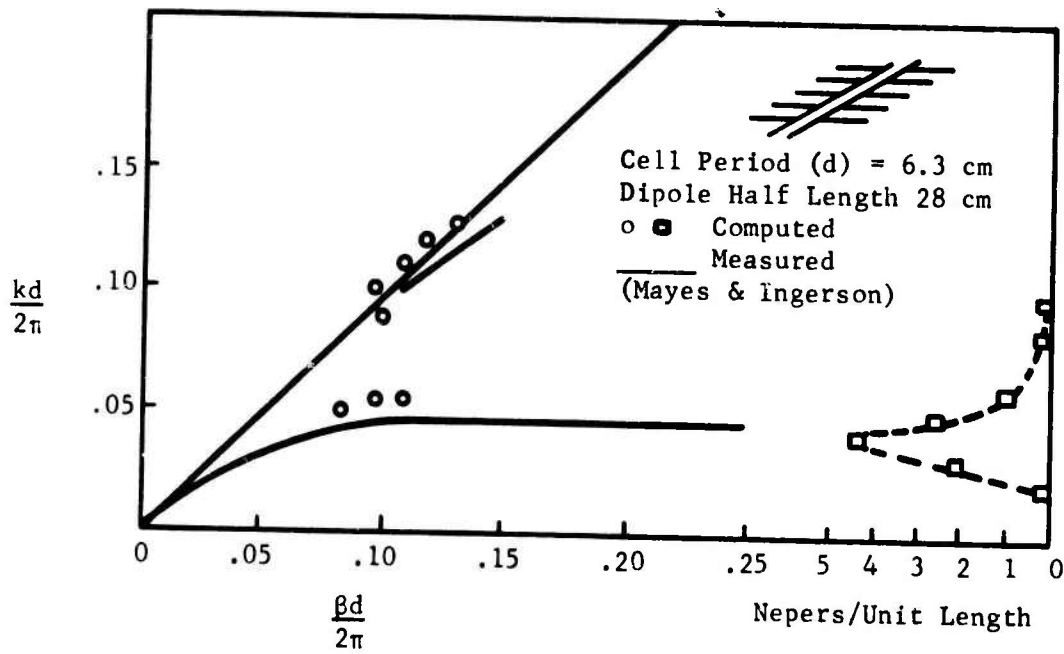


Fig. 34. Brillouin diagram for unreversed uniform dipole array.

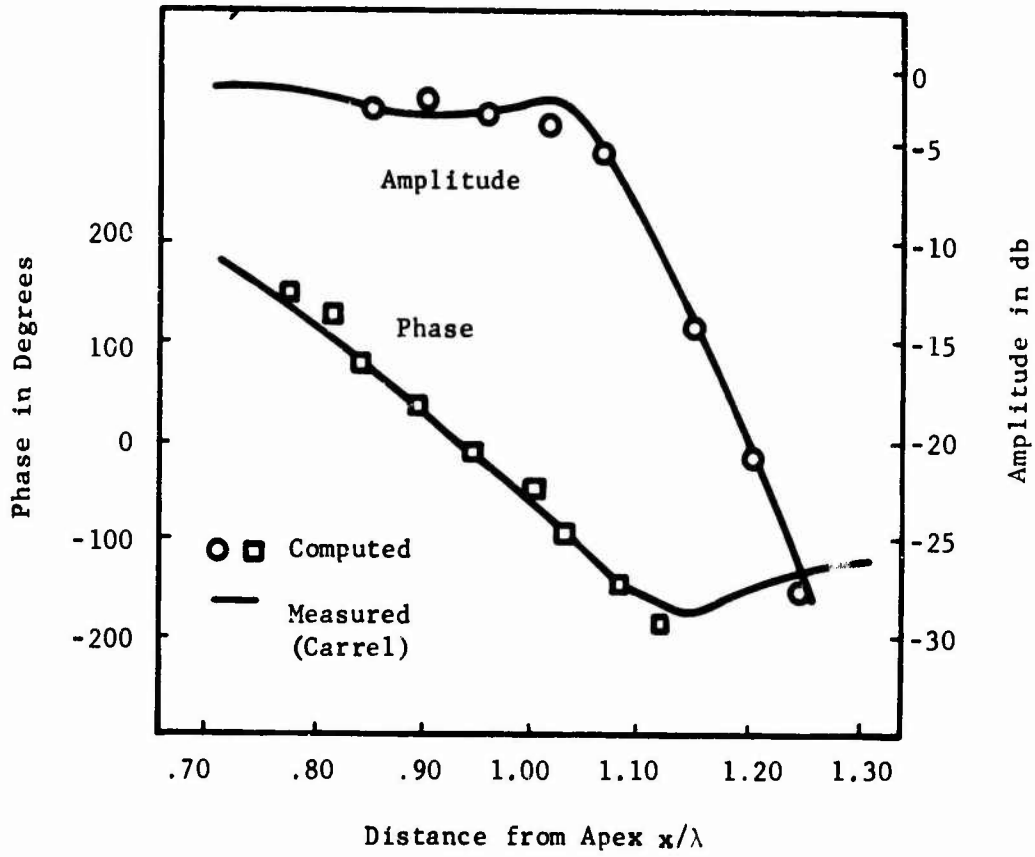


Fig. 35. Transmission-line voltage amplitude and phase curves for LP dipole array (theoretical) and comparison with experiment (Carrel [1]).

simple way, the amplitude and phase of the voltage along the antenna and the position of the active zone can be found by using only circuit and transmission-line theory.

A transmission line with resonant shunt circuits distributed in a log-periodic fashion can be adopted as a simple model. An even simpler model is a line loaded logarithmically (instead of log periodically). Mittra and Jones considered both these models. [44]. The latter, which is simpler, is the first they treated. In their terminology, Continuously Scaled, (C.S.) is synonymous with self-congruent, i.e., what we have always called in this report "frequency independent." Therefore, a C.S. line is one in which the voltage and current distribution remain unchanged if the frequency and the distance x to the point of observation are changed simultaneously, such that ωx remains constant. In other words for abscissae and frequencies such that:

$$\frac{\omega_1}{\omega_2} = \frac{x_2}{x_1}, \quad (2.4)$$

the impedance will be equal. Little reflection then leads to the conclusion that the impedance and the admittance for unit length of the line must have the following type of functional dependence upon x and ω :

$$Z(x, \omega) = \frac{Z(\omega x)}{x} \quad (2.5)$$

$$Y(x, \omega) = \frac{Y(x\omega)}{x} \quad (2.6)$$

If we put

$$x = \omega r,$$

it is easily found that the differential equations for the voltage and the currents are:

$$\frac{dV}{dr} = - \frac{Z}{\omega} I \quad (2.7)$$

$$\frac{dI}{dr} = - \frac{Y}{\omega} V \quad (2.8)$$

For purely shunt distributed RLC loading the expressions for the impedance and the admittance for unit length are:

$$Z = j\omega L \quad (2.9)$$

$$Y = j\omega C + \frac{1}{x[R + j(\omega L_1 x - \frac{1}{\omega C_1 x})]} \quad (2.10)$$

where L and C are the parameters of the uniform line (without the loading), while L_1 and C_1 are the ones due to loading.

It is convenient at this point to introduce the following definitions:

$$x_o^2 = \frac{1}{\omega_o^2 L_1 C_1} \quad (2.11)$$

$$L_o = L_1 x_o^2 \quad (2.12)$$

$$R_o = R x_o \quad (2.13)$$

$$Q = \omega_o L_o / R_o \quad (2.14)$$

where x_o is the point of the line where the load is resonant, and ω_o is an arbitrary frequency. If the propagation constant of the uniform line and the characteristic impedance are both taken equal to unity, by using formulas from (2.7) to (2.14), the following equation for V is obtained:

$$V'' + k^2(x) V = 0 \quad (2.15)$$

where

$$k^2(x) = 1 - \frac{x_o^2 / R_o Q}{x^2 - x_o^2 - j \frac{x_o}{Q} x}$$

If the wave along the line is essentially progressive, it is possible to treat (2.15) by WKB method [45]. It is also possible to consider the line made up of short sections of different uniform lines. By using this second method, it is not necessary to make any hypothesis about the amount of reflected energy along the line. Following this latter approach the authors have found a recurrence relationship for the complex amplitude of the incident and reflected wave. It is interesting to observe that as x tends to zero the characteristic impedance is purely resistive; see (2.9) and (2.10). The same happens for the input impedance, since the reflected wave has negligible amplitude, as the numerical results show. In Fig. 36 the amplitude and phase of the voltage along the structure is plotted as a function of $\beta_o x$ (β_o being the propagation

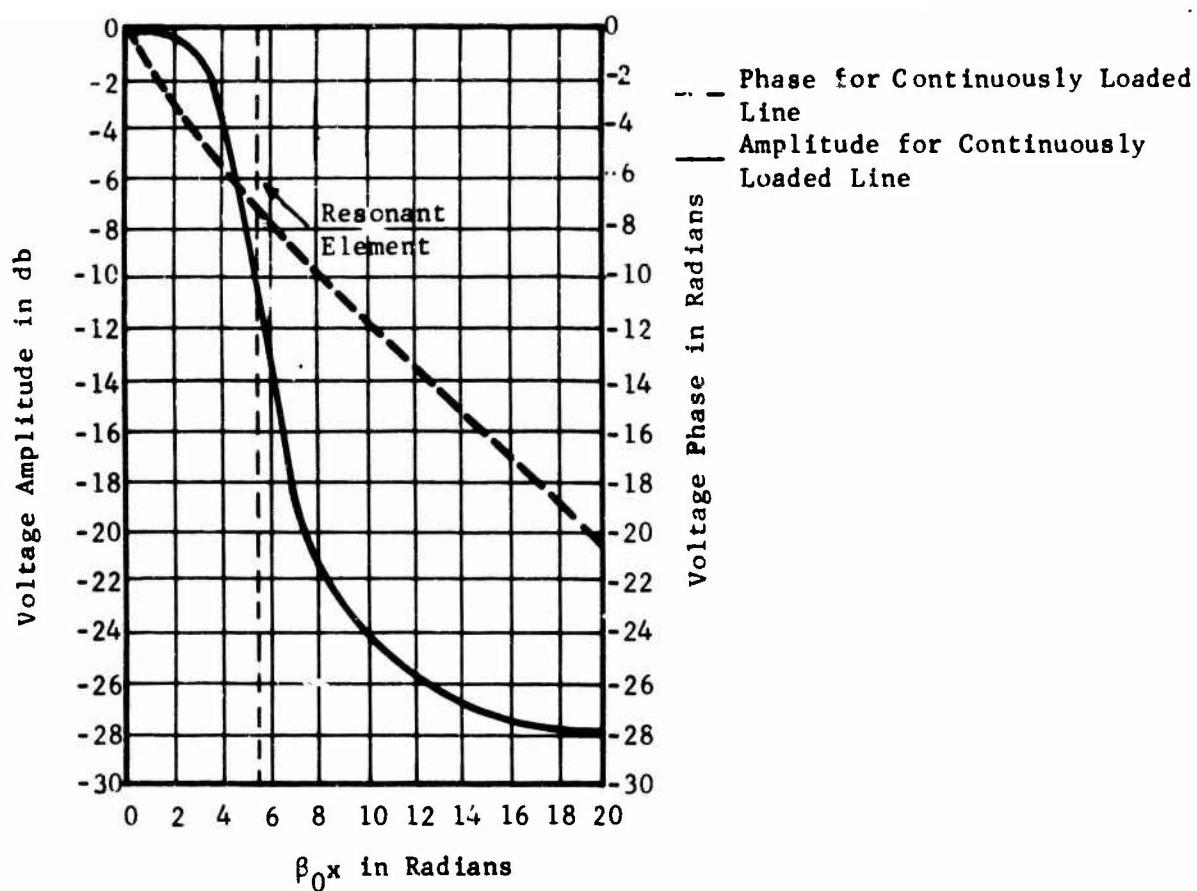


Fig. 36. Voltage amplitude and phase vs electrical distance with matched termination $R_o = 0.5$ and $Q = 2$.

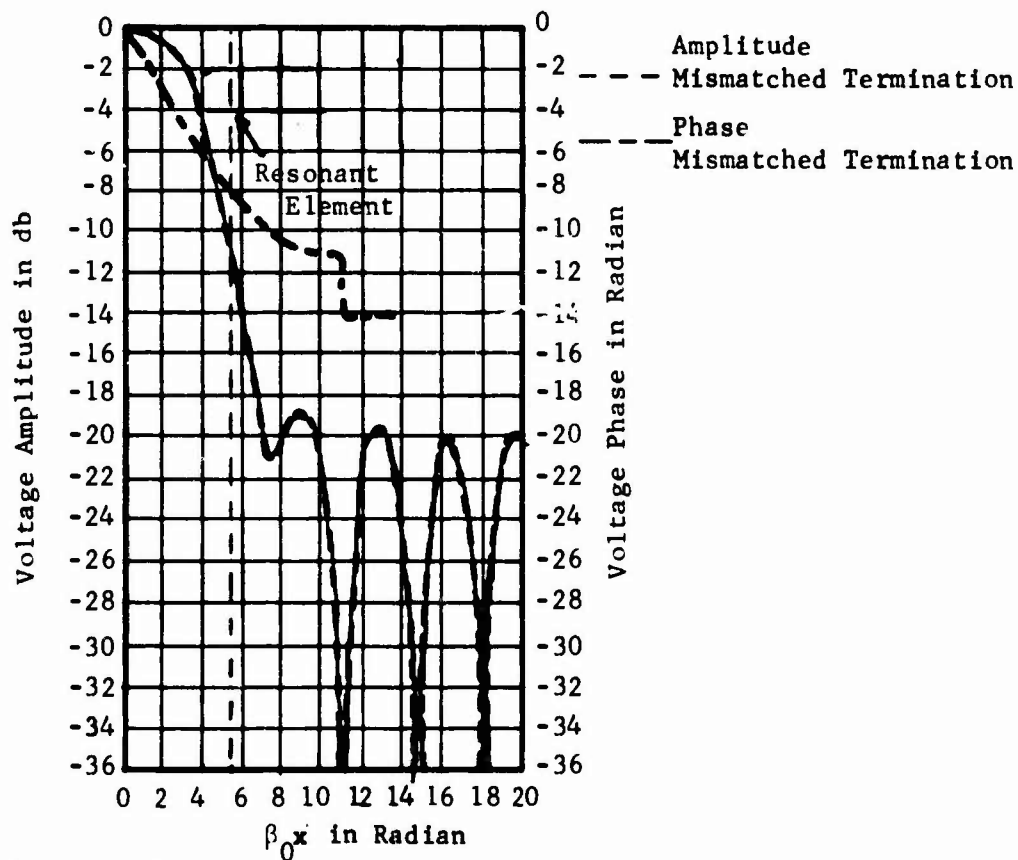


Fig. 37. Voltage amplitude and phase vs electrical distance with open circuit termination $R_o = 0.5$ and $Q = 2$

constant of the unloaded line at the frequency ω_0 considered). In the first part of the structure the attenuation is low and there is an approximately linear phase delay for unit length, of larger value than in the unloaded line. This means that near the input there is a slow-wave zone. Although the line is not uniform, the phase velocity is approximately constant. In the following region (the active zone), the attenuation is high, typically 20 - 25 db. In the final part of the structure, the amplitude decays very slowly, and the behavior of the voltage is heavily influenced by the nature of the termination, which has little or no influence in the input and active regions. In Fig. 37, the amplitude and phase behavior of the same structure of Fig. 36, but with a short-circuit termination, are plotted. The first part of the curves in Fig. 36 and Fig. 37 (before the active zone) are practically identical. This can be expected because of the large attenuation in the active zone which insulates the input from the load. The authors report that the computed reflection coefficient in the zone before the active region was about 10^{-3} , independent of the load. Behind the active region it was about 10^{-3} in the matched termination case and of the order of magnitude of the unity in the short circuit case. It is also interesting to consider the behavior of the active zone when Q is increased (for constant $R_0 Q$). The main effect is that the width of the active region decreases with Q ; the total attenuation however is not greatly affected. The authors have also computed the voltage distribution in the CS structure by using WKB methods, with numerical results very close to those obtained by using the method previously described.

In a well designed log-periodic structure, the performance not only repeats itself at log-periodic frequencies, but also deviates very little from the mean value for intermediate frequencies. The authors have shown, in fact, that if the C.S. model described above is modified by replacing the continuous loading of the line with a lumped one, according to a log-periodic sequence, the behavior of the voltage along the line does not change significantly. More precisely, they considered the line made up of an infinite number of log-periodic sections, loaded with shunt elements. The loads are equal to the length of a section times y [given by (2.10)]. We will not report here the details of the calculation procedure, which, essentially is standard circuit analysis. The interesting numerical results are plotted in Fig. 38 where D is the ratio between the length of a section and the wavelength corresponding to the frequency of resonance of the load. We see that in the region between the feed point and the active zone, and at some extent in the active zone itself, the LP and the CS models have practically identical behavior. Other computations (not reported here) show that if D , and/or Q are sufficiently large, the behavior of a log-periodic structure becomes different from that of the corresponding CS one, (with smaller attenuation in the active zone and increase in the input SWR).

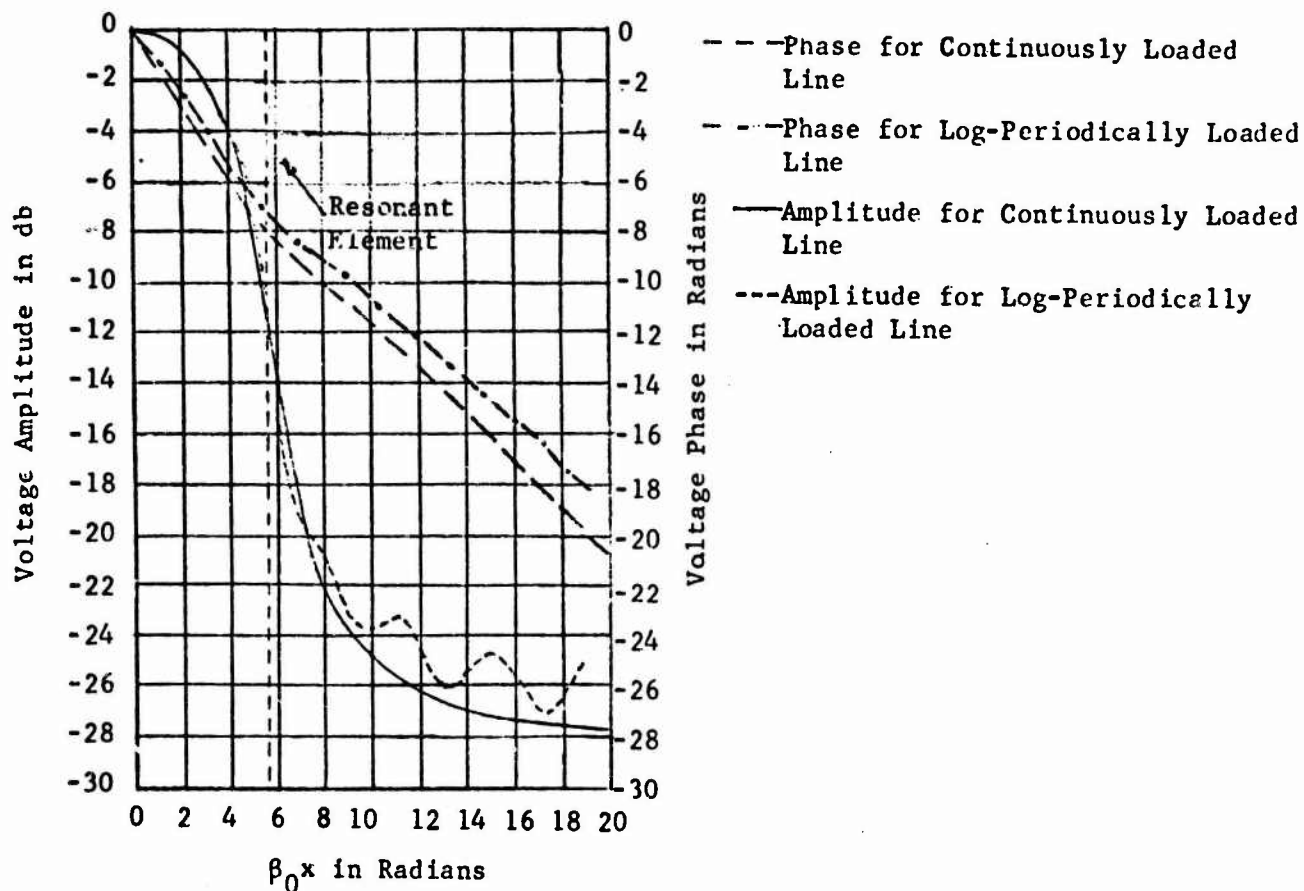


Fig. 38. Comparison of voltage amplitude and phase on LP and CS transmission lines with $\tau = 0.9$, $D = 0.5$, $R_0 = 0.5$, $Q = 2$, and $Z_0 = 1$.

In conclusion the study made by Mittra and Jones, although not concerned with the electromagnetic behavior of log periodic antennas, is however an important contribution to understanding their circuit behavior. The following two main points have been clarified:

- (a) The input SWR of a log-periodic structure is low if several elements are "active" (i.e. absorb power) at a certain frequency. The line acts as a continuous impedance transformer. The active zone insulates the input by the final load, and therefore, the antenna is insensitive of its termination.
- (b) In a certain range of the τ , D , Q , and R parameters a LP structure is a good approximation of a CS one. In other words, as far as the "internal" behavior is concerned, log-periodic and frequency-independent antennas may be considered equivalent.

2.3 NUMERICAL ANALYSIS OF THE LOG-PERIODIC DIPOLE ARRAY

2.3.1 Numerical Approach

Conceptually, the most satisfactory approach to the analysis of frequency-independent and log-periodic antennas is to consider the structure as a whole, to determine the "modes" (i.e., the types of waves which can be supported by a given geometry), and to determine which modes can be excited by certain given sources. This is, in principle, as it is well known, a standard procedure in solving problems of mathematical physics.¹ This type of approach certainly can lead to a deep understanding of the electromagnetic behavior of the structure, and can clarify the role played by the various geometrical parameters. However, the analytical difficulties associated with this problem are formidable; even the simpler problems posed by the periodic counterparts of these antennas are generally impossible to solve at the present state-of-the art. We have seen in the previous sections that in order to have an insight into the behavior of these structures it was necessary either to resort to extremely simplified models (i.e., different from the actual case as in Section 2.2.2), or to study a simply periodic line loaded with dipoles (Subsection 2.2.3), or to investigate only the interior problem of the antenna by considering either a "continuous scaled" or a log-periodic line loaded in a particular way, (Subsection 2.2.4). This section will be devoted to a review of a paper of R. Carrell dealing with an analysis, essentially numerical, of a particular kind of log-periodic antenna, which has wide application: the log periodic array of (reversed) dipoles of the type first

¹ A reasonably simple and readable reference (for the electromagnetic problems) can be, for example, Reference [46].

considered by Isbell [41]. Clearly this structure is simpler to analyze than, for example, that one of Fig. 25, since it is possible to use well-developed linear antenna theory to determine the interaction among the radiating elements. The approach utilized by Carrell is relatively straightforward [1]. A mathematical model of the antenna of Fig. 39, which very closely represents the physical structure under investigation, is built in the form of a uniform transmission line logarithmically loaded with dipoles. The question can be thus split in two parts; interior problem--to determine the current at the terminals of each dipole; and exterior problem--to find the radiated field and the phase center of the antenna (compare Subsection 2.2.3). We will see in the next subsections that as a result of the numerical investigation and experimental results, design information is presented in useful formulas and nomographs. Several pages will be devoted in this report to the survey of Carrell's paper because of its usefulness for design purposes and completeness of data.

2.3.2 Formulation of the Problem

The antenna analyzed by Carrell is depicted in Fig. 39, and schematized in Fig. 40. The ratio τ has the usual significance of expansion ratio and it is the ratio of the lengths of two adjacent dipoles.² A line through the ends of the dipole elements on one side of the antenna subtends an angle α with the center line of the antenna at the virtual apex 0. The spacing factor σ is defined as the ratio of the distance between two adjacent elements to twice the length of the larger element, and is constant for a given antenna. Parameters σ , τ , and α are related by the formula

$$\sigma = \frac{1}{2} (1 - \tau) \cot \alpha \quad (2.16)$$

The largest element is called element number 1. The half length of the element is denoted by h_n . Therefore

$$h_n = h_1 \tau^{n-1}$$

The distance d_n from element n to element $n+1$ is given by (compare Section 2.1)

$$d_n = d_1 \tau^{n-1}$$

If a_n is the radius of element number n , the a_n 's are given by:

$$a_n = a_1 \tau^{n-1}$$

² Rigorously speaking, because of the inversion of the dipoles the ratio between two dipoles is the square root of the expansion ratio. We will follow here however the definition used in [1].

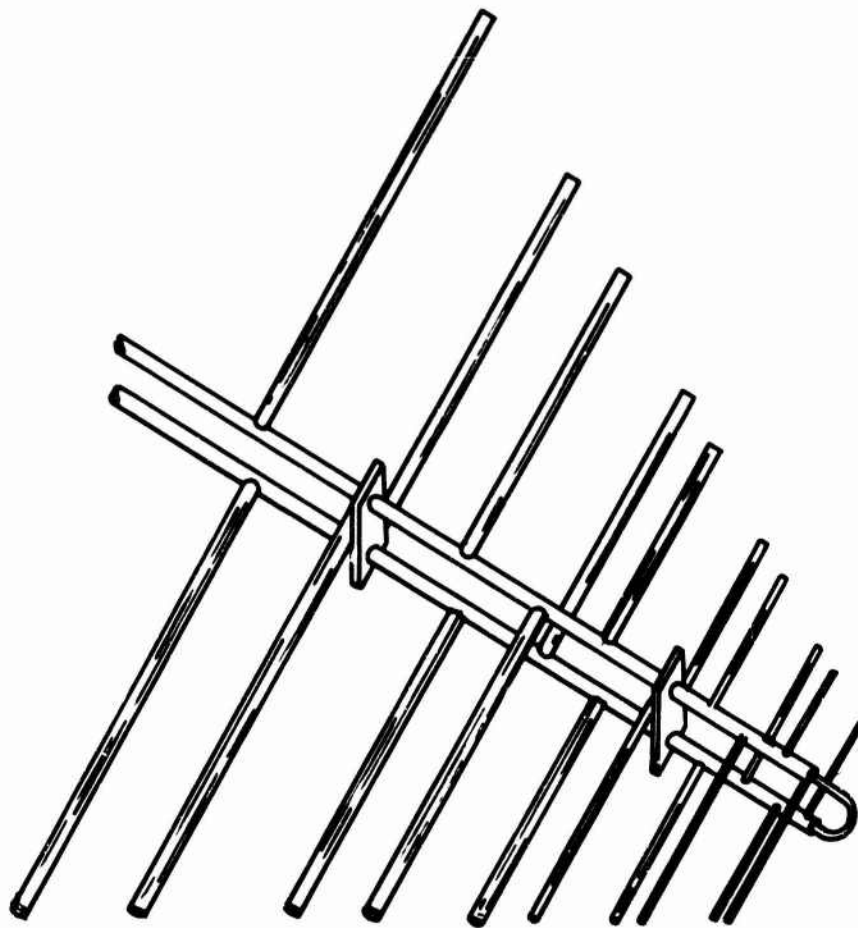


Fig. 39. Log-periodic array of reversed dipoles.

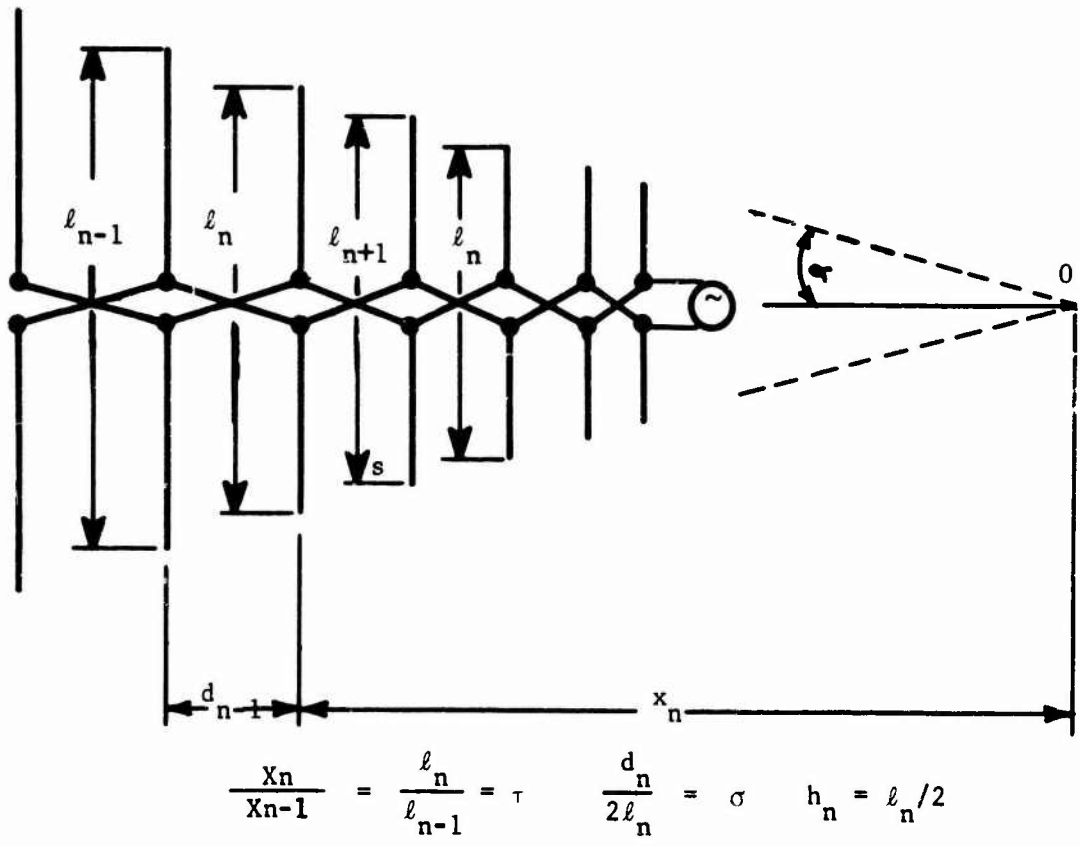


Fig. 40.. A schematic of the log-periodic dipole antenna, including symbols used in its description,

The ratio of element height to radius is the same for all elements in a given antenna and will be denoted by h/a .

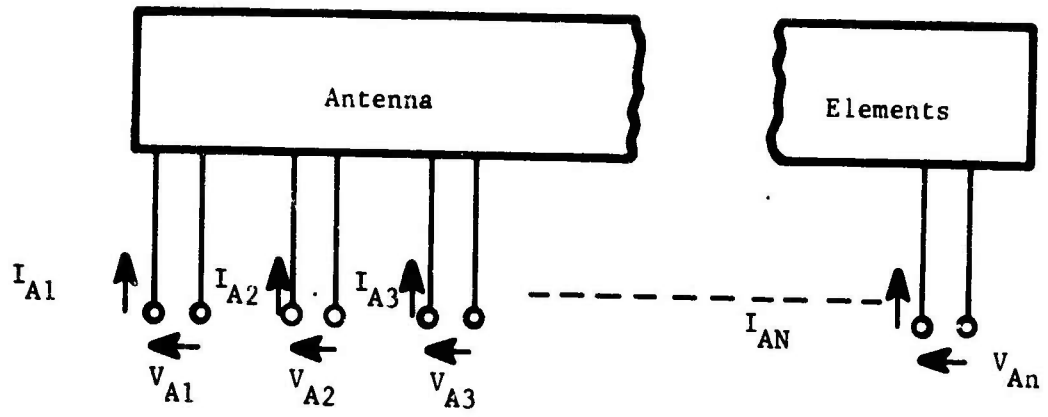
The antenna can be fed through a coaxial line inserted through the back of one of the hollow feeder conductors (Fig. 39). The shield of the coax is connected to its half of the feeder at the front of the antenna, the central conductor of the coax is connected to the other side of the feeder. With this method, an infinite balun is obtained in a way conceptually similar to that described for the log-spiral antennas. When the operating frequency is within the design limits, radiation is end-fire toward the feeding point, and the radiation occurs essentially in an active zone. Therefore behind such region the current is very attenuated and the nature of the load which terminates the feeder line is to a large extent immaterial (compare Subsection 2.2.4).

The dipoles are assumed to be very thin ($a/h \ll 1$) and the current on the dipoles is considered sinusoidal. Therefore, once the interior problem has been solved and the input current of the elements have been found, the current distribution on the various dipoles is also known. It is then possible, by using the standard formulas for linear current distribution, to determine the radiation pattern of the array.

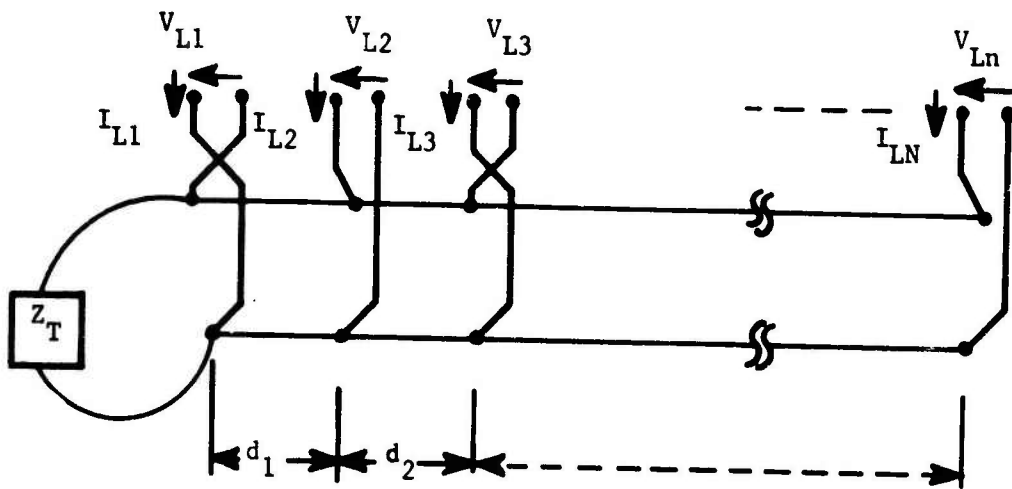
2.3.3 The Interior Problem

In order to solve the interior problem the antenna is considered as the parallel connection of two networks representing respectively the feeder and the radiating system (Fig. 41). The admittance matrix of the feeder circuit is $[Y_F]$ and its elements are trigonometric functions. If we call β_0 the propagation constant of the unloaded line and Y_0 its characteristic admittance from elementary transmission line theory it is simple to ascertain that $[Y_F]$ has the form:

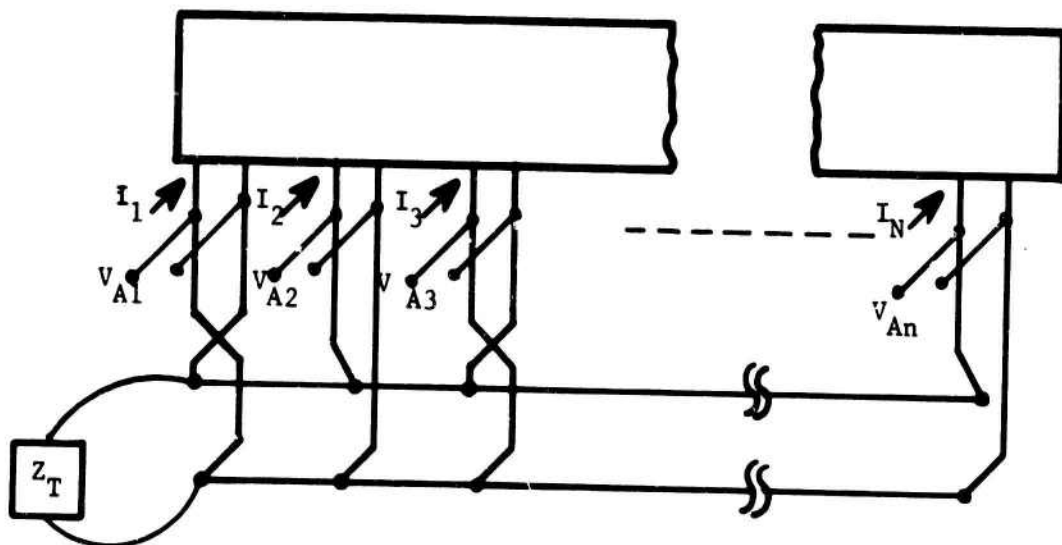
$$[Y_F] = \begin{bmatrix} (Y_T - jY_0 \cot B_0 d_1) & -jY_0 \csc B_0 d_1 & 0 & \dots & 0 \\ -jY_0 \csc B_0 d_1 & -jY_0 (\cot B_0 d_1 & -jY_0 \csc B_0 d_2 & \dots & 0 \\ & + \cot B_0 d_2) & & & \\ 0 & -jY_0 \csc B_0 d_2 & -jY_0 (\cot B_0 d_2 & \dots & 0 \\ & & + \cot B_0 d_3) & & \\ \dots & \dots & \dots & \dots & \dots \\ \dots & \dots & \dots & \dots & \dots \\ 0 & 0 & 0 & \dots & -jY_0 \cot B_0 d_{N-1} \end{bmatrix}$$



(a) Element Circuit



(b) Feeder Circuit



(c) Complete Circuit

Fig. 41. Schematic circuits for the LPD interior problem.

The relationship between the voltages and input currents in the feeder circuit is obviously

$$\vec{I}_F = [Y_F] \vec{V}_F \quad (2.17)$$

where \vec{I}_F and \vec{V}_F are column matrices which represent the driving currents and response voltages of the feeder circuit. Similarly if $[Y_A]$ is the admittance matrix of the antenna elements,

$$\vec{I}_A = [Y_A] \vec{V}_A \quad (2.18)$$

where \vec{I}_A and \vec{V}_A are the sets of input currents and voltages at the terminals. If the corresponding terminals of the feeder and dipole circuits are connected in parallel, a new circuit is obtained as shown in Fig. 41c. It is evident that

$$\vec{V}_A = \vec{V}_F$$

Therefore from (2.17) and (2.18), since the current column matrix is now

$$\vec{I} = \vec{I}_A + \vec{I}_F ,$$

it follows that

$$\vec{I} = ([Y_A] + [Y_F]) \vec{V}_A .$$

Setting $[Z_A] = [Y_A]^{-1}$

gives the

$$\vec{I} = ([Y_A] + [Y_F]) [Z_A] \vec{I}_A = ([U] + [Y_F] [Z_A]) \vec{I}_A \quad (2.19)$$

where $[U]$ is the unitary matrix. If we consider the matrix \vec{I} and the circuit of Fig. 41c it is clear that \vec{I} has only the first term, which represents the input current of the entire array. Formula (2.19) gives the solution to the problem. In fact, if the matrix,

$$[T] = [U] + [Y_F] [Z_A] ,$$

is inverted the input currents of the dipoles are given by

$$\vec{I}_A = [T]^{-1} \vec{I} .$$

The form of the matrix $[Y_F]$ has been already indicated. $[Z_A]$ is the matrix of the mutual and self impedance of dipoles, and can be formed, as we said in Subsection 2.2.3, by the standard e.m.f. method [43].

Besides \vec{I}_A , quantities of interest resulting from this analysis are the ones we have considered already many times: the voltage distribution along the feeder given by

$$\vec{V}_A = [Z_A] \vec{I}_A ,$$

and the location, the extension, and the power absorption of the active zone.

2.3.4 Radiation Pattern

Once the element base currents are found the radiation pattern can be calculated. Suppose that I_{An} are the elements of the column matrix \vec{I}_A . Standard computations then give the radiation pattern. Assuming that the current on the antenna is

$$I_n = I_{An} \sin \beta(h_n - |z|)$$

where β is the free space wave number, the amplitudes of the H and E planes radiation patterns, if the coordinate systems is that indicated in Fig. 42 are the following:

H plane:

$$\left| P_A(\varphi) \right| \sim \left| \sum_{n=1}^N I_{An} (1 - \cos \beta h_n) e^{j\beta x_n \cos \varphi} \right| \quad (2.20)$$

E plane:

$$\left| P_e(\theta, \varphi) \right| \sim \left| \sin \varphi \sum_{n=1}^N I_{An} \cos \left[(\cos \beta h_n \cos \varphi) - \cos \beta h_n \right] e^{j\beta x_n \sin \theta \cos \varphi} \right| \quad (2.21)$$

The phase patterns are given by the phase of the expression under sign of modules in the left side of (2.20) and (2.21).

2.3.5 Numerical Computations

Extensive numerical computations were performed by the method indicated in the previous subsections. The following quantities were computed:

- (a) the matrix $[Z_A]$ of the exterior couplings among the elements;
- (b) the matrix $[Z_L]$ of the line circuits;
- (c) the voltage \vec{V}_L i.e. the behavior of the voltage along the feeder;
- (d) the input currents of the dipoles \vec{I}_A ; and
- (e) the radiation patterns.

A plot of the voltage along the line is shown in Fig. 43 as a function of normalized distance $\frac{x}{\lambda}$ from the Apex. The frequencies are denoted by:

$$f_j = f_1 \tau^{1-j} \quad (2.22)$$

where f_1 is the frequency at which dipole number one is one-half wavelength long. For comparison purpose in Fig. 43 the data taken from measurements on an experimental model

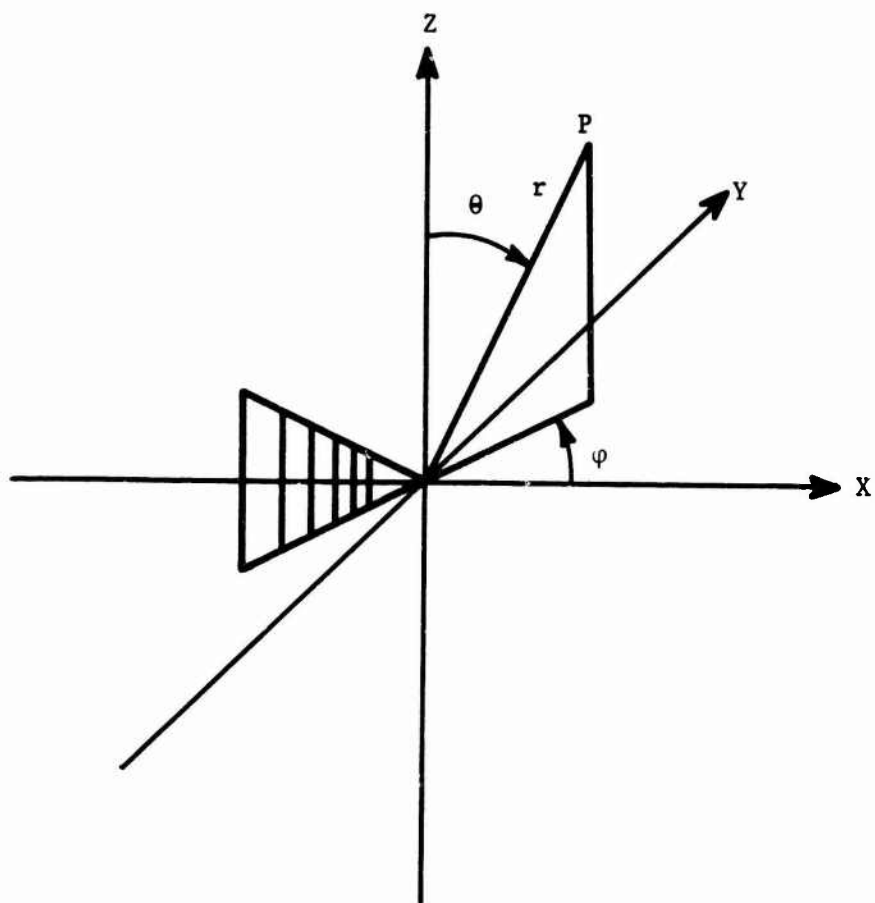


Fig. 42. Coordinate system used in the computation of the far field radiation patterns.

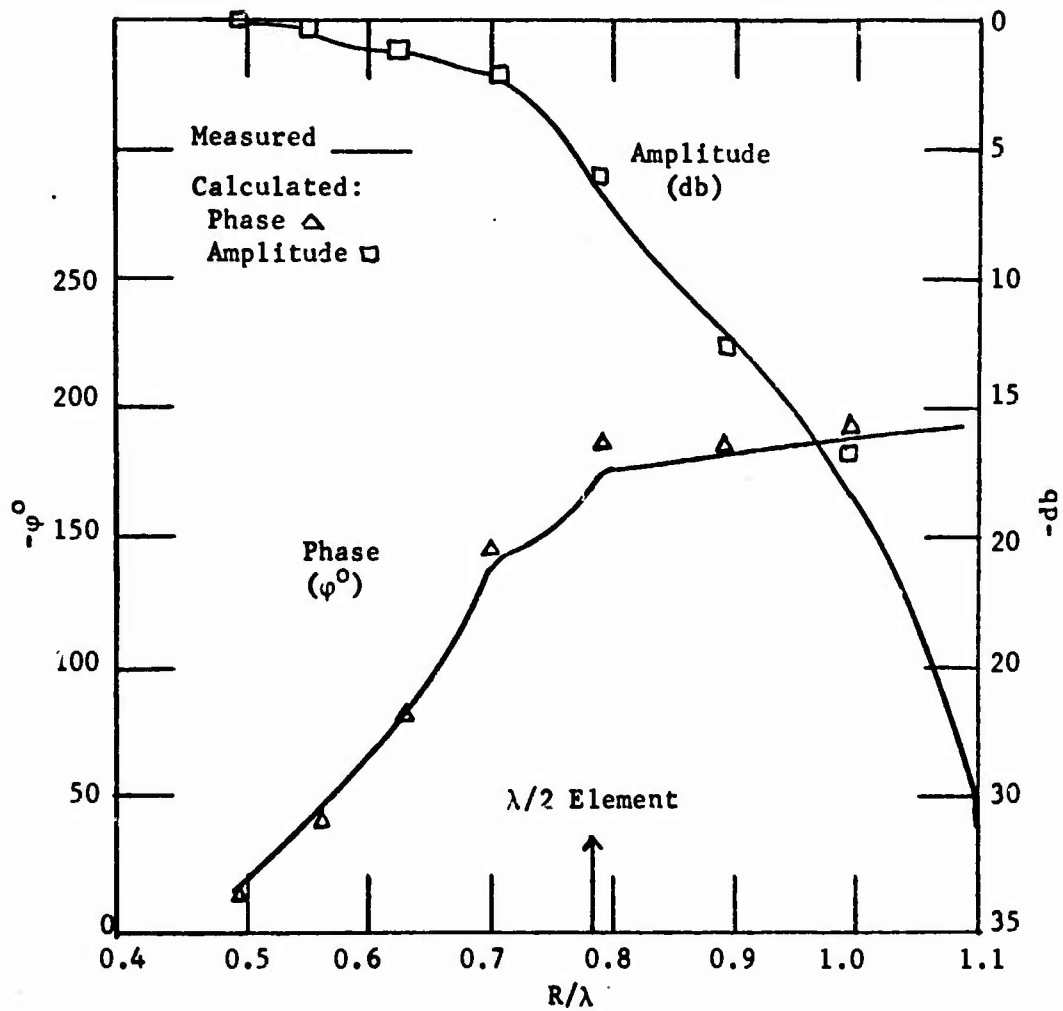


Fig. 43. Relative magnitude and phase of feeder voltage vs R/λ at f_3 , $\tau = 0.888$, $\sigma = 0.089$, $\alpha = 17.5^\circ$, $N = 8$, $Z_0 = 100$, $h/a = 125$, short circuit termination 0.128λ behind element number one.

are indicated too. The agreement is indeed excellent. The plot shows a steadily decreasing voltage going away from the feed point to the largest element. In the first zone there is essentially propagation without radiation: the small elements fed out of phase act as small shunt capacitors. For $\frac{x}{\lambda} > 1$ the feeder voltage decreases very rapidly, due to the coupling of energy into the elements of nearly half wavelength (active region). As the frequency is changed, the shape of the curve remains unchanged, and the position of the active zone moves along the antenna. The active region becomes deformed as it begins to include the front or back element of the antenna, and this establishes the upper and lower frequency of the antenna.

The ratio of operating frequency limits of the antenna is somewhat smaller than the ratio of the longest to the smallest elements on the antenna, which is:

$$B_s = \frac{\ell_1}{\ell_N} \tau^{1-N} \quad (2.23)$$

The operating bandwidth is instead

$$B = \frac{B_s}{B_{ar}} \quad (2.24)$$

where B_{ar} is a factor larger than 1. Notice that B_s , B and B_{ar} are non-dimensional numbers. The plot of Fig. 44 obtained by performing numerous computations shows the dependence of B_{ar} upon α for different values of τ .

The amplitude and phase of the base currents are plotted in Fig. 45. The phase curve shows the presence of a backward wave in the active region. The amplitude peak occurs for a dipole length somewhat smaller than $\frac{\lambda}{2}$. In Fig. 46 many computed patterns are compared with the experimental ones given by Isbell [41]. From the patterns it is possible to obtain an approximate estimation of the directivity from the E and H plane half power patterns:

$$D_{db} = 10 \log \frac{41000}{(BW_E)(BW_H)} \quad (2.25)$$

Fig. 47 contains computed curves which are very useful for design. The curves of constant directivity are plotted vs σ and τ , and for every τ is given the value of σ_{opt} (i.e., that value of σ which maximizes the gain). For values of σ greater than the optimum, large sidelobes appear on the radiation pattern.

The directivity is found to be independent of the characteristic impedance of the feeder. However, the element height to radius does affect the directivity: for each doubling of h/a the directivity decreases by about 0.2 db in the range $50 < h/a < 10000$.

The phase center of the antennas has been calculated too. In general, rigorously speaking, no antenna has a true phase center. As a matter of fact, the existence of

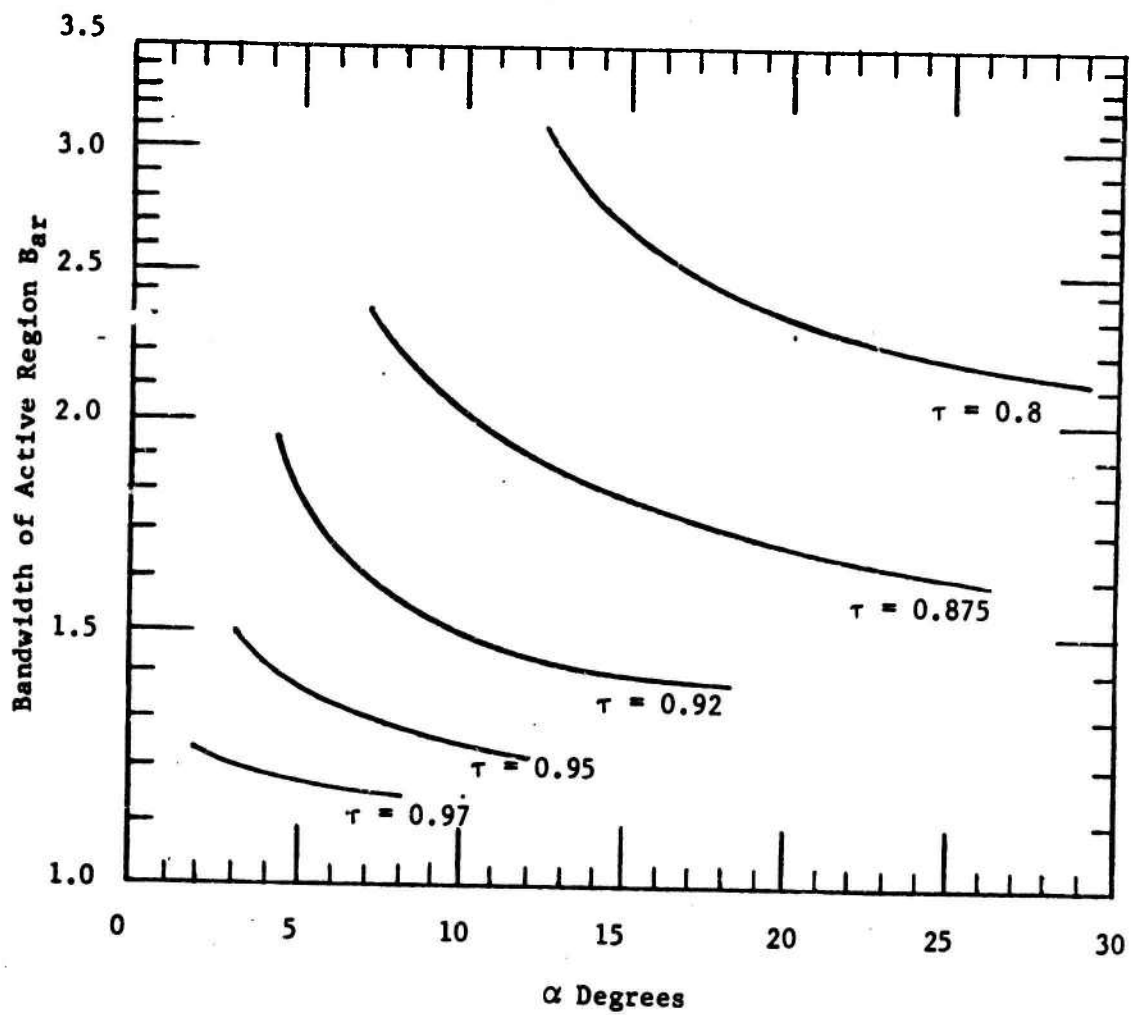


Fig. 44. Bandwidth of action region B_{ar} vs α for several values of τ , for $Z_o = 100\Omega$, $h/a = 125$.

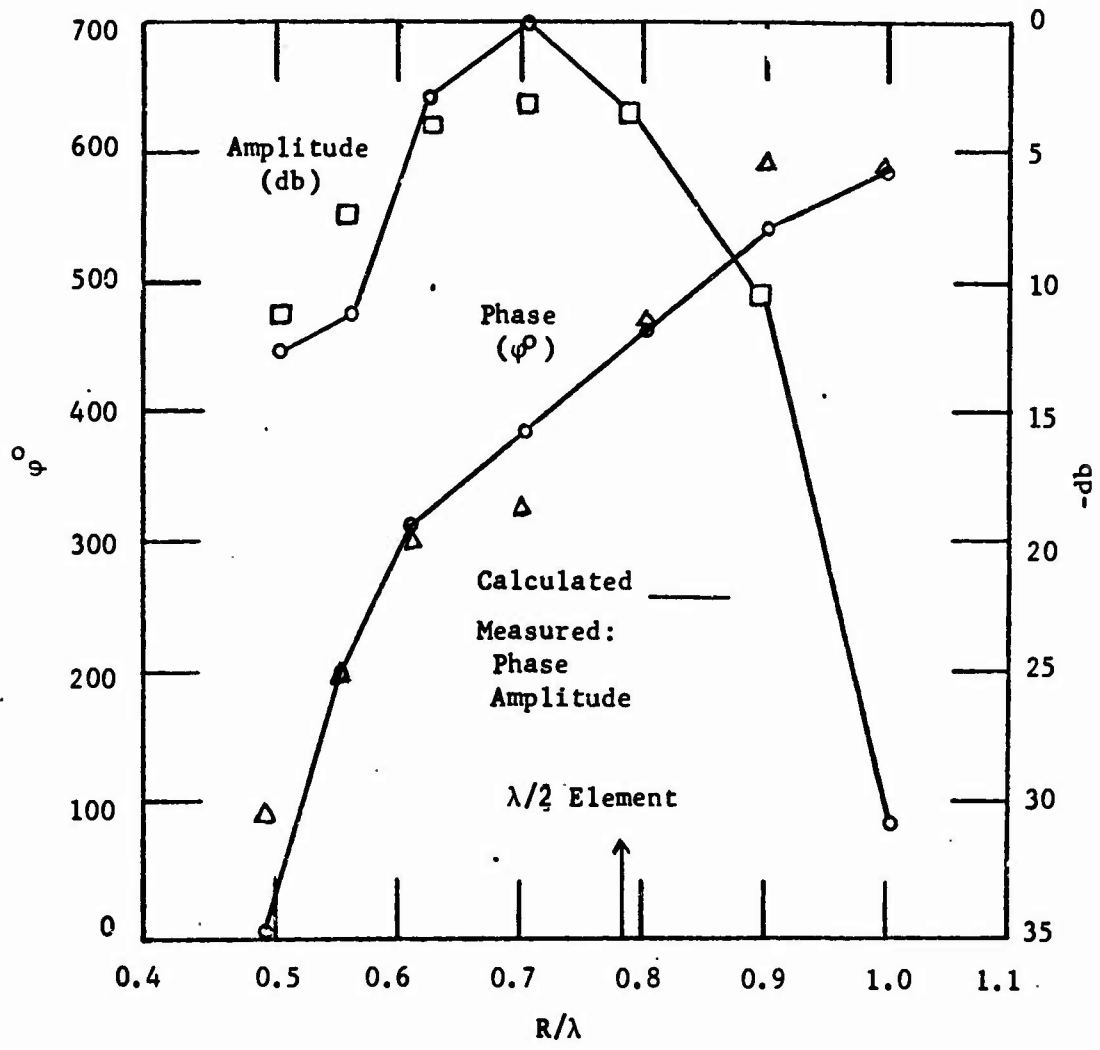


Fig. 45. Relative magnitude and phase of element base current vs R/λ at f_3 , $\tau = 0.888$, $\sigma = 0.089$, $\alpha = 17.5^\circ$, $N = 8$, $Z_0 = 100\Omega$, $h/a = 125$, short circuit termination 0.128λ behind element number one.

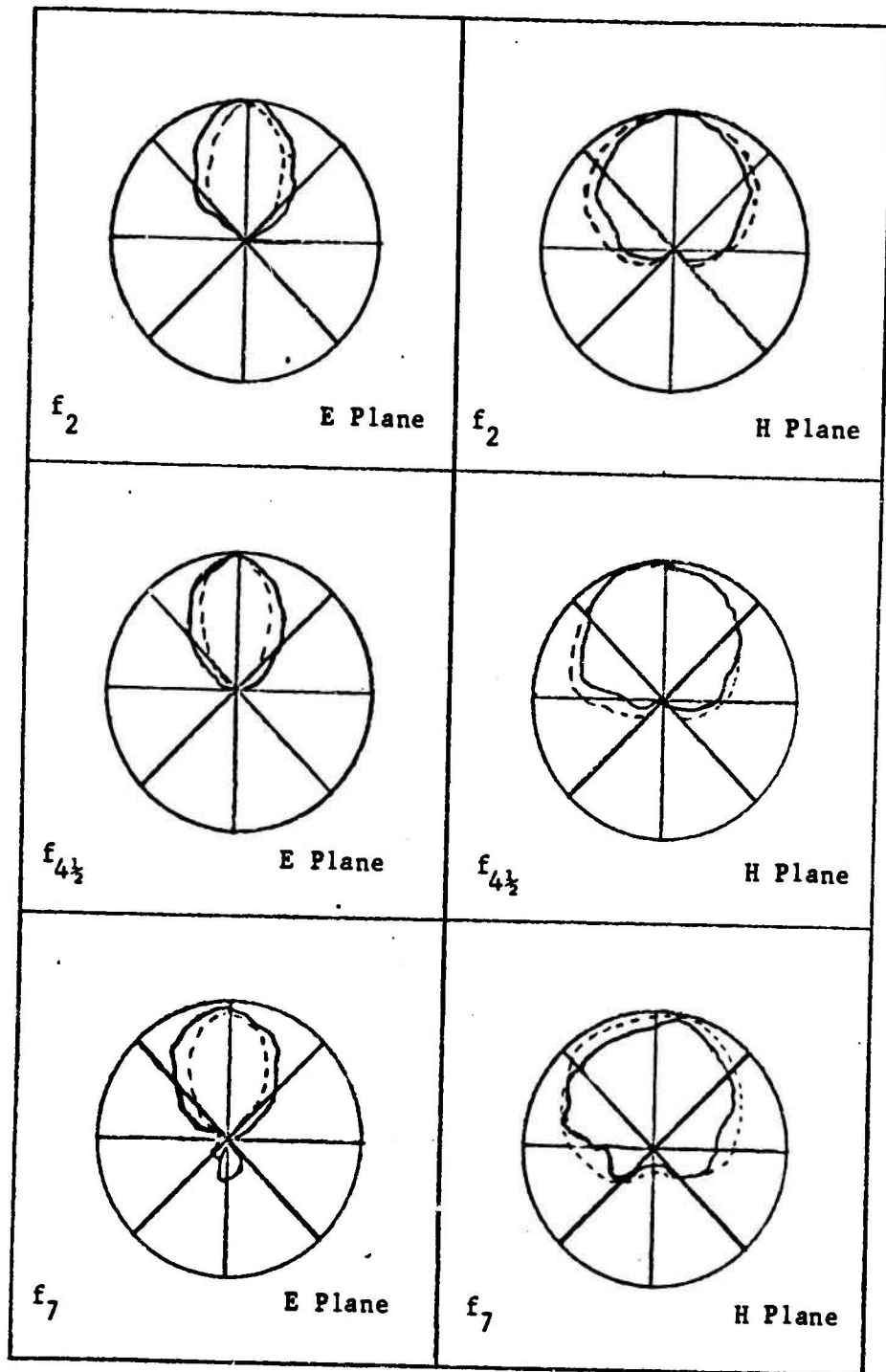


Fig. 46 . Computed and measured patterns, $\tau = 0.888$,
 $\sigma = 0.089$, $\alpha = 17.5^\circ$, $Z_0 = 100 \Omega$, $h/a = 125$,
 $Z_T = \text{short at } 0.1\lambda_{\text{max}}$ behind element number one.

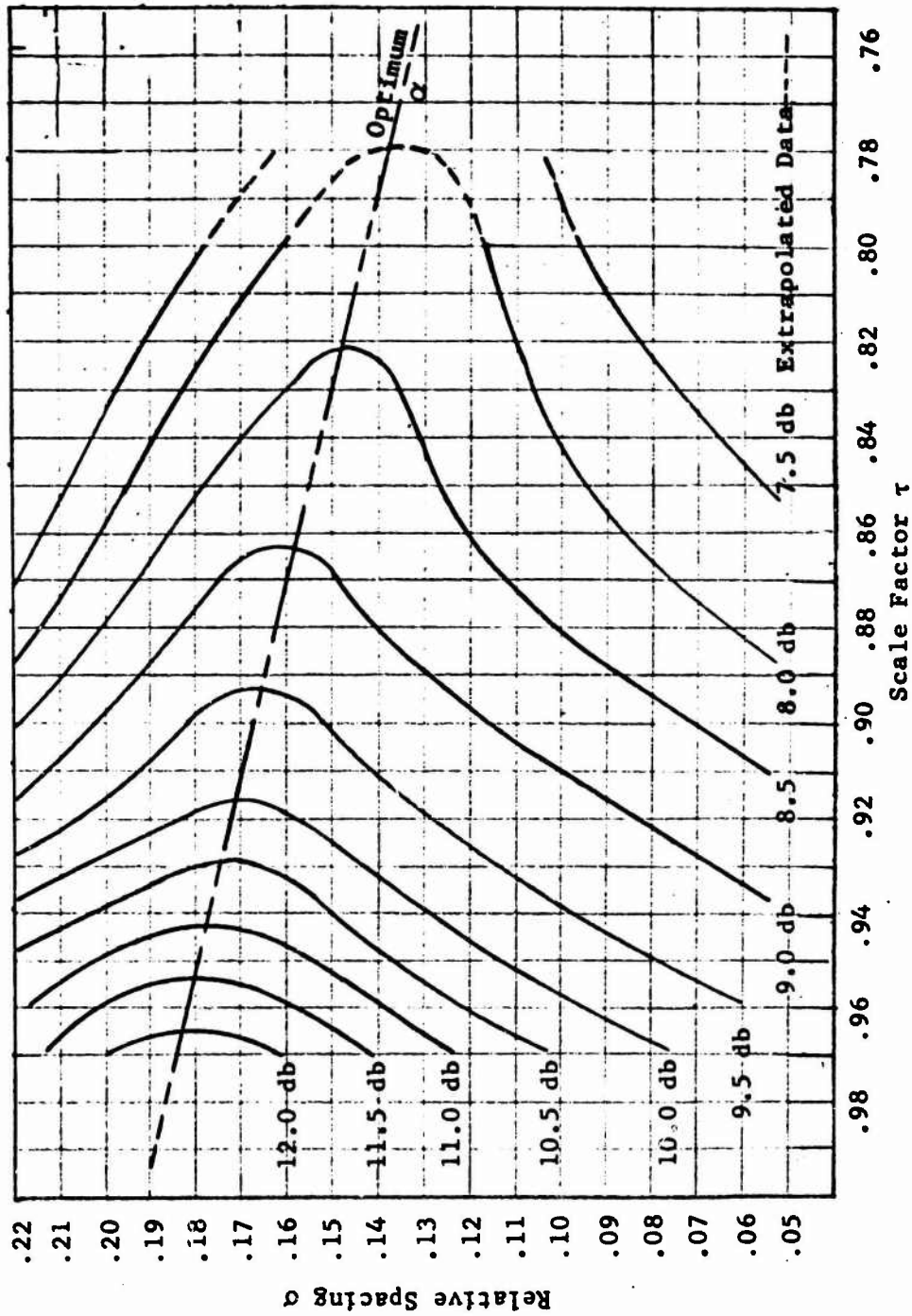


Fig. 47. Computed contours of constant directivity vs τ , σ , and α ; $Z_0 = 100$, $Z_T = \text{short}$ at $h_1/2$, $h/a = 177$.

a phase center would imply that the phase front of the radiation field of the antenna would be spherical, and this is true only for very particular sources. However for every direction θ, ϕ it is always possible to find the centers of curvatures of the sections of the phase front with two orthogonal planes. These define two "phase centers" relative to the direction and the plane under consideration. In this way, from the expression of the radiation patterns, the phase centers relative to the peak of the radiation pattern have been calculated for the E and H planes. The results for the H plane are plotted in Fig. 48. For the range of α shown, the location of the phase center is independent of τ and σ . The E plane phase center lies always ahead of the H plane one. In all cases it lies between the apex of the structure and the element whose length is one-half wavelength.

Considering the input impedance, the mean value of the resistance is given by the approximate formula

$$R_o = \frac{Z_o}{\sqrt{1 + \frac{Z_o \sqrt{\tau}}{4\sigma Z_a}}} \quad (2.26)$$

where Z_o is the characteristic impedance of the feeder and

$$Z_a = 120 \left(\ln \frac{h}{a} - 2.25 \right) \quad (2.27)$$

is an average characteristic impedance of a short dipole as a function of h/a . The SWR with respect to R_o has a minimum value of about 1.1:1 at the optimum value of σ . As σ is decreased below the optimum, the SWR rises above 1.8:1 at $\sigma = 0.05$. These calculated values represent lower bounds; the measured SWR is usually greater.

2.3.6 Design Data

The numerical analysis considered in this section can be applied directly to the design of the log-periodic dipole array. Moreover, in a qualitative way the same data can be useful as a guideline for the development of other types of log-periodic antennas. In this subsection we will consider how to utilize such data for design purposes.

The first step in the design is a choice of τ and σ , keeping in mind that a large value of τ (i.e., τ close to the unity) increases the number of the elements. The boom length (distance between the smallest and largest element) is determined mainly by σ , increasing with σ . For a certain required directivity, a preliminary choice of τ and σ can be made from the graph of Fig. 47. The dependent parameter α is then given by (2.16). The bandwidth, B_{ar} of the active region, for the given values of τ and α can be found from the graph of Fig. 44. The bandwidth of the structure B_s is then given by

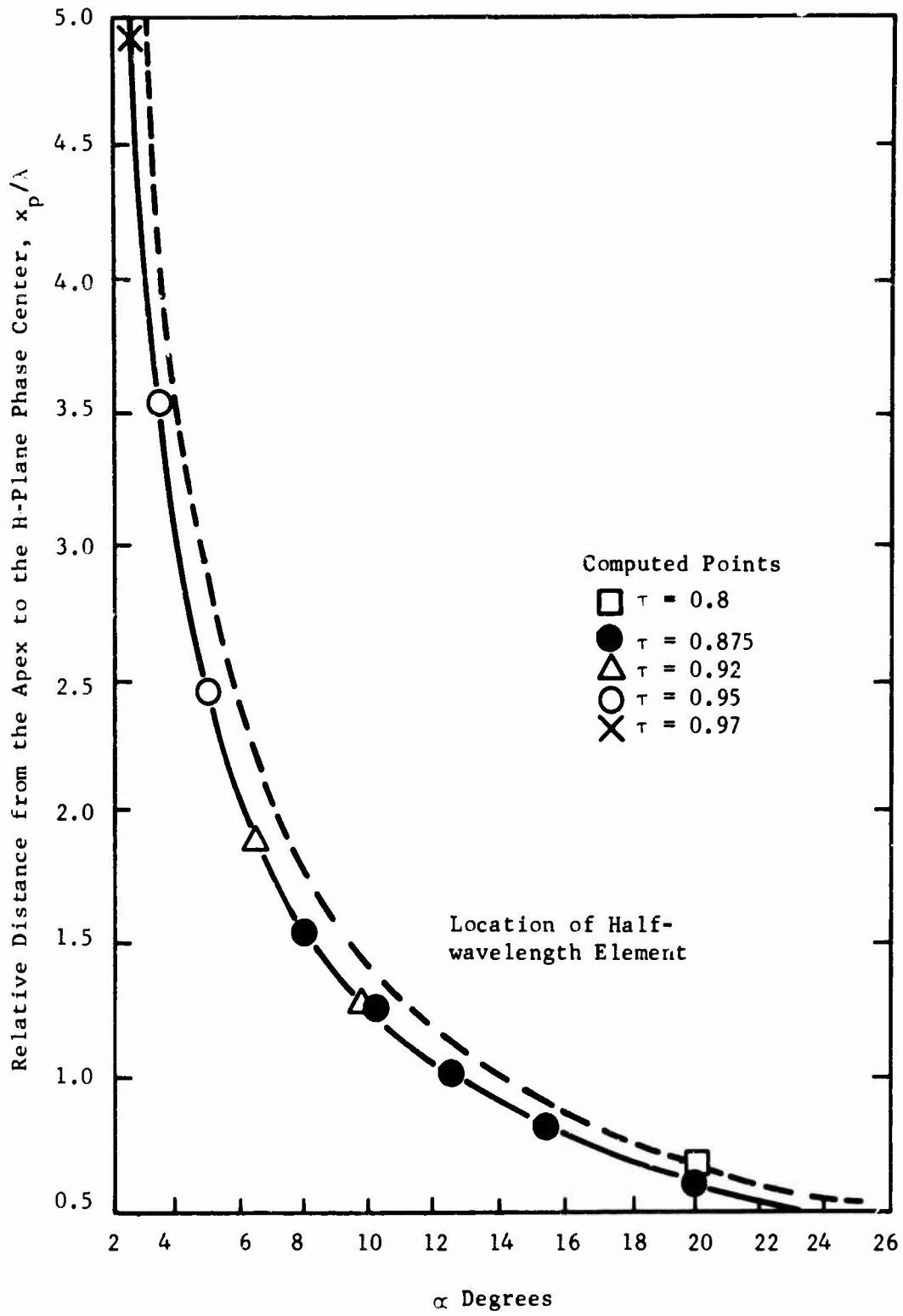


Fig. 48. Location of the phase center in wavelengths from the apex.

$$B_s = B B_{ar} \quad (2.28)$$

where B is the required operating bandwidth. The geometry of the log-periodic dipole antenna provides the following relationship between the boom length L and the longest operating wavelength λ_{\max} :

$$\frac{L}{\lambda_{\max}} = \frac{1}{2} \left(1 - \frac{1}{B_s}\right) \cot \alpha \quad (2.29)$$

because the length of the first element is $\lambda_{\max}/2$. L is the boom length between the largest and smallest element. The number of elements required is found from the equation

$$N = 1 + \frac{\log B_s}{\log 1/\tau} \quad (2.30)$$

The principal log-periodic dipole parameters are thus determined. It is likely that the first estimate of τ and σ will lead to a longer boom length than is necessary, so a revision must be made in τ and σ , repeating the above procedure several times until the minimum boom length is found.

In order to obtain a required input impedance R_o , the characteristic impedance of the feeder must be specified. Structural considerations generally determine h/a and Z_a is obtained by (2.27). Inverting (2.26), the characteristic impedance of the feeder relative to R_o is found

$$\frac{Z_a}{R_o} = \frac{1}{8\sigma' Z_a/R_o} + \sqrt{\frac{1}{(8\sigma' A_z/R_o)^2} + 1} \quad (2.31)$$

where $\sigma' = \sigma/\sigma_\tau$.

All the elements for the design are now available. Carrell suggests short-circuiting the terminal of element number 1 (the longest), since at the lowest frequency the shorted element acts as a passive reflector.

In conclusion, the work of Carrell seems the most exhaustive parametric analysis available for this type of structure. Although specifically concerned with log-periodic dipole arrays, the large amount of information given in it can be used also for other kinds of log-periodic antennas. The data in Table 1 show the effects of parameter modifications [1].

2.4 MISCELLANEOUS LOG-PERIODIC ANTENNAS

The log-periodic principle can be realized in a variety of geometries. As mentioned previously, the present state-of-art does not permit predicting the performance

Table 1 . LPD Parameters and Their Effect on the Observed Performance

Table entries denote the change in performance for an increase in the parameters of the first column.

Increasing LPD Parameter*	Bandwidth of Active Region B_{ar}	Input Impedance (Always less than Z_0)	Directivity	Phase Center Distance to the Apex x_p	Boom length L/λ_{max} for a fixed Operating Bandwidth B
τ (σ constant)	decrease	small decrease	increase	increase (depends on α)	Decrease to a point depending on B, then increase
τ (α constant)	decrease	small decrease	small increase	independent	decrease
σ (τ constant)	increase	increase	increase	increase (depends on α)	increase
σ (α constant)	increase	increase	small decrease	independent	increase
Z_0	independent but location of AR moves toward apex	increase	small decrease	small decrease	small decrease
h/a	independent, but location of AR moves away from apex	increase	small decrease	small increase	small increase

* The table entries hold true over the following range of parameters for which frequency independent operation has been verified: $0.875 < \tau < 0.98$. $0.05 < \sigma < \sigma_{optimum}$, $100 < Z_0 < 500$, and $20 < h/a < 10000$. Any one of τ , σ , or Z_0 may take on other values provided the remaining parameters are suitably restricted as explained in the text.

of a novel type of structure. Due to this lack of theoretical insight, a large amount of experimental work has been devoted to the development of different kinds of new antennas. We will briefly consider some of the most interesting miscellaneous structures which have been proposed.

Log-Periodic Folded Monopole Array

At the Radiolocation Research Laboratory Department of the Electrical Engineering Dept. of the University of Illinois, a limited investigation has been performed on a new type of unidirectional, vertically-polarized, log-periodic antenna, the log-periodic folded monopole array [47]. Such an antenna in its most promising version is constructed by a series of folded vertical log-periodic dipoles on a ground plane fed by a coax feeder line. The outer conductor is log-periodically broken and the folded monopole is fed in series as shown in Fig. 49. The ground plane clearly increases the directivity. The radiation patterns obtained are fairly satisfactory, but the SWR is not generally very good. Since this structure was judged not to have many advantages over the zigzag or coaxial fed monopole arrays, no attempt was made to improve its impedance characteristic.

Log-Periodic Cavity-Backed Slot Antennas

The usual types of log-periodic antennas are not suitable for use on aerospace vehicles traveling at high speed in the atmosphere, because such vehicles cannot employ protruding objects from the surface of the vehicle. Therefore, it is highly desirable for such applications to develop a flush-mounted antenna based on the log-periodic principle.

Perhaps the most successful attempt in this sense has been made at the University of Illinois [48]. The device proposed is constituted by an array of slots, each one backed by a cavity. The sizes of the slots, their spacings, and the cavity dimensions follow a log-periodic law. The cavities are excited by a series of loops in series on a feeder line and the energy is radiated through the slots. It is clear that the number of variable parameters in this type of antenna are much larger than in the case of log-periodic dipole array. Therefore, the choice of optimum parameter is more difficult. A program was conducted to find a satisfactory set of parameters, including tests on a single radiating element (i.e., slot and backing cavity to establish the optimum size and position of the magnetic loop). Design data are not given in [48]. Although the results are not too satisfactory, at least the feasibility of an antenna of this type has been demonstrated.

Other Log-Periodic Slot Arrays

Other different log-periodic slot arrays have been proposed with moderate success. Various techniques have been tried by utilizing ground-plane slots as radiating elements. Fig. 50 shows a fairly successful array remarkable for the simplicity and

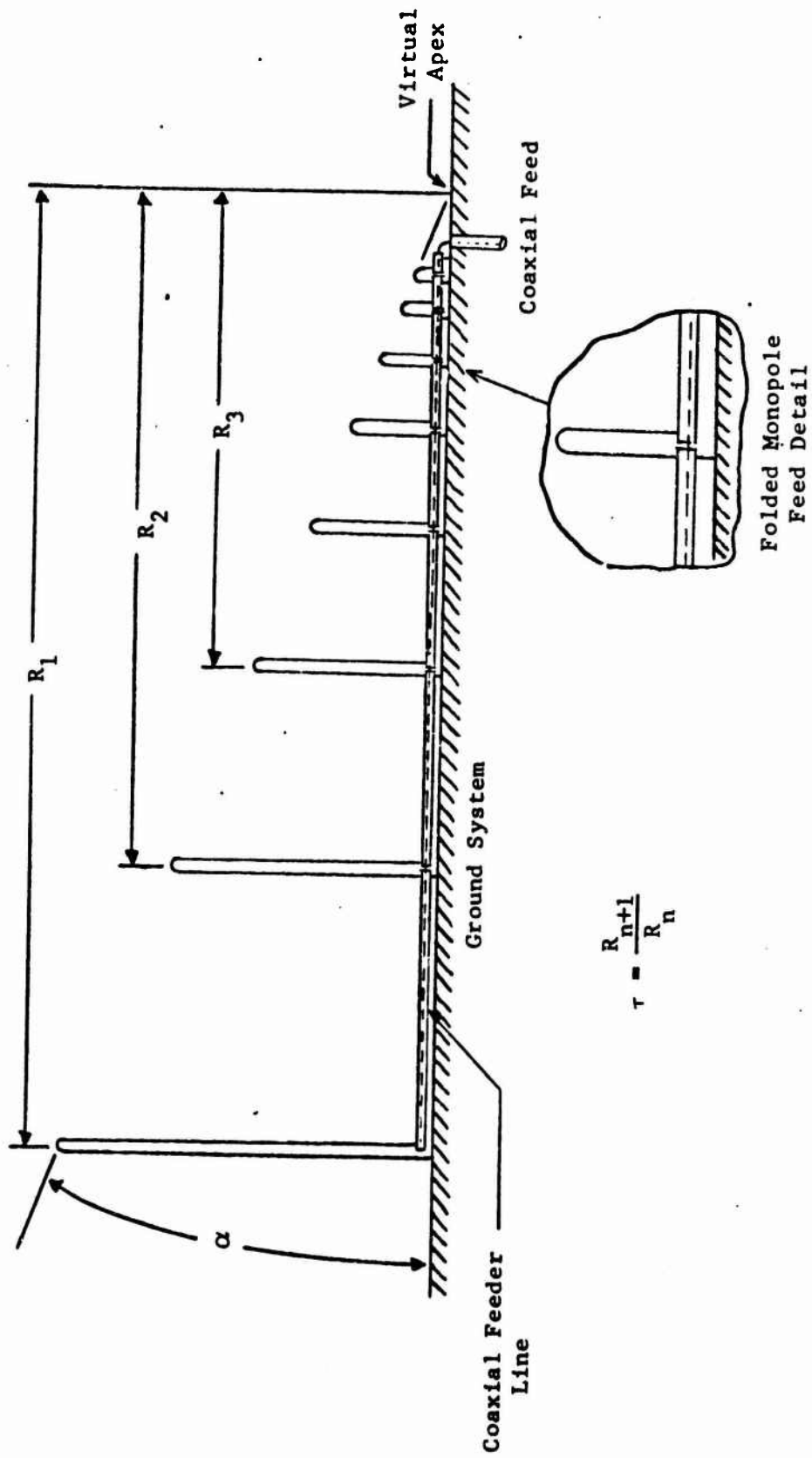


Fig. 49. Log periodic, folded monopole array.

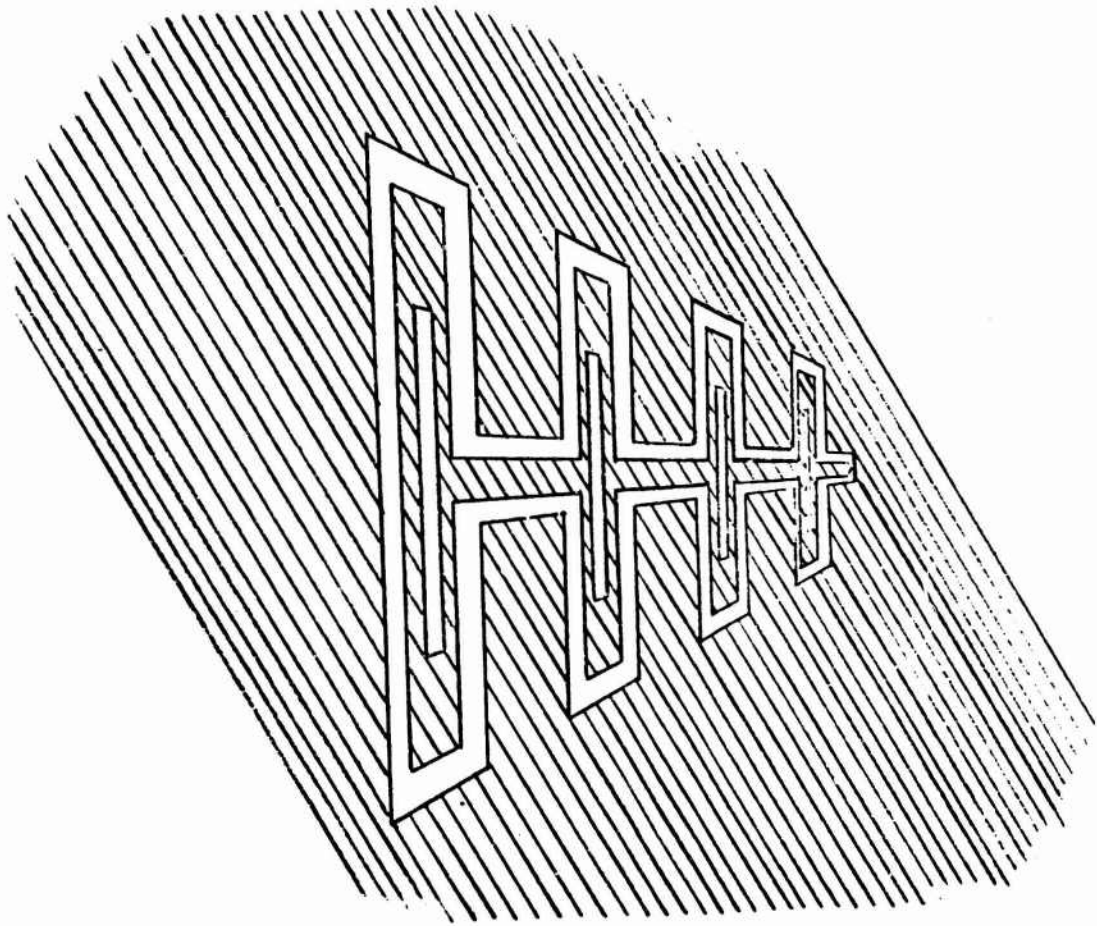


Fig. 50. Log-periodic folded slot array.

cleanness of design is shown [50]. A completely printed construction is adopted. Antenna currents flowing on the ground plane on the array axis are parallel to a line bisecting the elements (i.e., the axis of the array). Thus, the ground plane can be cut along the array axis and sections of a printed circuit transmission line inserted therein. The radiating elements are "folded slots," the dual of folded dipoles. The smaller (inner) slot of each element can be used for the fine phasing of the elements. It has been experimentally determined that the optimum length for these phasing slots is in the neighborhood of one-half the length of the outer slots. Appreciable deviations from this optimum length are accompanied by pattern degradation. Some radiation patterns are shown in Fig. 51. It is to be noticed that the radiation is bidirectional. Attempts to make it unidirectional with the addition of a backing cavity were not very successful.

Circularly-Polarized Log-Periodic Antennas

A peculiar property of log-periodic antennas, which seems quite general although not analytically proven, is the so-called phase rotation phenomenon: if the phase of the field is measured relative to the phase of the input current, the phase of the received signal will be delayed of 2π if the structure is expanded through a period [50]. The relation between the log of the frequency and the phase rotation is practically linear, with deviations of less than about 15° from the exact law. This allows frequency-independent phasing of the array elements. Consider now two log-periodic structures, placed at right angles to each other, with one structure scaled by the factor $\tau^{\frac{1}{2}}$ with respect to the other. The situation is depicted in Fig. 52. (Notice that the period τ is as indicated, because of the reversal of feeding connections of the dipoles). The phase rotation phenomenon guarantees that circular polarization independent of frequency is obtained on the peak of the beam. Not only the dipole array but also other different structures can be arranged according to the same idea, to give circular polarization. For example, two trapezoidal tooth structures of the type of Fig. 25, can be arranged in a pyramidal shape. Axial ratios greater than 2:1 can be obtained on the entire bands of the component antennas. The circular polarization obtained with antennas of the type shown in Fig. 52 is generally better than that given by trapezoidal tooth structures [51].

Reduced Size Log-Periodic Antennas

We have already mentioned some attempt to reduce the size of log-spiral antennas. Loading the antenna with lumped elements, or with a continuous dielectric or magnetic material has been suggested [52]. However, it seems that the most promising approach, is one proposed at the University of Illinois: the log-periodic helical zigzag antenna, essentially a modification of the log-periodic zigzag antenna on a ground plane [53 and 54]. This antenna is constituted of a single conducting wire, arranged in a log-periodic way as indicated in Fig. 53. A disadvantage of such an antenna, which does

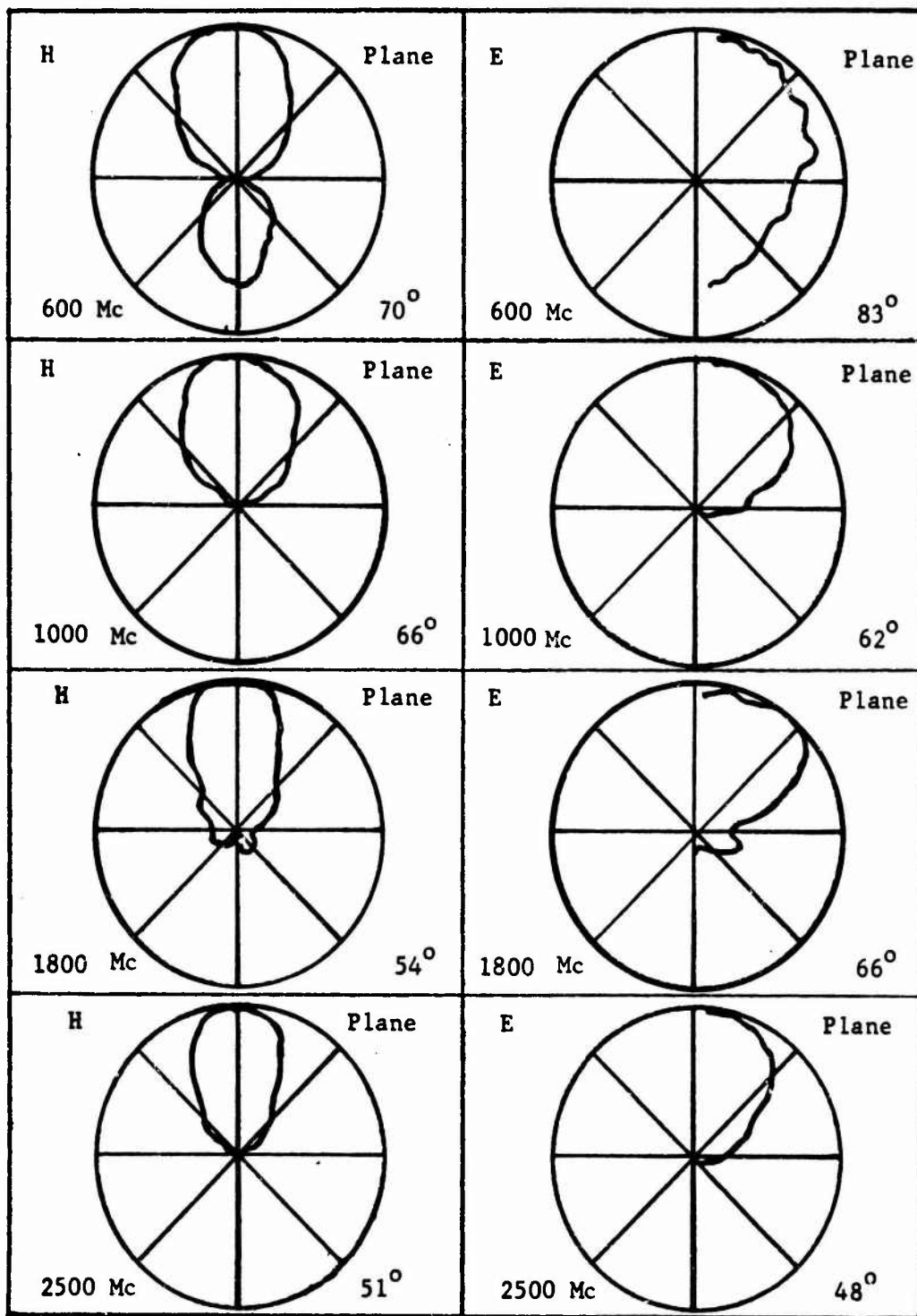


Fig. 51. Some radiation patterns of the slot array of Fig. 50.

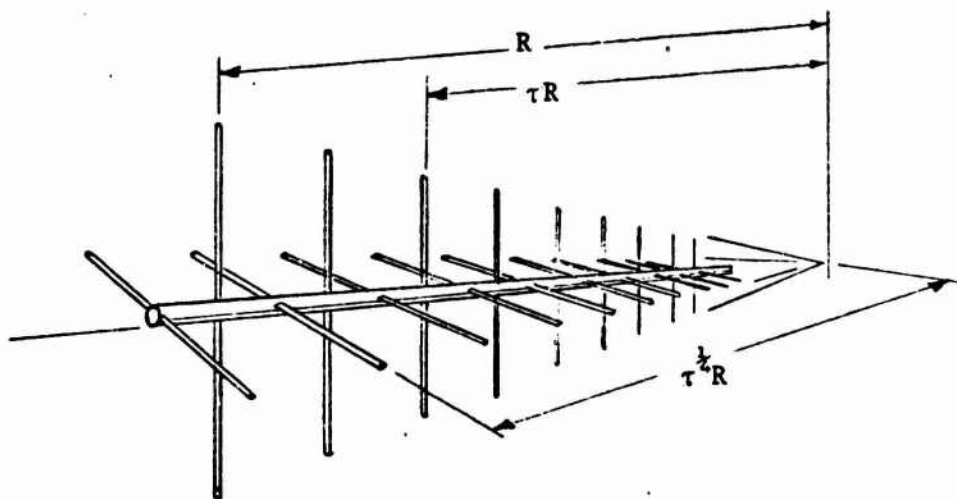


Fig. 52. A circularly polarized log periodic dipole array.

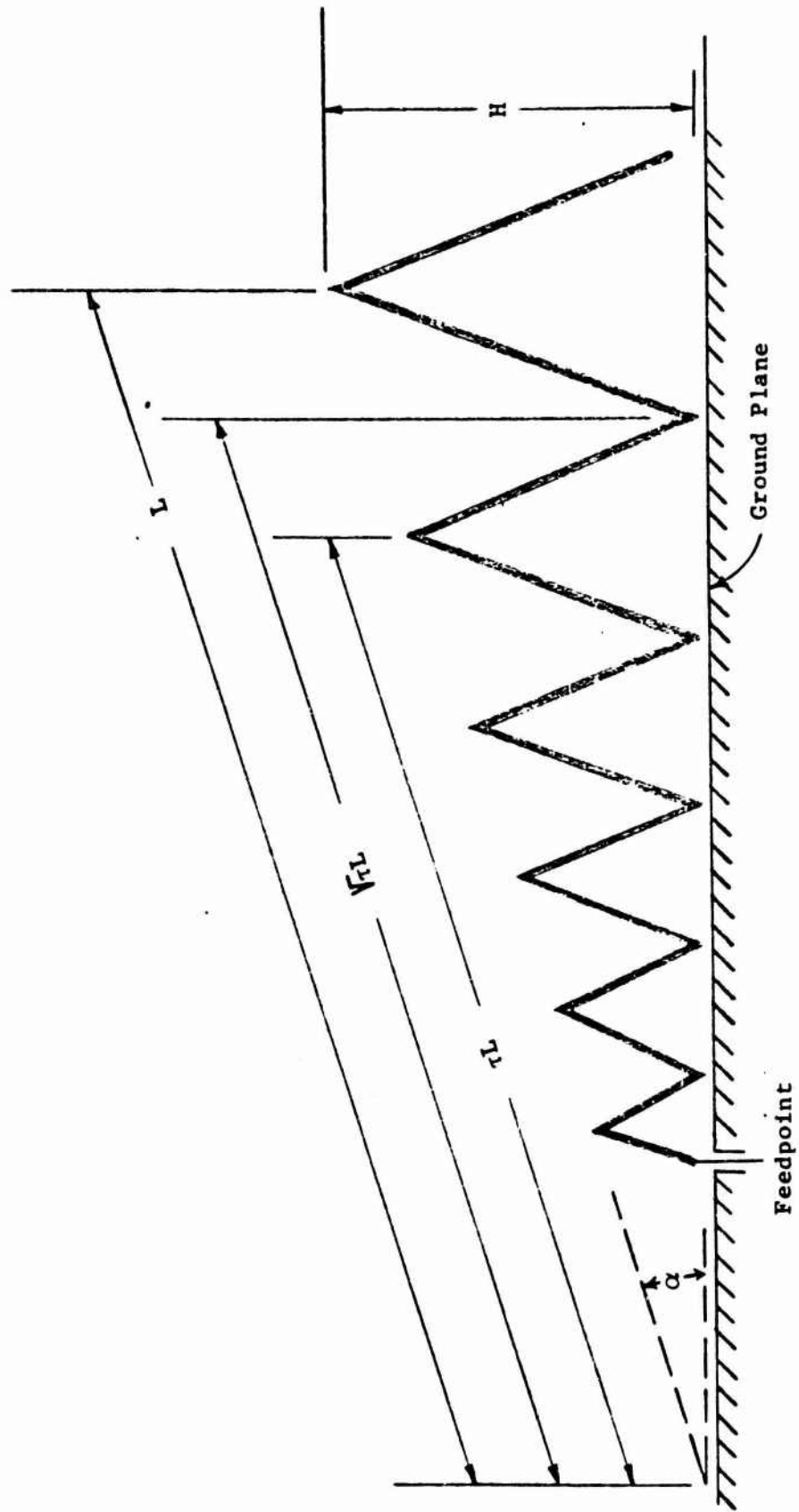


Fig. 53. Log periodic zigzag antenna on a ground plane.

not make it attractive at low frequencies, is that the height is rather large, exceeding one-half the maximum wavelength on the band covered.

The method of size reduction utilized in the log-periodic helical zigzag antenna is conceptually very simple. The linear conductors of the structure of Fig. 53 are replaced by helical ones (Fig. 54), the cell-to-cell phasing is then adjustable by changing the pitch angle of the helix. In fact, according to the discussion in Section I, the phase velocity along the wire of the helix is approximately that of light. Consequently, the propagation along the helix axis occurs at a velocity smaller than in the case of the simple linear conductor of Fig. 53, and the active zone occurs over increments considerably shorter than a half wavelength. However, to get the same directivity as a simple zigzag antenna, it is necessary to increase the length of the active zone since a reduction of broadside effect must be compensated by an increase of end-fire effect. In fact, the author suggests as a satisfactory set of parameters; a pitch angle of the helix, $\varphi = 30^\circ$, expansion factor $\tau = .9$ and $\alpha^\circ = 10^\circ$. Notice that such a small α gives origin to a long structure (see Section 2.3). Therefore, it is not clear whether the overall size of the antenna can be reduced. However, a reduction of one dimension at the expense of an increase of another can be useful for particular applications.

Array of Log-Periodic Structures

In Section 2.3, a special type of log-periodic antenna, the log-periodic array of dipoles, was considered in detail. It is a planar structure and therefore, in some respects is simpler than the one depicted in Fig. 25. Almost all the other practical structures consist of non-planar arrangements. In order to increase the gain, two log-periodic planar structures may be arrayed in a log-periodic fashion. This arrangement also simplifies the feeding problem, since it is possible to feed one-half structure against the other half. Arrangement of more than two structures are seldom used, because of difficulty in the feeding problem, and more importantly, because the increase of gain is modest while the radiation pattern is not too satisfactory. This is due to the inherent phase error, since for log-periodic operations, the phase centers must lie on a circle (see Subsection 1.4.2).

Let us consider an array of two-planar elements as in Fig. 25. If φ is the observation direction in the E plane and ψ is the angle between the planes of the two elements, the radiation pattern is given by

$$E = \cos^n\left(\frac{\varphi + \psi}{2}\right) \exp\left(j\beta d \sin\frac{\psi}{2} \sin\varphi\right) + \cos^n\left(\frac{\varphi - \psi}{2}\right) \exp\left(-j\beta d \sin\frac{\psi}{2} \sin\varphi\right) \quad (2.32)$$

where d is the distance of the phase center from the virtual apex and $\cos^n\frac{\varphi}{2}$ is an assumed function form for the element pattern. Although in (2.32) the interaction

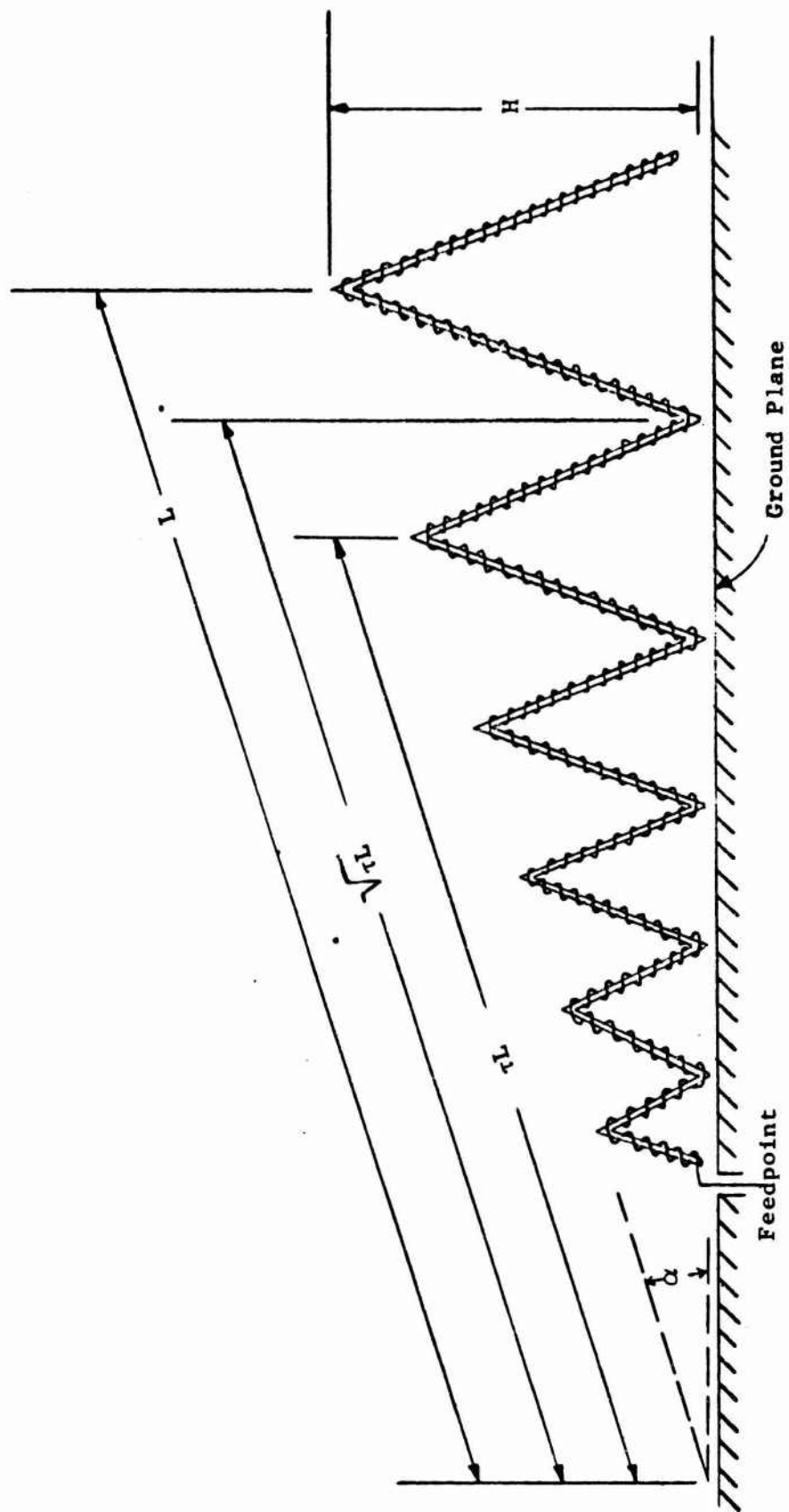


Fig. 54. Log periodic helical zigzag antenna on a ground plane.

effects between the two component structures are neglected, the expression is reasonably accurate. To practically find n , the beamwidth of a component structure is first determined. This can be obtained by data in the literature. Duhamel gives a plot of the pattern characteristics of wire trapezoidal tooth elements as a function of α for the minimum value of τ (for smaller τ the pattern degrades considerably) (Fig. 55 and [4]). It is then possible by using the empirical graph of Fig. 56, to obtain n , and therefore by using (2.32), to predict approximately the H plane pattern. The E plane pattern is the same as that for a single component structure and can be obtained by using the graph of Fig. 57, where the front-to-back ratio is also indicated.

The impedance behavior of these structures as a function of the various parameters is not clear. In general, it appears that a wire structure has a characteristic impedance somewhat higher than a sheet structure. There is no definite trend in the variation of impedance with τ . Some data on the impedance and SWR as a function of τ and ψ for particular structures can be found in the Antenna Handbook [4].

2.5 DESIGN OF LOG PERIODIC ANTENNAS

The design of a log-periodic array is still in many aspects an art rather than a science. Cut-and-try procedures, assisted by good physical intuition, are necessary to develop an antenna meeting given specifications. As pointed out in Section 1.5 about log spirals; it is rather simple to design a log-periodic antenna behaving reasonably well, but it is sometimes very hard to obtain a behavior closely following given specifications.

In reviewing the design procedure, we distinguish between antennas constituted by a single planar log-periodic structure (as the log-periodic dipole array), and by two component structures arrayed (as in Fig. 25).

Single Planar Structures

The only important antenna constituted by a single planar radiating structure is the log-periodic array of dipoles. Design data are discussed rather thoroughly in Section 2.3.6. Therefore, we will repeat only briefly the steps of the design procedure.

Assume that certain directivity and impedance are specified. A τ and σ can thus be chosen, taking in account that the number of the elements increases with τ , and that the boom length increases with σ . Given a certain specified directivity, the use of the graph of Fig. 47 allows determination of τ and σ . The angle α is a dependent quantity according to (2.16). The above procedures can be repeated in order to reduce the minimum beam length, keeping in mind that the best front-to-back ratio can be obtained by using a value of σ which is close to the optimum. The input impedance determines the characteristic impedance of the feeder line according to (2.31).

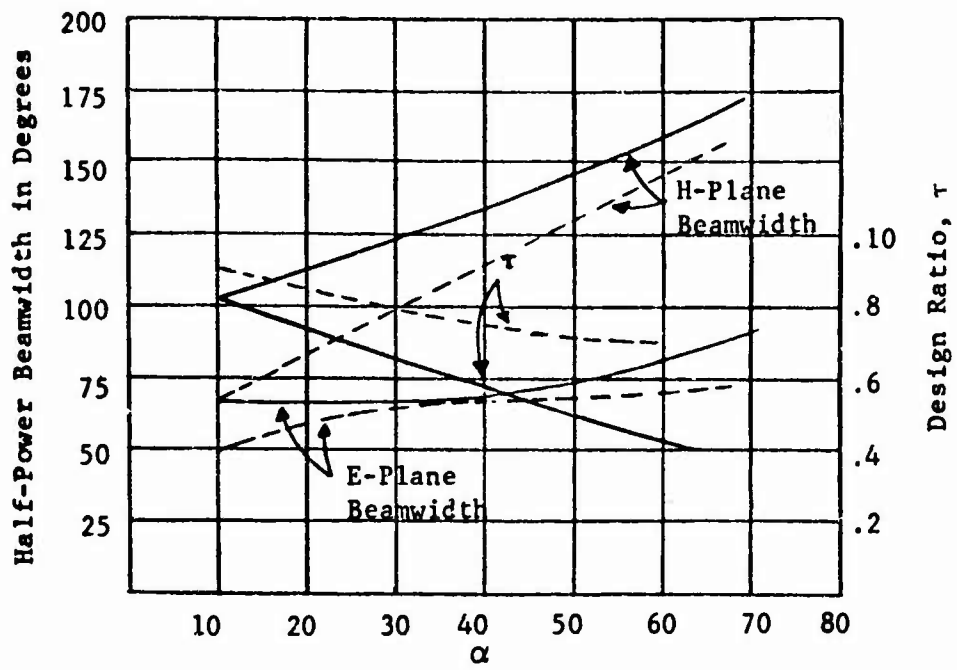


Fig. 55. Pattern characteristics of wire trapezoidal tooth element for: ——— approximate minimum value of τ .
 - - - A larger value of τ .

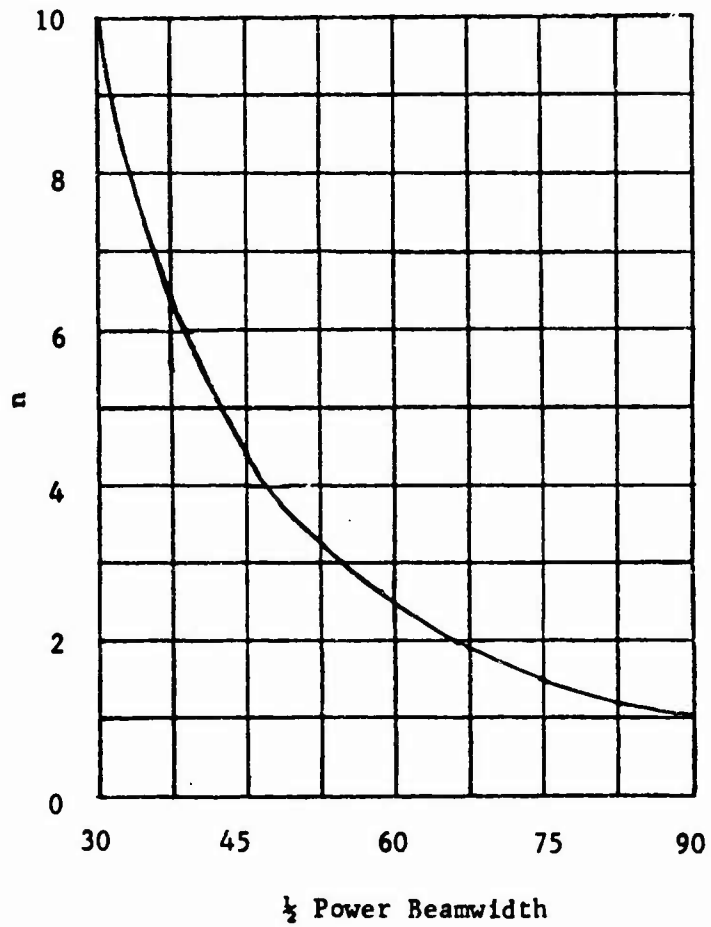


Fig. 56. Relation between element beamwidth and n .

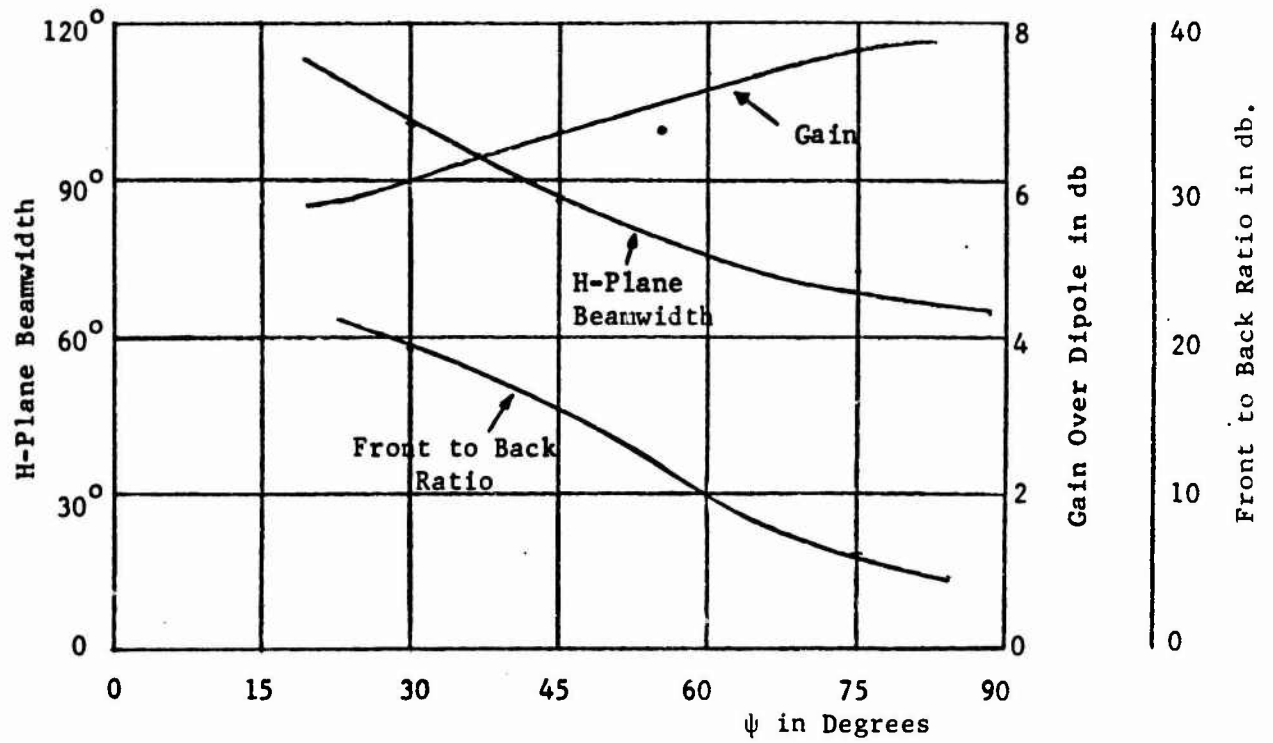


Fig. 57. Effect of angle ψ on pattern characteristics for antenna with $\alpha = 60^\circ$ and $\tau = 0.6$.

Array of Two Component Structures

Suppose that in the H plane the required beam is too narrow to be obtained by means of a single planar structure. In such a case, it is necessary to resort to an array configuration (Fig. 25). The equivalent broadside aperture D (distance between the phase centers of the two components structures) can be given by the following semi-empirical formula,

$$\frac{D}{\lambda} = \frac{40}{\psi} \quad (2.33)$$

which takes into account the directivity of a single structure (due to the end-fire effect). Aperture D can be computed with the data given by Fig. 48 (which holds approximately for any kind of log-periodic antenna). The design data given in 2.3.6 can be used (according to the procedure reported above) to determine all the other necessary parameters. Of course, for wire and tooth structures the data given by Carrell can be useful only for a very qualitative prediction of the radiation patterns. Alternatively, the graph of Fig. 55, where some data for wire and tooth structures are given, can be used. By using Fig. 56, the parameter n to be introduced into (2.32) can be determined. After choosing an angle ψ , (2.32) can give an idea of how the radiation pattern will look. The computation can be repeated several times to find a suitable value of ψ . The graph of Fig. 27 can help in a preliminary evaluation of the gain and the front-to-back ratio.

III. BROADBANDING CONVENTIONAL ANTENNAS

3.1 THE "SMALL ANTENNA" PROBLEM

We have seen in the previous Sections that the way to obtain antennas with frequency bands extremely extended is to use a certain class of structures geometrically characterized by being self-congruent, and having a peculiar type of current attenuation along the structure. The power (in transmission type of operation) is radiated by an active zone whose size counted in wavelengths is constant with frequency: this means that when the antenna is operated in the upper frequency range not all the structure is utilized. The size of this active zone is always of the order of one or several wavelengths and the gain obtainable from these antennas is low or moderate.

There are cases when the small size is desirable and the gain is not an important factor. This occurs generally at frequencies in the range of the Mc or of the tenths of Mc, often in vehicular applications. In such instances, if broadbanding is required, the basic F.I. or L.P approach is out of question. The antenna geometry is generally very simple (a simple stylus, for example, or a biconical structure), and broadbanding is attempted using an input network which matches the impedance rapidly varying with frequency.

It turns out that this approach has strong limitation in principle. In fact, as in any other linear network, the rate of variation of the input impedance of an antenna is rapidly increasing with the increase of the reactive energy (stored in the neighborhood of the antenna), which in turn increases at an extremely high rate if the size of the antenna is decreased behind a certain point. This and related questions (as the possibility of supergain antennas) have been the subject of some classical papers, and now are well clarified [55-57].

Chu considered the question of the physical limitations of an antenna omnidirectional in the azimuthal plane, and showed that the Q of the antenna, defined in a suitable way, increases at an astronomical rate if the size of an antenna is decreased under a certain value dependent upon the gain [55]. Later Harrington considered the more general case of a directive antenna [56], and showed that the maximum gain obtainable from a broadband antenna is approximately equal to that of a circular uniformly illuminated aperture whose diameter is equal to the maximum size of the antenna.

Here we will limit ourselves to the consideration of the omni-azimuthal case (which is the most important for this kind of application) and will examine the question of the limitation which the size of the antenna imposes on the frequency band. We will only require that the band is a maximum, without imposing any

requirement on the gain. We will find that the antenna which has the potentially broadest band is one which has a radiation pattern corresponding to that of an infinitesimally small dipole. This in turn leads to the conclusion that, for small antennas, trying to devise very complex structure is not a very promising approach to broadbanding, which must rather be attempted through a careful design of the input network. However, the results which can be expected are quite limited, if losses are not purposely introduced to reduce the Q, and consequently the efficiency, of the radiating system.

3.2 THE Q OF A RADIATING ELECTROMAGNETIC SYSTEM

The first exhaustive treatment of this problem has been given by Chu who found a lowest bound for the Q of a lossless antenna (defined later), once its maximum size is given, which is strictly related to its broadbanding potentiality.

Let the largest size of the antenna be $2a$, and let us imagine the complete antenna structure (including the source of power) enclosed inside a geometrical spherical surface of radius a . It is well known that the field outside the sphere is completely determined by the distribution of equivalent currents on the spherical surface and can be due to infinitely different distributions of sources inside the sphere. The Q of the antenna is defined as

$$Q = \begin{cases} \frac{2\omega W_e}{P} & \text{if } W_e > W_m \\ \frac{2\omega W_m}{P} & \text{if } W_m > W_e \end{cases} \quad (3.1)$$

where W_m and W_e are the average magnetic and electric energies stored in the neighborhood of the antenna and P is the power supplied at the antenna input. The justification of the definition (3.1) can be simply given by considering that the antenna will be always tuned with a reactance to give a resistive input. This therefore implies that the total average energy stored by the antenna and tuning network is as given in the numerator of (3.1).

It is rather difficult to determine the energy stored in the localized reactive field and to separate it from the radiation field. One method consists of recognition of the fact that the power flow from an antenna is equal to an energy density ($U_e + U_m$) multiplied by a velocity of energy flow. Then, for infinite U_e, U_m and the power flow may be readily evaluated and the velocity of energy flow determined [57]. If U_e and U_m are subtracted from the expressions

$\frac{\epsilon}{4} \underline{E} \underline{E}^*$ and $\frac{\mu}{4} \underline{H} \underline{H}^*$, giving the total energy density in the field, the remainder is the energy density associated with the reactive field. Chu's method, which is the one considered here, consists instead of finding for each of the spherical modes an equivalent network and reducing therefore the problem to circuit analysis [55].

3.3 EXPRESSION OF THE FIELD OF AN OMNIAZIMUTHAL ANTENNA

If we assume that the antenna is omniazimuthal and the system of current is vertical, i.e., in the direction of an axis z , associated in a standard way with a system of polar coordinates R, θ, φ , we have as the only nonvanishing field components:

$$\begin{aligned} H_{\varphi} &= \sum_n A_n P_n^1(\cos \theta) h_n(kR) \\ E_R &= -j \left(\frac{\mu}{\epsilon} \right)^{\frac{1}{2}} \sum_n A_n n(n+1) P_n(\cos \theta) \frac{h_n(kR)}{kR} \\ E_{\theta} &= j \left(\frac{\mu}{\epsilon} \right)^{\frac{1}{2}} \sum_n A_n P_n^1(\cos \theta) \frac{k}{kR} \frac{d}{dR} [R h_n(kR)] \end{aligned} \quad (3.2)$$

where $P_n(\cos \theta)$ is the Legendre polynomial of order n , $P_n^1(\cos \theta)$ is the first associated Legendre polynomial, $h_n(kR)$ is the spherical Hankel function of the second kind, $k = 2\pi/\lambda$, $\sqrt{\mu/\epsilon}$ is the wave impedance of a plane wave in free space and $1/\sqrt{\epsilon\mu}$ is the velocity of light. The A_n 's are a set of coefficients, generally complex.

The asymptotic expression for the field (i.e., that one valid in the far zone) is:

$$\begin{aligned} E_{\theta} &= \sqrt{\frac{\mu}{\epsilon}} \frac{e^{-jkr}}{kR} \sum_n A_n (-1)^{(n+1)/2} P_n^1(\cos \theta) \\ H_{\varphi} &= \sqrt{\frac{\epsilon}{\mu}} E_{\theta} \end{aligned} \quad (3.3)$$

The directivity gain is:

$$G(\theta) = \frac{|E_{\theta}|^2}{\int_0^{\pi} \int_0^{2\pi} |E_{\theta}|^2 \sin \theta d\theta d\varphi}$$

Putting $\theta = \frac{\pi}{2}$, (i.e., considering the directivity in the equatorial plane) and using the orthogonality properties of the associated Legendre polynomials we get, assuming all the A_n in phase (for maximum gain):

$$G\left(\frac{\pi}{2}\right) = \frac{\sum' A_n (-1)^{(n+1)/2} P_n^1(0)^2}{\sum' A_n^2 \frac{n(n+1)}{2n+1}} \quad (3.4)$$

where Σ' represents the sum over odd n only [55].

3.4 EQUIVALENT CIRCUITS OF THE VARIOUS MODES

The flow of the complex power computed at the surface of the sphere is the integral of the complex Poynting vector over the same sphere:

$$P(a) = j2\pi \sqrt{\frac{\mu}{\epsilon}} \sum' \frac{A_n^2}{k} \frac{n(n+1)}{2n+1} \rho h_n(\rho) \quad (3.5)$$

where $\rho = ka$, $h_n = h_n(\rho)$, $\rho h_n = \frac{d}{d\rho} \rho h_n(\rho)$. The real part is the average radiated power:

$$P_r = 2\pi \sqrt{\frac{\mu}{\epsilon}} \sum' \frac{A_n^2}{k} \frac{n(n+1)}{2n+1} \quad (3.6)$$

The expression (3.5) in which the orthogonal properties of the wave functions are clearly apparent, can be the starting point to devise an equivalent circuit for the various modes. If we replace the space outside the sphere by number of independent equivalent circuits (Fig. 58), each of them corresponding to a mode, their input voltages, currents and impedances are:

$$V_n = \sqrt{\frac{\mu}{\epsilon}} j \frac{A_n}{k} \left[\frac{4\pi n(n+1)}{2n+1} \right]^{\frac{1}{2}} (\rho h_n)' \quad (3.7)$$

$$I_n = \sqrt{\frac{\mu}{\epsilon}} \frac{A_n}{k} \left[\frac{4\pi n(n+1)}{2n+1} \right]^{\frac{1}{2}} \rho h_n \quad (3.8)$$

$$Z_n = j \frac{(\rho h_n)'}{\rho h_n} \quad (3.9)$$

The method which is used in [55] to find the reactive energy stored stems from the recognition that the impedance (3.9) (which is physically realizable)

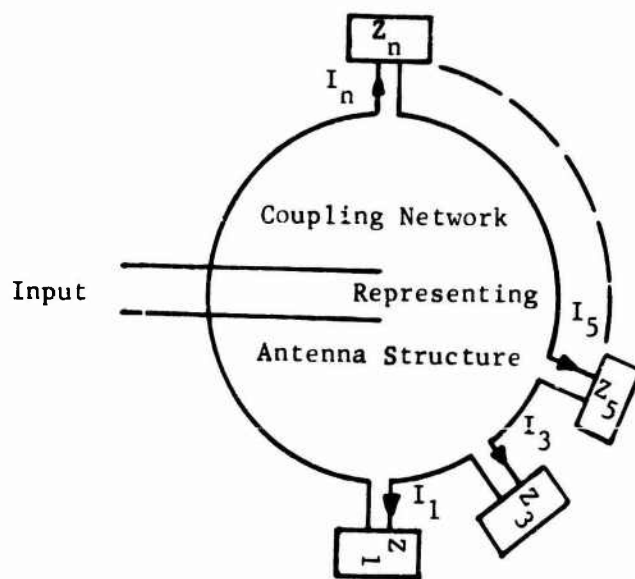


Fig. 58. Equivalent circuit of a vertically polarized omni-directional antenna.

can be written as a continued fraction by using some recurrence relations of Bessel functions:

$$Z_n = \frac{n}{j\rho} + \frac{1}{\frac{2n-1}{j\rho} + \frac{1}{\frac{2n-3}{j\rho} + \dots + \frac{1}{\frac{3}{j\rho} + \frac{1}{\frac{1}{j\rho} + 1}}}} \quad (3.10)$$

The circuit interpretation is a cascade of series capacitances and shunt inductances terminated with a unit resistance (Fig. 59). For $n = 1$, the field is the same as that of an elementary dipole and the equivalent circuit is shown in Fig. 60. It is apparent from (3.10) that the resistive element is hidden at the end of a series of high pass filter cells. The effect of an increase of frequency is equal to an increase of the radius of the sphere. It is therefore clear that practically, for an antenna of very small size with respect to the wavelength, the higher modes contribute only to the reactive energy and the radiation pattern is essentially that of a dipole. In principle, however, if the amplitudes of the higher modes are exceedingly high, it is possible to obtain arbitrarily shaped radiation patterns with an arbitrarily small antenna at the expense of an enormous increase of the reactive energy of the antenna.

To calculate the energy stored in the reactive elements of the equivalent bipolar network Z_n of Fig. 59 is a rather long procedure. However, in the neighborhood of the operating frequency, Z_n can be approximated by a simple series RLC circuit. The R_n , L_n , and C_n of the simplified equivalent circuit can be found by equating the resistance, reactance and frequency derivative of Z_n to these of the series RLC circuit. The results are:

$$R_n = |\rho h_n|^{-2}$$

$$C_n = \frac{2}{\omega} \left[\frac{dX_n}{d\omega} - \frac{X_n}{\omega} \right]^{-1}$$

$$L_n = \frac{1}{2} \left[\frac{dX_n}{d\omega} + \frac{X_n}{\omega} \right]$$

where

$$X_n = \left[\rho j_n (\rho j_n)' + \rho n_n (\rho n_n)' \right]$$

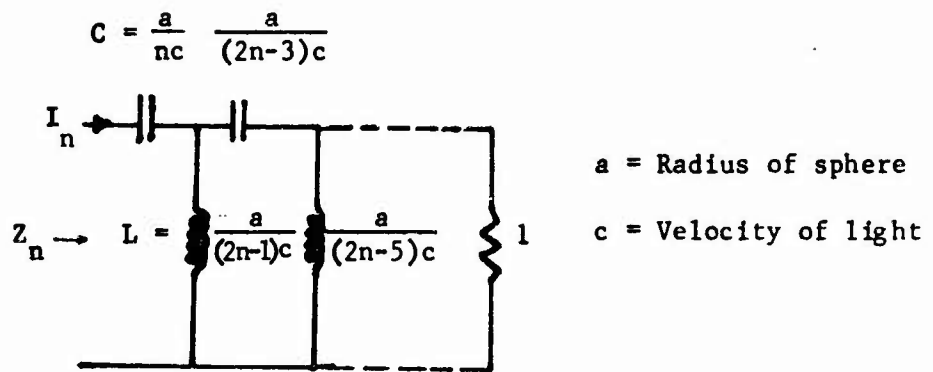


Fig. 59. Equivalent circuit of TM_n spherical wave.

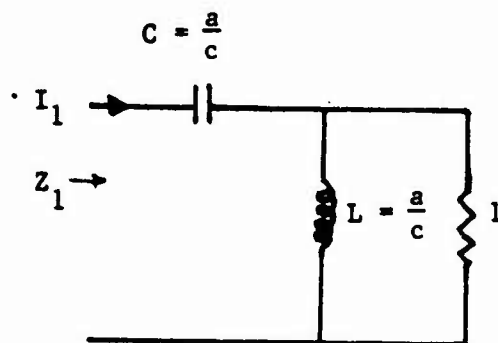


Fig. 60. Equivalent circuit of electric dipole

and j_n and n_n are the spherical Bessel functions of the first and second kind. The simplified circuit describes Z_n accurately enough in the immediate neighborhood of the operating frequency. If a Q_n for the n mode is defined

$$Q_n = \frac{2\omega W_n}{P_n} \quad (3.11)$$

where W_n is the average electric energy stored (which is higher than the magnetic energy) and P_n is the average dissipated power in Z_n . From the simplified circuit, there is obtained:

$$Q_n = \frac{1}{2} |\rho h_n|^2 \left[\rho \frac{dX_n}{d\rho} - X_n \right] \quad (3.12)$$

The bandwidth of Z_n (when externally matched with a proper amount of magnetic energy to make it resonant) is approximately equal to the reciprocal of Q_n . A plot of Q_n vs $2\pi a/\lambda$ for various n is given in Fig. 61. When $2\pi a/\lambda$ is of the order of n , Q_n is of the order of unity, and increases extremely fast when $2\pi a/\lambda$ decreases.

3.5 THE MINIMUM Q OF A SMALL LOSSLESS ANTENNA

For all n such that $\rho = 2\pi a/\lambda < n$ the spherical Hankel function $h_n(\rho)$ is essentially an imaginary positive quantity. Thus the currents of the equivalent circuits Z_n for n greater than the argument ρ are essentially in phase. This means therefore, that the electric energy stored in all the equivalent circuits oscillates in phase. It is clear then, that if the antenna is assumed lossless, its Q (defined in 3.1) is simply equal to

$$Q = \frac{2\omega \sum W_n}{\sum P_n} \quad (3.13)$$

where we recall that W_n and P_n are respectively the average reactive electric energy and the radiated power associated with the n th mode. We have assumed for the internal circuitry of the antenna (i.e., inside the spherical box of Fig. 58) the most favorable condition: no electrical energy stored, and magnetic energy in the right quantity to make the antenna resonate, i.e., the magnetic energy stored in the input network is equal to the sum of all the electrical energy stored in the Z_n equivalent circuits. In this hypothesis, (3.13) results consistent

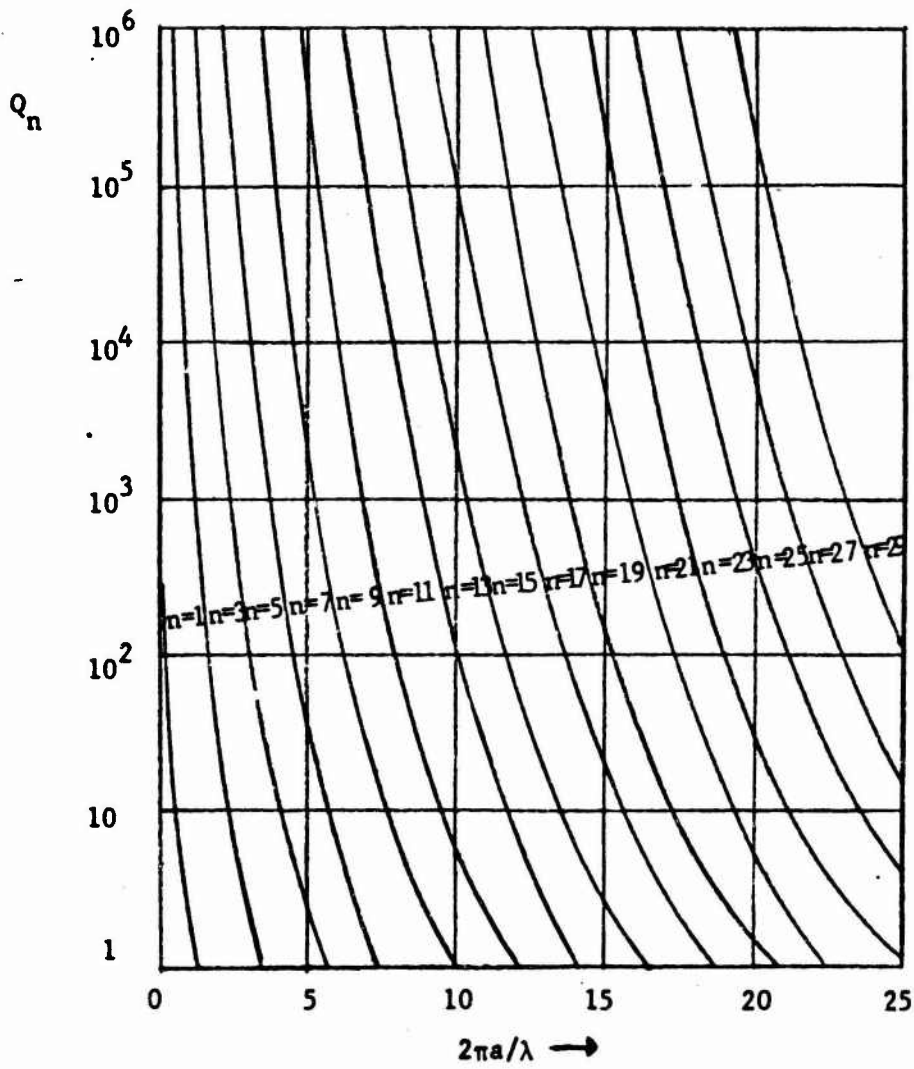


Fig. 61. Q_n of the equivalent circuit.

with the usual definition of Quality Factor for a circuit. It is easy to check that Q can be written

$$Q = \frac{\sum_n A_n^2 \frac{n(n+1)}{2n+1} Q_n(ka)}{\sum_n A_n^2 \frac{n(n+1)}{2n+1}} \quad (3.14)$$

where Q_n 's are given by (3.11) and the dependence upon a is explicitly pointed out. The Q so defined, when it is high, can be interpreted as the reciprocal of the fractional frequency bandwidth of the antenna. When it is low, however, it can be considered only qualitatively as an indication that the antenna is broadband.

It is possible to minimize (3.14) under the constraint of a certain gain and can be shown that the maximum gain which can be obtained with a reasonable value of Q is $\approx 4a/\lambda$. We will consider however the other related question which is perhaps more important for omni-azimuthal antennas: which is the minimum Q of an antenna of a given size when no constraint on the gain is given? Or in other words, which is, for a given a , the optimum combination of the model coefficients A_n 's in order to obtain the absolute minimum Q? From the expression (3.14) the answer is apparent. Since the various Q_n have different values, and the minimum is Q_1 , it results that the antenna generating a field outside the sphere corresponding to the first transverse magnetic mode (i.e., the field of an elementary dipole) is the one with greater broadband potentiality. The gain of this antenna is 1.5.

3.6 QUALITATIVE DISCUSSION

The discussion in the previous section has been rather theoretical. We have considered an antenna in free space and have seen what the radiation pattern must be in order to obtain the minimum Q or, equivalently, the maximum band of the antenna. We have not considered the effect of the nearby objects which will always be present. The only case in which the effect of a physical structure can be easily taken in account is when a ground plane is present, and in such a case the theory is still valid with only minor modifications. For every practical structure the theory is unable to predict the effects, except in a rough qualitative way. For example, let us suppose that the antenna current distribution has been carefully chosen to have a gain higher than $4a/\lambda$ when isolated

(and we do not want to consider here the difficulties of fulfilling this task). This means that the antenna has also high Q , and large reactive fields in its neighborhood. If the antenna is in proximity of other structures, these fields (and of course the radiation field) will induce currents on them. The radiation pattern will as a result be modified, with a decrease of the gain. On the basis of this consideration it does not seem advisable to try to devise complicated structures for small antennas in an attempt to increase the gain. Moreover, a high Q means also (for every practical structure) very high conduction losses, which will reduce the efficiency of the antenna. The general conclusions which can be deduced by Chu's analysis are the following:

- For small antennas, there is a practical impossibility of obtaining gain higher than 1.5 (the gain of an elementary dipole). This does not completely exclude the possibility of modest increase of directivity at the expense of correspondent increase in losses.
- The Q of the antenna is the lowest if the antenna generates a pure dipole field. This is clearly impossible for practical structures, but can be better approximated if complicated geometries are avoided. We have to take in account however that the "output surface" of a practical antenna is not a sphere. For example, for a simple stylus it is a cylinder. Therefore, even if outside the sphere (having its diameter equal to the maximum size $2a$ of the antenna) all the waves different from the dipole mode are strongly attenuated; nevertheless, the reactive field can be very strong in the space between the output surface, increasing the Q of the antenna. This again suggests use of a structure with simple geometries, and avoidance of conductors with small radius of curvature¹.

Once the maximum size ($2a$) of one antenna is given, the maximum bandwidth of its input impedance (obtained by using a proper matching network) is determined. In fact, the Q of the antenna (supposed lossless) is always less than $Q_1(ka)$. Therefore, assuming this value for the Q and assuming an equivalent circuit as in Fig. 60, is a conservative hypothesis. A theoretical study on the possibility of broadbanding a given bipolar network by using a matching quadripole was made by Fano [58]. Based on its computation Chu gave a curve, valid for an antenna

¹ It is well known, for example, that a thick dipole is more broadband than a thin one, and a biconical antenna is more broadband than a dipole.

having $Q = Q_1(ka)$. Fig. 62 shows the fractional bandwidth, for an assumed allowable reflection coefficient, as a function of the size of the antenna, when the antenna is optimally matched (i.e., is connected to the generator through a passive lossless network which gives a constant amplitude of the reflection coefficient throughout the band). This curve can be very useful in determining an upper bound on the frequency bandwidth to be expected from a given antenna. For example, consider a short dipole with length 0.1λ , and assume an allowable reflection coefficient of 0.5 (which corresponds to a SWR of approximately 3 and an efficiency of about 75%). In this case we obtain from the graph of Fig. 62

$$-\frac{2}{\pi} \frac{\Delta B}{f} \log |\Gamma| \approx .1$$

which gives $\Delta B/f \approx 25\%$. From the curve it is seen that the band decreases very fast with the size. For example, for an antenna whose size were 0.01λ , in absence of conduction losses, the band for the same maximum reflection coefficient is approximately .022%. However, for antennas of such a small size the theory is hardly applicable since very large reactive currents and very high conduction losses also occur. For example, antennas for VLF (which are always electrically small) can have conduction losses ranging from 80% to 90% of the input power.

3.7 NETWORK THEORETICAL APPROACH

In the previous section the problem of the minimum Q (and therefore of the maximum bandwidth) of a lossless antenna of a given overall size has been investigated. Chu's theory allows to predict an upper bound of what can be expected from a small antenna. A practical antenna will have a model structure different from the ideal antenna having $Q = Q_1$. The configuration of the field will certainly be more complicated with a doublefold effect: to increase the reactive energy and also to increase the power loss because of the currents on the structure. As a consequence of these two contrasting effects, it is not clear which will be the overall effect on the Q of a structure. The present state of the theory clarifies what we cannot expect from a certain structure but it is not, however, able to predict the actual behavior of a practical antenna given its physical configuration, or to suggest which configurations can be recommended in order to have a behavior close to the theoretical limit.

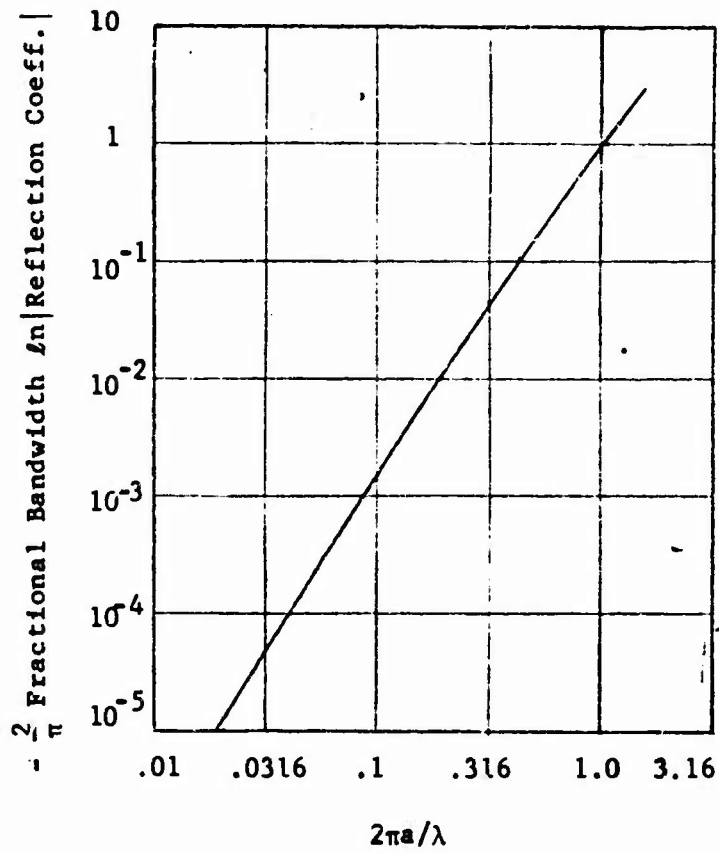


Fig. 62. Bandwidth of an ideal dipole with ideal matching network.

Instead of attempting to design an optimum structure, a less ambitious program can be followed: designing the antenna on an empirical or semiempirical basis, taking measurements of its input impedance behavior with frequency, and then from the knowledge of these data, rationally designing the "best" network (in some sense). This sort of approach, in other words, does not investigate the electromagnetic behavior of the structure and reduces the question to a network theoretical type of problem [59].

The input impedance of a lumped element circuit can be analytically described, as it is well known, by a rational algebraic function. Distributed systems on the other hand can be described, in general, by meromorphic functions. To show this point in a simple way, (related to the treatment of the previous section), we can say that for an arbitrary structure in general the mode expansion of the field will contain an infinite number of terms; therefore, the equivalent circuit of Fig. 58 will be constituted by an infinite number of bipolar networks. Consequently, the input impedance function will contain an infinite number of poles; i.e., will be a meromorphic function. The idea in Ref. [59] is to approximate the actual impedance function with a rational algebraic function (or equivalently to substitute the distributed circuit with a lumped one), and then to match it with a quadri-polar lossless network.

As a first approximation of the impedance, the simple rational function

$$\mu(p) = \frac{C_1 p^2 + C_2 p + C_3}{p^3 + C_4 p^2 + C_5 p} \quad (3.15)$$

can be chosen where the C_i 's are constant to be determined and

$$p = \sigma + ja$$

is the complex frequency.

The first requirement for this function is to be "positive real" or in other words to represent a physical network. Furthermore, the real part must be evidently zero at zero frequency. These are general requirements which impose constraints on the C_i 's. The determination of the C_i 's will be then completed by requiring that (3.15) behaves as close as possible to the actual antenna impedance. Without reporting here the details of the method which the authors of Ref. [59] used, it can be said that essentially the modulus of the difference between the reflection coefficient (amplitude and phase) obtained by actual measurement and that one calculated from the expression (3.15), (with the C_i 's still

unknown) is minimized with respect to the C_i 's. When (3.15) is so determined, network theory allows finding the optimum matching quadripole given a certain value of the maximum allowed reflection coefficient on the operating bandwidth. We will not consider here this last problem, which is essentially a network theoretical problem.

The authors give some example of the application of this method, showing, for example, that with a proper matching network a slot backed by a cavity has a band of about 50% narrower than its "end loaded" version (which is the magnetic equivalent of the capacitance loaded dipole).

BLANK PAGE

IV. CONCLUSIONS AND RECOMMENDATIONS

4.1 CONCLUSIONS

The overall size is perhaps the physical quantity which most strongly constrains the characteristics obtainable from an antenna. The frequency band of an antenna "electrically small" is always very limited, even if the theoretically optimum input network is used. Its actual value, of course, depends upon the size. Practical small antennas are generally linearly-polarized and the directivity is that of a small dipole.

Logarithmic spiral and logarithmic periodic antennas are different from all other antennas because of the peculiar property of being "active" only in a limited part of their structure, in such a way that their electrical size, so to speak, remains constant in terms of wavelengths for a wide band of frequencies. In theory, the frequency band can be made as large as wanted, just by increasing the overall size of the antenna. From an engineering point of view, however, in this way only the lower limit of the frequency band is determined. The upper bound is determined by different factors, such as structural mechanical problems and fabrication tolerance considerations. The geometrical and electrical requirements which must be satisfied are the following:

(a) The antenna must be geometrically self-congruent after an expansion with respect to an infinite discrete (in the case of log periodic) or continuous (for log spiral) set of expansion ratios.

(b) The current must decay along the structure faster than the inverse of the distance from the feeding point.

These antennas are not small in terms of wavelengths. Their size is always of the order of magnitude of the largest operating wavelength. The gain is small or moderate and the polarization can be either linear or circular.

The theory of log periodic and frequency independent antennas is not well developed; we have seen that the only approach having thus far been developed is the analysis of the periodic counterpart of the structure. If this analysis can be accomplished, the Brillouin diagram can be used in an approximate way for the slowly-tapered structure. The analysis of the simplified problem is still very difficult. The array of dipoles is the only practical structure which has been solved [40]. In this case, the solution was only approximate and was found by considering the coupling of each radiator with the closest elements only. The approximation is good for large spacings but degrades for spacings smaller than a wavelength. This degradation of solution accuracy is unfortunately the case for log periodic arrays of dipoles, since the ratio between spacing

*In Table 2, some of the characteristics of these broad classes of antennas considered in this report, i.e., frequency independent, log periodic, and small antennas are indicated. Of course, the table has only indicative values.

Table 2. Summary of Usual Values of Some Physical Parameters of the Antennas Considered in this Report

	Polarization	Directivity with Respect to an Isotropic Radiator	3 db Beamwidth	Bandwidth	Input Impedance
Log Spiral (Frequency Independent Antennas)	Circular	3 - 7 db	70° - 180°	Can be in principle made as large as wanted	Essentially resistive 70 - 200 ohms
Log Periodic Antennas	Linear or Circular	4 - 15 db	E plane 80° - 100° H plane 70° - 180°	Can be in principle made as large as wanted	Essentially resistive 50 - 200 ohms
"Small" Antennas	Generally Linear	~ 2 db	E plane ~ 90°	Generally very narrow	Rapidly varying with frequency (can be compensated on a narrow band, very sensitive to the environment)

and wavelength in the active zone is usually smaller than 0.1. It would be desirable to find a method by which the approximation improves with decrease in spacing. A promising method based on the use of Fourier Analysis is described briefly in the following section.

4.2 RECOMMENDATIONS FOR FURTHER STUDIES

Because of the general nature of this survey and the Army's broad interest in antennas for many applications covering the entire frequency spectrum (i.e., all frequencies of use to communications and radar) and a wide variety of antenna characteristics, the recommendation is for a theoretical study which has the purpose of developing a better understanding of the behavior of wideband antenna structures. The body of this report clearly indicates the lack of adequate theoretical treatment. This recommendation for further studies leaves open the approaches which may be considered; obviously, this must be nature of research studies in order to allow generation and evaluation of new concepts. However, to show that further meaningful research in this area may be conducted, a rather specific approach to the solution of periodic-like structures is outlined below.

The use of Fourier Transforms in certain types of electromagnetic problems can be often very convenient [59, 60]. It has been used to determine the driving point impedance of a phased planar array of dipoles in a rectangular arrangement [62], and in a general periodic arrangement [63]. It has not been used to the author's knowledge to determine the surface waves or the leaky waves in an (either bidimensional or linear) array of dipoles (similar to Fig. 30). To indicate how this method can be used for this problem, consider the following approach: It is possible to determine an expression of the impedance of an element complex in the form of a series, the terms of which are proportional to the square of the bidimensional Fourier transform of the current in the single element with respect of the coordinates in the plane of the array, sampled at certain points depending upon the unknown complex propagation constant. We can equate this impedance to the opposite of the impedance looking into the feeding line (Fig. 30 and 32). A "Transverse Resonance" equation is thus established in a form of a series whose terms contains the unknown propagation constant. The various solutions are the propagation constants of the various modes. An interesting feature of this equation is that it is simplified as element spacing is decreased; it is possible to show that the number of non negligible terms of the series increases with the spacing.

Following this Fourier Analysis approach, it may be possible to achieve new steps in the development of the theory of log periodic antennas. It is highly desirable that

further theoretical work be done. New insight on the behavior of these interesting and peculiar structures is very important to put the design criteria on a sounder theoretical ground. Further work on this field could include the following tasks:

(a) Analysis of the modes in a structure composed of an infinite number of dipoles fed by a line (Fig. 30). This could be done, as mentioned previously, by using a Fourier analysis technique. It would be very interesting to compare these results with those obtained for the same problem as described in Ref. [40].

(b) With the analytical results of task (a), it is believed that solutions to the "source problem" can be achieved. In other words, to consider not just the free modes on the structure (without excitation), but the radiation when an element is driven.

(c) Research in a different direction could be an attempt to use the method outlined above to analyze a periodic structure of a more complex type (e.g., the periodic counterpart of the sawtooth structure of Fig. 25). The results of this analysis as compared with the results concerning the array of dipoles would clarify how the nature of the single element influences the behavior of the array. These results would be extremely useful for design purposes.

(d) A fourth (and more ambitious) task will be to seek a method for treating not the simple periodic, but the actual log periodic array. Although it can be anticipated that the fulfillment of this task will be very difficult, there are hopes that the use of some special functional transform can be a first step toward the solution of this challenging problem.

V. REFERENCES

- [1] Carrel, R.L., "Analysis and Design of the Log-Periodic Dipole Antenna," Technical Report No. 52, Contract AF 33(616)-6079, Antenna Laboratory, University of Illinois, Urbana, Illinois, October 1961.
- [2] Rumsey, V. H., "Frequency Independent Antennas," IRE National Convention Record, Pt. I, pp. 114-118
- [3] Mitra, R., and K.E. Jones, "On Continuously Scaled and Log-Periodic Structures," Technical Report No. 73, Contract AF 33(657)-10474, Antenna Laboratory, University of Illinois, Urbana, Illinois, Sept. 1963.
- [4] Deschamps, A., and R. H. Duhamel, "Frequency-Independent Antennas," Chapter 18, Antenna Engineering Handbook, edited by Henry Jasik, McGraw-Hill, Inc., 1961.
- [5] Cheo, B.R.S., V.H. Rumsey, and W.J. Welch, "A Solution to the Frequency Independent Antenna Problem," IRE Transactions on Ant. and Prop., Vol. AP-9, No. 6, Nov. 1961, pp. 527-534.
- [6] Rumsey, V.H., "A New Way of Solving Maxwell's Equations," IRE Transactions on Ant. and Prop., Vol. AP-9, No. 5, Sept. 1961, pp. 461-466.
- [7] Cheo, B.R.S., "A Solution to the Equiangular Spiral Antenna Problem," University of California, Berkeley, Cal., Institute of Engineering Research Report, Series No. 60, Issue No. 324, Nov. 1960, U.S. Army Signal Research and Development Laboratory Contract No. DA-36-039 SC-84923.
- [8] Bernard, G.D., and Akira Ishumaru, "A Class of Equiangular Spiral Antenna Excited by A Vertical Dipole," University of Washington, College of Engineering, Dept. of EE, Technical Report No. 92, Dec. 1964.
- [9] Copeland, J.R., "Radiation From the Balanced Conical Equiangular Spiral Antenna," Ohio State University Research Foundation Report, Sept. 1960.
- [10] Turner, E.M., "Spiral Slot Antenna," WADC, Dayton, Ohio, Tech. Note WCLR-55-8 (1955) Unpublished.
- [11] Turner, E.M., "The Scimitar Antenna," Proc. IRE Nat'l. Aerospace Electronics Conf., (1956).
- [12] Turner, E.M., "Broadband Radiators," Proc. IRE Nat'l. Aerospace Electronics Conf., (1958).
- [13] Jones, S.R., and E.M. Turner, "Polarization Control with Opposely Sensed Circularly Polarized Antennas," Proc. IRE Nat'l. Aerospace Electronics Conf., pp. 588-595, (May 1959).
- [14] Bawer, R., and J.J. Wolfe, "The Spiral Antenna," IRE International Convention Record, Pt. 1, 84-95 (1960).

- [15] Kaiser, J.A., "The Ardimedeian Two Wire Spiral Antenna," IRE Trans. on Ant. and Prop., Vol. AP-8, pp. 312-323.
- [16] Donnellan, J.R., "Second Mode Operation of the Spiral Antenna," IRE Trans. AP-8, p. 637 (Nov. 1960).
- [17] Curtis, W.L., "Spiral Antennas," IRE Trans. of Professional Group on Ant. and Prop., Vol. AP-9, May 1960.
- [18] Tamir, T., "Wave Types on Open Periodic Structure," Proceedings of the Applications Forum on Antenna Research, Univ. of Illinois, Urbana, Ill., 1964.
- [19] Tamir, T., and A.A. Oliner, "Guided Complex Waves; Part I - Waves at an Interface," Proceedings of the IEEE, Vol. 110, No. 2, (Feb. 1963), pp. 310-324.
- [20] Tamir, T., and A.A. Oliner, "Guided Complex Waves: Part II - Relation to Radiation Patterns," Proceedings of the IEEE, Vol. 110, No.2 (Feb. 1963), pp. 325-355.
- [21] Tamir, T., and A.A. Oliner, "The Spectrum of Electromagnetic Waves Guided by a Plasma Layer," Proceedings of the IEEE, Vol. 51, No. 2 (Feb. 1963), pp. 317-332.
- [22] Collin, R.E., Field Theory of Guided Waves, McGraw-Hill, Inc., 1960, pp. 453-506.
- [23] Watkins, D.A., "Topics in Electromagnetic Theory," John Wiley and Sons, Inc., 1958, Chapter 1.
- [24] Collin, R.E., "Op. cit.," Chapter 9.
Chapter 9.
- [25] Mayes, P.E., and G. A. Deschamps, and W. T. Patton, "Backward-Wave Radiation from Periodic Structures and Application to the Design of Frequency Independent Antennas," Proceedings of the IRE, Vol. 49, No. 5 (May 1961), pp. 962-963.
- [26] Mayes, P.E., G.A. Deschamps, and W. T. Patton, Technical Report No. 60, Contract AF 33(616)-8460, (Dec. 1962), Dept of EE, Univ. of Illinois, Urbana, Illinois.
- [27] Sensiper, S., "Electromagnetic Wave Propagation on Helical Conductors," S.D. Thesis, Mass. Inst. of Tech., Cambridge, Mass., 1951.
- [28] Watkins, D.A., "Op. cit.," Chapter 3.
- [29] Watkins, D.A., "Op. cit.," Chapter 2.

- [30] Dyson, J.D., "The Equiangular Spiral Antenna," Univ. of Illinois, Urbana, Illinois, Tech. Report No.21, Contract AF(33) 616(3220), Sept. 15, 1957.
- [31] Dyson, J.D., "The Equiangular Spiral Antenna," IRE Trans. on Ant. and Prop., Vol. AP-7, April 1959, pp. 181-188.
- [32] Dyson, J.D., "The Unidirectional Equiangular Spiral Antenna," IRE Trans. on Ant. and Prop., Vol. AP-7, Oct. 1959, pp. 329-334.
- [33] McClelland, O.L., "An Investigation of the Near Fields on the Conical Equiangular Spiral Antenna," Univ. of Illinois, Urbana, Illinois, Antenna Lab Tech. Report No. 55 Contract AF 33(657)-8460.
- [34] Tang, C.H., "A Class of Modified Log-Spiral Antennas," IEEE Trans. on Ant. and Prop., Vol. AP-11, No. 4, July 1963, pp. 424-427.
- [35] Dyson, J.D., and P.E. Mayes; "New Circularly-Polarized Frequency Independent Antennas with Conical Beam or Omnidirectional Patterns," Trans. on Ant. and Prop., Vol. AP-9, No. 4, July 1961, pp. 334-341.
- [36] Dyson, J.D., "The Coupling and Mutual Impedance Between Balanced Wire-Arm Conical Log Spiral Antennas," Univ. of Illinois, Urbana, Ill., Ant. Lab, Tech. Report No. 54, Contract AF33 (657)-8460.
- [37] Norman, J.E., S.B. Rhee, G.G. Rossivier, and A.I. Simanyi, "Study and Investigation of a UHF and VHF Antenna," Univ. of Michigan, College of Eng., Dept of EE, Contract No. AF33 (657) 10607, Sept. 1964.
- [38] Duhamel, R.H., and D.E. Isbell, "Broadband Logarithmically Periodic Antenna Structures," IRE Nat'l. Convention Record, Pt. I, pp. 119-128, 1957.
- [39] Rumsey, V.H., "Propagation Over a Sheet of Sinusoidal Wires and Its Application to Frequency Independent Antennas," Elec. Res. Lab., Univ. of Cal., Tech. Report Series No. 60, No. 479, Contract DA-36-039 SC-88924.
- [40] Mittra, R., and K.E. Jones, "Theoretical Brillouin ($k-\beta$) Diagrams for Monopole and Dipole Arrays and Their Application to Log Periodic Antennas," IEEE Trans. on Ant. and Prop., Vol. AP-12, Sept. 1964.
- [41] Isbell, D.E., "Log-Periodic Dipole Arrays," IRE Trans. on Ant. and Prop., May 1960, pp. 260-267.
- [42] Mayes, P.E., and P.G. Ingerson, "Near-Field Measurements on Backfire Periodic Dipole Arrays," Research Studies on Problems Related to Antennas, Ant. Lab., Univ. of Ill., Quarterly Prog. Rep. No. 1, Jan. 1963.
- [43] Kraus, J.D., Antennas, McGraw-Hill Book Co., Inc., 1950, Chapt. 10.
- [44] Mittra, R., and K.E. Jones, "On Continuously Scaled and Log-Periodic Structures," Dept. of EE, Univ. of Ill., Ant. Lab., Tech. Report No. 73, Jan. 1964.
- [45] Morse, P.M., and H. Feshbach, Chapter 9, pp. 1092-1106.

- [46] Rumsey, V.H., "A Short Way of Solving Advanced Problems in Electromagnetic Fields and Other Linear Systems," IEEE Trans. on Ant. and Prop., Vol. AP-11 Jan. 1963, pp. 73-86.
- [47] Ore, F., "Log Periodic Folded Monopole Array," Radiolocation Res. Lab., Dept. of EE, Univ. of Ill., RRL. No. 247.
- [48] Mikenas, V.A., "A Log-Periodic Cavity-Backed Slot Antenna," Dept. of EE, Univ. of Ill., June 1964.
- [49] Freiser, J.W., "Research of Log-Periodic Array of Slots," Tech. Rep. No. 3, Ant. Lab., Dept. of EE, Univ. of Ill., Jan. 1964.
- [50] Duhamel, R.H., and F.R. Ore, "Logarithmically Periodic Antenna Designa," 1958 IRE Nat'l, Conv. Record, Pt. 1, pp. 161-174.
- [51] Collins Radio Co., Dallas, Texas, Final Progress Report on Development of Antenna AN/TLA-7, Aug. 1963.
- [52] Univ. of Pennsylvania, The Moore School of Electrical Engineering, "Study of Power Density Measurement Techniques," Moore School Rep. No. 62-19.
- [53] Yaminy, R.R., "The Log-Periodic Helical ZigZag Antenna," Tech. Rep. No. 9, Dept. of EE, Univ. of Ill., June 1965.
- [54] Carr, J.W., "Some Variations in Log-Periodic Antenna Structures," IEEE Trans. on Ant. and Prop., Vol. AP-9, No. 2, p. 229, March 1961.
- [55] Chu, L.J., "Physical Limitations of Omni-Directional Antennas," J. of Applied Physics, Vol. 19, Dec., 1948, pp. 1163-1175.
- [56] Harrington, R.F., "Effect of Antenna Size on Gain, Bandwidth, and Efficiency," J. Res. NBS, Vol. 64D, No. 1, pp. 1-12, Jan., 1960.
- [57] Collin, R.E., and S. Rothychild, "Evaluation of Antenna Q," IEEE Trans. on Ant. and Prop., Vol. AP-12, No. 1, Jan. 1964, pp. 23-27.
- [58] Fano, R.M., "Theoretical Limitations on the Broadband Matching of Arbitrary Impedances," R.L.E. Tech. Report No. 41, Jan. 1948.
- [59] Borgiotti, G. V., "Fourier Transform Method in Aperture Antennas Problems," Alta Frequenza, Vol. 32, No. 11, Nov. 1963.
- [60] Rhodes, D. R., "On a Fundamental Principle in the Theory of Planar Antennas," Proc. of IEEE, Sept. 1964.
- [61] Stark, L., "Radiation Impedance of a Dipole in an Infinite Planar Array," Radio Science, Vol. 1 (New Series) pp. 361-377, March 1966.
- [62] Borgiotti, G. V., "Impedance and Gain of a Dipole in an Infinite Periodic Phased Array," Research Triangle Institute, Tech. Report RTI-TMR22, March 4, 1966.

Unclassified

Security Classification

DOCUMENT CONTROL DATA - R&D		
<i>(Security classification of title, body of abstract and indexing annotation must be entered when the overall report is classified)</i>		
1. ORIGINATING ACTIVITY (Corporate author) Research Triangle Institute		2a. REPORT SECURITY CLASSIFICATION Unclassified
		2b. GROUP NA
3. REPORT TITLE A Survey of Available Information Relative to Achieving Ultimate Antenna Bandwidths		
4. DESCRIPTIVE NOTES (Type of report and inclusive dates) Final Report 31 Jul 66		
5. AUTHOR(S) (Last name, first name, initial) Borgiotti, G. V.		
6. REPORT DATE 31 July 1966	7a. TOTAL NO. OF PAGES 118	7b. NO. OF REFS 62
8a. CONTRACT OR GRANT NO. DA31-124-ARO-D-396	9a. ORIGINATOR'S REPORT NUMBER(S) RTI Program RU-224	
b. PROJECT NO. 2T023201A710	9b. OTHER REPORT NO(S) (Any other numbers that may be assigned this report) 6030.1-E	
c.		
d.		
10. AVAILABILITY/LIMITATION NOTICES Distribution of this document is unlimited. The findings in this report are not to be construed as an official Department of the Army position, unless so designated by other appropriate authorities.		
11. SUPPLEMENTARY NOTES None	12. SPONSORING MILITARY ACTIVITY U. S. Army Research Office-Durham Box CM, Duke Station Durham, N. C. 27706	
13. ABSTRACT This report is concerned with a survey of the presently available literature concerning broadband antennas, in order to determine the capabilities and the limitations of the various techniques which have been investigated. The report is divided into three main parts, concerned with the following subjects: I. Frequency Independent Antennas. II. Logarithmic Periodic Antennas. III. Electrically Small Antennas. In the first part the present state of the theory of frequency independent antennas is discussed. The experimental work on these structures is then briefly reviewed. In Section II, a parallel treatment is made for log periodic antennas. Section III is mainly concerned with the theoretical question of the bandwidth limitation of an antenna "small" in terms of wavelength.		

14. KEY WORDS	LINK A		LINK B		LINK C	
	ROLE	WT	ROLE	WT	ROLE	WT
Antennas Broadband antennas Frequency Independent antennas Logarithmic periodic antennas Electrically small antennas						

INSTRUCTIONS

1. **ORIGINATING ACTIVITY:** Enter the name and address of the contractor, subcontractor, grantee, Department of Defense activity or other organization (*corporate author*) issuing the report.
- 2a. **REPORT SECURITY CLASSIFICATION:** Enter the overall security classification of the report. Indicate whether "Restricted Data" is included. Marking is to be in accordance with appropriate security regulations.
- 2b. **GROUP:** Automatic downgrading is specified in DoD Directive 5200.10 and Armed Forces Industrial Manual. Enter the group number. Also, when applicable, show that optional markings have been used for Group 3 and Group 4 as authorized.
3. **REPORT TITLE:** Enter the complete report title in all capital letters. Titles in all cases should be unclassified. If a meaningful title cannot be selected without classification, show title classification in all capitals in parenthesis immediately following the title.
4. **DESCRIPTIVE NOTES:** If appropriate, enter the type of report, e.g., interim, progress, summary, annual, or final. Give the inclusive dates when a specific reporting period is covered.
5. **AUTHOR(S):** Enter the name(s) of author(s) as shown on or in the report. Enter last name, first name, middle initial. If military, show rank and branch of service. The name of the principal author is an absolute minimum requirement.
6. **REPORT DATE:** Enter the date of the report as day, month, year; or month, year. If more than one date appears on the report, use date of publication.
- 7a. **TOTAL NUMBER OF PAGES:** The total page count should follow normal pagination procedures, i.e., enter the number of pages containing information.
- 7b. **NUMBER OF REFERENCES:** Enter the total number of references cited in the report.
- 8a. **CONTRACT OR GRANT NUMBER:** If appropriate, enter the applicable number of the contract or grant under which the report was written.
- 8b, 8c, & 8d. **PROJECT NUMBER:** Enter the appropriate military department identification, such as project number, subproject number, system numbers, task number, etc.
- 9a. **ORIGINATOR'S REPORT NUMBER(S):** Enter the official report number by which the document will be identified and controlled by the originating activity. This number must be unique to this report.
- 9b. **OTHER REPORT NUMBER(S):** If the report has been assigned any other report numbers (*either by the originator or by the sponsor*), also enter this number(s).

10. **AVAILABILITY/LIMITATION NOTICES:** Enter any limitations on further dissemination of the report, other than those imposed by security classification, using standard statements such as:

- (1) "Qualified requesters may obtain copies of this report from DDC."
- (2) "Foreign announcement and dissemination of this report by DDC is not authorized."
- (3) "U. S. Government agencies may obtain copies of this report directly from DDC. Other qualified DDC users shall request through _____."
- (4) "U. S. military agencies may obtain copies of this report directly from DDC. Other qualified users shall request through _____."
- (5) "All distribution of this report is controlled. Qualified DDC users shall request through _____."

If the report has been furnished to the Office of Technical Services, Department of Commerce, for sale to the public, indicate this fact and enter the price, if known.

11. **SUPPLEMENTARY NOTES:** Use for additional explanatory notes.

12. **SPONSORING MILITARY ACTIVITY:** Enter the name of the departmental project office or laboratory sponsoring (*paying for*) the research and development. Include address.

13. **ABSTRACT:** Enter an abstract giving a brief and factual summary of the document indicative of the report, even though it may also appear elsewhere in the body of the technical report. If additional space is required, a continuation sheet shall be attached.

It is highly desirable that the abstract of classified reports be unclassified. Each paragraph of the abstract shall end with an indication of the military security classification of the information in the paragraph, represented as (TS), (S), (C), or (U).

There is no limitation on the length of the abstract. However, the suggested length is from 150 to 225 words.

14. **KEY WORDS:** Key words are technically meaningful terms or short phrases that characterize a report and may be used as index entries for cataloging the report. Key words must be selected so that no security classification is required. Identifiers, such as equipment model designation, trade name, military project code name, geographic location, may be used as key words but will be followed by an indication of technical context. The assignment of links, rules, and weights is optional.